2018

Metabolism and Gas Phase Reactions of Peroxide Explosives Using Atmospheric Pressure Ionization Mass Spectrometry

Kevin Colizza
University of Rhode Island, kcolizza@gmail.com

METABOLISM AND GAS PHASE REACTIONS OF PEROXIDE EXPLOSIVES USING ATMOSPHERIC PRESSURE IONIZATION MASS SPECTROMETRY

BY

KEVIN COLIZZA

A DISSERTATION SUBMITTED IN PARTIAL FULFILLMENT OF THE

REQUIREMENTS FOR THE DEGREE OF

DOCTOR OF PHILOSOPHY

IN

CHEMISTRY

UNIVERSITY OF RHODE ISLAND

2018

DOCTOR OF PHILOSOPHY IN CHEMISTRY DISSERTATION

OF

KEVIN COLIZZA

APPROVED:

Dissertation Committee:

Major Professor Jimmie C. Oxley

James L. Smith

Matthew Kiesewetter

Roberta King

Nasser H. Zawia

DEAN OF THE GRADUATE SCHOOL

UNIVERSITY OF RHODE ISLAND

2018

ABSTRACT

The toxicity or pharmacodynamics of many of the nitrated explosives have been well documented. Trinitrotoluene (TNT) is known to cause liver toxicity while nitrate esters (nitroglycerine) are known vasodilators. One class of explosive that has been on the rise due to the ease of manufacturing from household products are the peroxides. Of particular interest are the cyclic peroxides used for many home-made explosives (HME): triacetone triperoxide (TATP) and hexamethylene diamine triperoxide (HMTD). Very little is known about the toxicity or potentially beneficial effects of these compounds. This may be primarily due to the difficulty in detecting or working with these materials, particularly when they are extracted from living tissues. The use of liquid chromatography (LC) mass spectrometry (MS) is ideally suited to handle this type of sample, provided that the proper detection limits can be achieved. Additionally, this technique provides a very sensitive detection with gentle ionization for more definitive confirmation of the chemical in question over many other techniques historically chosen.

In our efforts to reduce the limits of quantification for TATP and HMTD, several remarkable discoveries were made. Most importantly, acetonitrile, one of the most commonly used LC/MS solvents used throughout many industries has shown direct inhibition of ionization. The proposed mechanism of this suppression is by the formation of neutral aggregates of the nitrile moiety with various, common functional groups. Peroxides are one of the most intensely affected moieties. Also, TATP and methyl ethyl ketone peroxide (MEKP) have been shown to react with one or more alcohols under atmospheric pressure ionization (API) conditions to produce new

species which may be exploited to improve limits of detection. Caution must be used while working with these products since the conditions can directly affect the signal intensity and multiple related analytes can all provide this common product. Lastly, HMTD has been found to react with both primary and secondary amines and alcohols in the gas phase to produce unique products related to the nature of the amine or alcohol. This research has allowed limits of detection to improve by 20 to 50 times our original analysis limits.

Toxicity of HMTD and TATP were primarily in question. However, with the volatility associated with TATP, it seems prudent that this should be the first compound studied since the exposure to this chemical entity is highly probable for any scientist or animal (bomb-sniffing canines) working with it. Simple *in vitro* analysis using canine liver microsomes (DLM) and lung microsomes (DLgM) in the presence of NADPH (electron donor) were performed to determine the rate, product and nature of the metabolism. Since most of the Phase I metabolism associated with the cytochrome P450 (CYP) enzymes requires molecular oxygen, the incubations are performed in open containers. The exceptional volatility of solid TATP extended to solutions of the compound as well, thus preventing this technique for experimentation. To overcome this issue, oxygen gas was bubbled through the buffered solution used as the matrix for the *in vitro* studies prior to sealing the containers for the duration of the experiment. Based on this work, several discoveries have been made. The metabolism that does occur appears to be NADPH-dependent, which limits the types of enzymes with may be responsible. The affinity for the non-specific metabolism is very high, with a K_m value of 2.21 μM (±14.8%) with a V_{max} of 1.13 nmol/min/mg

protein (±3.27%). This also indicates that the enzyme responsible for the metabolism is saturated at relatively low concentrations. Work with recombinant isoforms of specific CYP enzymes (rCYP) has shown that only rCYP2B11 has any effect (of the 5 major liver 5CYP's commercially available) and that this metabolism is enhanced by the presence of cytochrome b5. The metabolism of CYP2B11 does not seem to account for all of the total metabolism of TATP.

Only one metabolite has been identified, the mono-oxidation of a single primary methyl carbon (TATP-OH), for TATP. Monitoring the relative amount of this metabolite has been performed. After the rate of metabolism of TATP begins to level, the TATP-OH begins to drop, without detection of a second metabolite. Attempts to trap a second metabolite with semicarbazide (for aldehydes and ketones) or glutathione (for soft electrophiles) did not provide any conclusive products related to the metabolism of these species. With the successful synthesis of TATP-OH, we were able to directly incubate this metabolite. Although it was metabolized more rapidly that TATP, we were unable to detect any metabolites. It was also shown to degrade to acetone in oxidized aqueous buffer, but this did not appear to be related to the metabolism. TATP metabolism was not affected by the presence of TATP-OH or additional undetected metabolite(s). TATP-OH is metabolized only by rCYP2B11, providing evidence that TATP and TATP-OH competitively compete for the same enzyme and TATP dominates this competition. Of particular note is that very little metabolism was observed with the lung microsomes compared to liver. This may have the consequence of significant systemic exposure to those coming into contact with this material.

ACKNOWLEDGMENTS

I cannot thank my major professors, Dr. Jimmie C. Oxley and Dr. James L. Smith, enough for their support of my research and faith in my ability to provide positive results in research with considerable risk of failure. Not many would so generously invest as much as they have in a single student. I would also like to thank Ms. Jacqueline M. Tyler for her love, support and dedication throughout this endeavor. My colleagues in the lab have my immense gratitude for all of their support. Without their help, much of this work could not have been realized. I would like to particularly acknowledge the help of my co-authors of the papers presented in this thesis: Alexander V. Yevdokimov, Keira Mahoney, Lindsay McLennan, Matt Porter and particularly, Michelle Gonsalves, for all of her hard work. And of course, I would like to thank all of the funding agencies that supported my efforts and provided me with the tools to achieve this accomplishment.

DEDICATION

I would like to dedicate this work to my mother, Beverly A. Bachman, who supported me in every way in this endeavor as well as in everything else in my life. Thank You!

PREFACE

The work contained in this thesis is presented in Manuscript Format for specific reasons. The initial idea for research efforts began with the concept of performing energy resolved mass spectrometry (ERMS) on explosive and energetic materials. This technique involves infusion of a specific compound into the liquid chromatography mass spectrometry (LC/MS) source and isolating the ion of interest using quadrupole mass filtering. Once isolated, the ion can be fragmented by slowly increasing the energy to perform collision activated dissociation (CAD) with resonance excitation (ion trap) or collision induced dissociation (CID) by voltage differential (triple quadrupole). Parent depletion and fragment formation can be monitored to render relative energy values for the initiation of fragmentation, 50% depletion and 100% depletion of the parent. Analysis of this data may provide insight into the nature of a compound that will explode, which must be fundamentally different from similar compounds that do not explode. This work may spin off other research projects for years to come.

Knowing which instruments to use to achieve success in this project was only a small piece of this endeavor. Between establishing the methods, circumventing minor issues (such as solubility), ionizing each molecule, selecting proper solvents, requiring specific additives (for adduct formation), working with vendors to correct software issues and stabilizing the signal for each compound, it soon became clear that this project would exceed the timelines for any one PhD project and should be considered a long-term vision. As a positive consequence, many of the problems overcome during this work were serving to provide optimal ionization for compounds that

required detection by LC/MS. This led to quantification or separation assays being developed for each class of energetic material, minimally including TNT, dinitrotoluene (DNT), dinitroanisole (DNAN), nitrotriazole-one (NTO), nitroguanidine (NG), pentaerythritol tetranitrate (PETN), erythritol tetranitrate ETN, HMTD, TATP, tetramethylene diperoxide diamine dialdehyde (TMDDD), MEKP, 1,3,5-trinitro-1,3,5-triazinane (RDX) and 1,3,5,7-tetranitro-1,3,5,7-tetrazocane (HMX).

Also included in my research proposal was an alternate idea for determining the energy associated with fragmentation of explosives. This was the concept of Argon Flash—argon gas in a shock wave emits detectable levels of visible and UV light. Since most triple quadrupole instruments use argon gas as a collision gas, the idea was to place a fiber optic into the second quadrupole (collision cell) and attempt to detect light emitted when fragmenting explosives. Although we were quite successful in getting the fiber optic into the quadrupole while maintaining the vacuum, we were unable to detect any emissions. Many problems surrounded this lack of signal detection, but there were two major issues which discontinued this work. First, we were moving the fiber optic in blindly, without knowing where the fiber was in relation to the quadrupoles. If we were sitting directly behind the quadrupole, it is unlikely that any signal would be detected. To properly address this, machining a hole into the very expensive quadrupole cell would be required so that the optics could be properly aligned. The second issue was that the light signal might be very weak and require amplification from external components such as photomultipliers. In short,

this concept was not pursued at this time, but with proper funding could provide worthwhile results.

Examination of peroxide explosives metabolism using *in vitro* techniques required significant efforts into the assay development to drop detection levels from 500 ng/mL to 10 ng/mL. Obstacles overcome while reducing these limits also led to discoveries of gas phase reactions or interactions with the solvents. For this reason, the bulk of my research efforts were spent on the gas phase reactions of peroxide explosives using atmospheric pressure ionization (API) techniques associated with LC/MS. Since the discoveries made while performing this work are important to many in the analytical community, especially those working in explosive detection, it was prudent to publish the information as soon as it could be confirmed. This is the reason the Manuscript Format is the most practical means of presenting this work.

TABLE OF CONTENTS

LIST OF TABLES

LIST OF FIGURES AND SCHEMES

LIST OF ABBREVIATIONS

Solvent Abbreviations

ACN	Acetonitrile
BrACN	Bromoacetonitrile
BuOH	Butanol
HP	Hydrogen Peroxide
MeOH	Methanol
IPA	Isopropanol
MEK	Methyl Ethyl Ketone
PrOH	Propanol
NH_4OAc	Ammonium Acetate
TBAH	Tetrabutyl Ammonium Hydroxide
t-BuOH	Tertiary-butanol
TMACN	Trimethylacetonitrile (pivalonitrile)

Chromatography/analytical Abbreviations

ANP	Aqueous Normal Phase
FIA	Flow Injection Analysis
GC	Gas Chromatography
IS	Internal Standard
LC	Liquid Chromatography
LLOQ	Lower Limit of Quantification

LOD	Limit of Detection
QC	Quality Control
RPLC	Reverse Phase LC
ULOQ	Upper Limit of Quantification
UV	Ultraviolet

Mass Spectrometry Abbreviations

API	Atmospheric Pressure Ionization
APCI	Atmospheric Pressure Chemical Ionization
APPI	Atmospheric Pressure Photoionization
AU	Arbitrary Unit
CAD	Collision Activated Dissociation
CID	Collision Induced Dissociation
Da	Dalton
DART	Direct Analysis in Real Time
DBDI	Dielectric Barrier Discharge Ionization
DESI	Desorption Electrospray Ionization
EESI	Extractive Electrospray Ionization
ERMS	Energy Resolved Mass Spectrometry
ESI	Electrospray Ionization
GPB	Gas Phase Basicity
HCD	High-energy Collisional Dissociation
HESI	Heated Electrospray Ionization

HRMS	High Resolution Mass Spectrometry
LIT	Linear Ion Trap
LTQ	Linear Trap Quadrupole
MRM	Multiple Reaction Monitoring
MS	Mass spectrometry
MS/MS	Multi-stage or Tandem Mass Spectrometry
MS^n	Ion Trap Fragmentation (n = number of experiments)
m/z	Mass to Charge Ratio
PA	Proton Affinity
SRM	Selective Reaction Monitoring
ToF	Time of Flight
TSQ	Triple Stage Quadrupole
XIC	Extracted Ion Chromatogram

<u>In vitro Analysis Abbreviations</u>

1-ABT	1-aminobenzotriazole
Cl_{int}	Intrinsic Clearance
CYP	Cytochrome P450
DLgM	Dog Lung Microsomes
DLM	Dog Liver Microsomes
FMO	Flavin-containing Monooxygenase
GSH	Reduced Glutathione
GSSG	Oxidized Glutathione

K_m	Michaelis-Menten Constant
NADPH	Reduced Nicotinamide Adenine Dinucleotide Phosphate
RLM	Rat Liver Microsomes
rCYP	Recombinant CYP
SC	Semicarbazide
$T_{1/2}$	Half-life
V_{max}	Maximum (Enzyme) Velocity

Explosives Abbreviations

AP	Acetone Peroxide
CP	Cyclic Peroxide (number represents polymer units)
DADP	Diacetone Diperoxide
DHP	Dihydro Peroxide (number represents polymer units)
DNAN	Dinitroanisole
DNT	Dinitrotoluene
ETN	Erythritol Tetranitrate
HME	Homemade Explosive
HMTD	Hexamethylene Triperoxide Diamine
HMX	1,3,5,7-tetranitro-1,3,5,7-tetrazocane
MEKP	Methy Ethyl Ketone Peroxide
NG	Nitroguanidine
NTO	Nitrotriazole-one
PETN	Pentaerythritol Tetranitrate

RDX	1,3,5-trinitro-1,3,5-triazinane
TATP	Triacetone Triperoxide
TMDDD	tetramethylene diperoxide diamine dialdehyde
TNT	Trinitrotoluene

Chapter 1 : Acetonitrile Ion Suppression in Atmospheric Pressure Ionization Mass Spectrometry

Status: Published

Journal of the American Society of Mass Spectometry, 2016 Nov; 27(11):1796-1804

Abstract

Efforts to analyze trace levels of cyclic peroxides by liquid chromatography/mass spectrometry gave evidence that acetonitrile suppressed ion formation. Further investigations extended this discovery to ketones, linear peroxides, esters and possibly many other types of compounds including triazole and menadione. Direct ionization suppression caused by acetonitrile was observed for multiple adduct types in both electrospray ionization and atmospheric pressure chemical ionization. The addition of only 2% acetonitrile significantly decreased the sensitivity of analyte response. Efforts to identify the mechanism were made using various nitriles. The ion suppression was reduced by substitution of an acetonitrile hydrogen with an electron-withdrawing group, but was exacerbated by electron-donating or steric groups adjacent to the nitrile. While current theory does not explain this phenomenon, we propose that polar interactions between the various functionalities and the nitrile may be forming neutral aggregates that manifest as ionization suppression.

Introduction

Ionization suppression caused by undetected or unknown impurities, contaminants or solvents has been an ongoing issue for mass spectrometry (MS) users. Whether the issue is caused by one of the numerous possible suppression factors outlined in the literature[1–3] or from reaction (either gas or liquid phase) of the analyte with the matrix,[4] these effects compromise the ability to detect the analyte.[1–3]

Furthermore, these problems are frequently very difficult to recognize;[5] ion suppression may easily be misinterpreted by the absence of an unknown component that significantly enhances ionization.[6] Efforts to minimize these effects have been extensive for electrospray ionization (ESI) and atmospheric pressure chemical ionization (APCI), although APCI typically experiences fewer of these issues.[2, 7] Usually co-eluting background interference from matrix components are the most significant problem and frequently can be addressed by changing the liquid chromatography (LC) conditions to separate undetected suppressors from the analyte.[5] Solvent suppression, either from aqueous mobile phase modifiers, pH adjustment, or organic solvent selection is typically identified in the initial analysis for the compound of interest.

Addition of some degree of organic solvent is known to improve ionization in atmospheric pressure ionization (API) sources by improving the volatility of the solution. The organic modification can disrupt surface tension of droplets and generally assist in the droplet evaporation process.[8–10] The two most abundantly used organic solvents in reverse-phase liquid chromatography (RPLC) are methanol (MeOH) and acetonitrile (ACN).[2, 8, 11, 12] They have low molecular mass, low reactivity, low UV cutoffs (<210 nm), similar dielectric constants, low surface tension, and good solvent strength for RPLC. The ability of ACN to inertly solvate many non-polar analytes makes it a common first choice for LC/MS analysis. Methanol may be preferred if a more polar or protic solvent is required, or if excessive solvent expense is an issue.[13] However, if chromatographic conditions are not favorable in MeOH, better ionization may be compromised for better peak shape using ACN. In most

cases, initial work will show which solvent provides a better MS signal or solvation, and LC development will focus on that solvent.

There are a few previous reports of ionization suppression by ACN. For example, Vieno et al., observing the phenomena with high levels of ACN in the mobile phase, contended that non-polar matrix constituents eluting at the end of the gradient were causing the suppression.[5] Examining BAY 11-7082, Hewavaitharana and Shaw accounted for the correlation between increased ACN concentration and decreased $[M+H]^+$ formation asserting that solvent polarity promoted the formation of the dimerized sodium adduct.[14] Duderstadt showed some significant signal loss using ACN or acetone versus MeOH for polyalkene compounds of various size and functionality using APCI and atmospheric pressure photoionization (APPI) sources with a gradient chromatography system; the extent of this effect was not fully determined or quantified.[11] Efforts within our lab to analyze trace levels of cyclic peroxides led to the discovery that ACN appears to be suppressing the formation of H^+, NH_4^+ and Na^+ adduct ions. Further investigation into this issue led to the discovery that this effect extended to ketones, linear peroxides, esters triazole and menadione. Acetonitrile, present at very low solvent concentrations, caused direct ion suppression for multiple adduct types in both ESI and APCI.

Materials and Methods

Chemicals and Reagents

Caution: The sensitive organic peroxides mentioned below are powerful explosives. Take all necessary precautions when working with these compounds.

General use water, acetonitrile, methanol (all Optima HPLC grade), ammonium acetate (NH_4OAc) (HPLC grade), methyl ethyl ketone and acetone (ACS grade) were from Fisher Chemical. Fluka Analytical LC/MS Ultra CHROMASOLV® acetonitrile and bromoacetonitrile were purchased from Sigma-Aldrich. A 1 L solution of aqueous 10 mM NH_4OAc was prepared at neutral pH unless otherwise stated. Hexamethylenetetramine (hexamine), pivalonitrile (trimethylacetonitrile), cyanamide, tetrabutyl ammonium hydroxide (TBAH), cyclopentanone and cyclohexanone were purchased from Acros Organics. 4,4′-Bis(dimethylamino)benzophenone, commonly called Michler's ketone, was supplied by Alfa Aesar. Hydrogen peroxide (HP, 50%) was purchased from Univar. Menadione and diphenyl isophthalate were obtained from MP Biomedical. Hexamethylene triperoxide diamine (HMTD) was produced in house by standard methods reported in previous work.[15] Triacetone triperoxide was synthesized according to the method previously published by our group.[16] Methyl ethyl ketone (MEK) peroxides (MEKPs) and MEK/acetone peroxides (MEK/AP) were produced by the addition of equimolar parts of hydrogen peroxide (50% solution), MEK (or 50/50 MEK/acetone) and sulfuric acid. The non-aqueous layer was pipetted into a clean test tube and washed with water. The organic layer (mixture of various MEKPs or MEK/APs) was pipetted into a tared vial, weighed and immediately diluted to 50 mg/mL with MeOH. Further dilutions were made as needed.

Instrumentation

Using a Thermo Electron LTQ Orbitrap XL and Exactive mass spectrometer equipped with either APCI or ESI interface, ions were generated and introduced into the ion

transfer tube set between 180 to 275 ºC (depending on the thermal stability of the compound). Tune conditions for positive ion mode APCI infusion experiments (20 µL/min flow) were as follows: discharge current, 5000 µA; N_2 sheath gas, 20 arbitrary units (AU); N_2 auxiliary gas, 10 AU; vaporizer temperature 220-250 ºC; ion transfer tube, 14 V; tube lens, 55 V; and skimmer offset, 0 V. ESI conditions were as follows: source voltage, 4200 V; N_2 sheath gas, 15 AU; N_2 auxiliary gas, 2 AU; ion transfer tube, 14 V; tube lens, 85 V; and skimmer offset, 0 V. Mass spectrometer source conditions for flow injection analysis (FIA) were optimized for an aqueous liquid flow of 300 µL/min. This included increasing the sheath gas to 40 AU (ESI) or 35 AU (APCI) and auxiliary gas to 20 AU (ESI) or 16 AU (APCI) to provide better de-solvation. Minor voltage changes were made at times to improve signal intensity for some compounds. Orbitrap mass resolution was set to 15000 for FIA and 30000 for direct infusion with mass calibrations done as needed using Pierce LTQ ESI positive or negative ion calibration solutions provided by ThermoFisher Scientific. Solvent delivery was performed using a Thermo Electron Accela quaternary pump. Sample injections were performed by a CTC Analytics HTS PAL autosampler directly from either Agilent Technologies amber, glass LC vials with PTFE septa or from Analytical Sales and Service polypropylene, 2 mL 96-well plates with pre-slit silicone plate covers. Sample preparation was done directly in the aforementioned vials or plates. Additional sample injections using identical solvent and sample delivery were performed on a Thermo Electron Quantiva triple quadrupole mass spectrometer equipped with a heated electrospray ionization (HESI) source. Conditions for HESI analysis were: positive ion spray voltage 4200 V; sheath gas 40 AU; auxiliary gas 12

AU; sweep gas 1 AU; ion transfer tube 220 ºC; and vaporizer temperature was 200 ºC. Ion transfer tube and vaporizer temperatures were 325 ˚C and 333 ºC, respectively for 1, 2, 4-triazole analysis. Data collection and analysis was performed with Thermo Xcalibur software version 2.2, SP 1.48.

Methods

TATP analysis

Using the LC vials, 7 solutions of 1000 μL were made at concentrations of ACN/MeOH/aqueous 10 mM NH4OAc of 50/0/50, 40/10/50, 30/20/50, 20/30/50, 10/40/50, 5/45/50 and 0/50/50. All volumes given as a "percent" are by volume. A solution of TATP (20 μL of 4.5 mM in ACN) was placed into each vial (final concentration of 90 μM, neglecting the addition of 2% ACN). Samples were individually infused onto the LTQ Orbitrap. Initial results suggested that the 2% ACN should not be neglected and a new 4.5 mM standard solution was created using MeOH. An eighth vial was added to include a 2/48/50 solution ratio and 10 μL of standard was added to each vial (neglecting the 1% addition of MeOH). These samples were re-infused and used to develop the FIA system.

Flow Injection Analysis (FIA)

An adequate number of scans (>10) across the peak and minimal mixing with the flow were required for this system. The system was acquiring full scan data (between m/z 50 to 400) at approximately 110 scans per minute for the LTQ Orbitrap (the slowest scanning of the 3 instruments used). Assuming the liquid was non-compressible,

tubing length (from injector to detector) and particularly the inner diameter (ID) were minimized using Poiseuille's law to keep viscosity differences in the sample plug and mobile phase negligible.[17] The system was optimized using a constant flow of 10 mM NH_4OAc in pump channel B at 300 μL/min flow to deliver sample volumes of 20 μL from a 20 μL injection loop to the LC/MS source. Wash solvent was exclusively 80/20 water/MeOH. Path length from injection port to source was approximately 0.5 meters using 0.005" ID red PEEK tubing. The auto-sampler was set for manual control, and peak to peak injection times were determined by needle, valve and port wash cycles. Contact closure triggered by the auto-sampler started sample acquisition. In order to avoid data loss from the slight delay of analysis start compared to the speed in which the first sample reached the source, the first injection of each run was blank water. Each analysis allowed triplicate injections for each solution with approximately 1.5 minutes between injections. Some solvents or analytes (e.g. diphenyl isophthalate) were not compatible with the 100% aqueous environment of the mobile phase, so conditions were modified to run with a binary mixture of 50/50 10 mM NH_4OAc/MeOH. Extracted ion chromatograms (XIC) were integrated using the Genesis peak detection algorithm in Thermo Xcalibur Qual Browser.

HMTD analysis

Since HMTD is poorly soluble in MeOH (but very soluble in ACN), to create an ACN-free solution, a dilute solution of HMTD (4.8 mM) in MeOH was made. This solution was almost imperceptibly cloudy, indicative of a very fine suspension. Prior to removing any sample, the standard solution was quickly vortex-mixed. Injections

were made with each final concentration of 48 μM (HMTD was fully solvated at this concentration).

MEKP and MEK/AP analysis

Immediately following MEKP or MEK/AP synthesis, material was pipetted into a tared vial and dissolved in MeOH to a volume of 50 mg/mL and 10 mg/mL, respectively. Since this synthesis produces multiple compounds, individual standards are not available and concentrations could not be accurately determined. Positive results for impact sensitivity confirmed the presence of the desired materials. Samples were produced at 10 and 1 μg/mL to assure that the observed results were not a concentration dependent effect.

Alternate nitrile solvents

Cyanamide (a white powder with aqueous solubility of 850 mg/mL) was dissolved in water to 786 mg/mL (18.7 M and comparable to the density of ACN). Samples were produced in a constant 20% MeOH while 10 mM NH_4OAc volume was altered to accommodate the increasing volume of cyanamide from 0-50%. Trimethylacetonitrile and bromoacetonitrile were immiscible in water; therefore, the 10 mM NH_4OAc was replaced with MeOH for these experiments (nitrile/MeOH going from 0/100 to 50/50). This was duplicated with ACN to assure the effect was consistent in a 100% organic environment.

Other analysis

All other compounds analyzed were directly weighed into glass vials and dissolved in MeOH to produce concentrations of standard solutions necessary to add 10 µL to produce the final concentrations in mixtures. Final sample concentrations were varied as needed for detection. MEK was run at 4.1 mM, menadione at 0.581 mM and hexamine required only 14.3 nM. Diphenyl isophthalate was run at 3.14 µM and 1, 2, 4-triazole was analyzed at 72.4 µM. Cyclohexanone analysis was performed at a concentration 1.02 mM for all experiments unless otherwise stated. For aqueous content analysis, MeOH was added to compensate for volume loss when 10 mM NH_4OAc was reduced from 50%; however, for the 80% aqueous run, the organic ratios were limited so the MeOH/ACN ratio was set at 0/20, 5/15, 10/10 (run 3 times to keep analyses consistent), 15/5, 18/2 and 20/0.

Calibration curves

A solid sample of diphenyl isophthalate was weighed into a glass vial and diluted to 1.26 mM in MeOH. From this solution, five, serial 2:1 dilutions were made in MeOH to the concentration of 39.3 µM. A sample of liquid cyclohexanone was weighed into a glass vial and diluted to 81.5 mM in MeOH. From this solution, five, serial 2:1 dilutions were made in MeOH to the concentration of 2.55 mM. For each compound, these standards were used to prepare calibration curves using 500 µL 10 mM aqueous NH_4OAc, 100µL of standard solution, and 400 µL MeOH. Three additional curves were prepared for each compound by replacing a portion of the MeOH with 20 µL, 50 µL, and 100 µL of ACN (e.g. 20 µL ACN with 380 µL MeOH). All samples were

analyzed in triplicate using the FIA system on the TSQ Quantiva. Linear regression was performed using Microsoft Excel version 14.0.4760.1000 (32-bit).

Results and Discussion

TATP is very soluble in ACN yet not solvated by MeOH at concentrations above 171 mM (38 mg/mL),[18] far above levels being examined in this work. Literature reports the LC/MS analysis of TATP yielding a significant signal for the ammonium adduct $[M+NH_4]^+$ of m/z 240 using APCI.[19] Using a solvent of 50/50 (v/v) aqueous 10 mM NH_4OAc and ACN, no signal of TATP or any related adduct could be observed in either APCI or ESI. Since previous work[19] stated that analysis was performed using MeOH, the solvent was changed to 50/50 (v/v) 10 mM NH_4OAc/MeOH. Infusion of this solution into the APCI source immediately yielded a large signal at m/z 240.1442. This anomaly was initially believed to be caused by signal enhancement due to the protic nature of MeOH. Keeping the aqueous portion constant (50% 10 mM NH_4OAc), ACN and MeOH ratios were varied. Rather than a linear increase in signal response corresponding to the increase of MeOH, an exponential increase in response was observed for decreasing ACN levels. Even 2% ACN (the neglected standard volume added to 50/50 NH_4OAc/MeOH) suppressed ionization by as much as 50%. As observed by Annesley for MeOH, it was considered that some trace contamination in the ACN lot might be responsible for this effect.[13] Several lots of Fisher ACN and one lot from Fluka were subsequently tested with identical results to our initial observation.

To determine if the suppression effect of ACN was occurring specifically under APCI conditions, the LC/MS system was switched to ESI. Infusion experiments showed that the effect persisted with similar results. In order to effectively quantify these results, a FIA method was developed to measure peak areas of analytes in specific solvent ratios. The required system had to carry the sample to the source interface with minimal mixing of the mobile phase. While this would require a high flow rate, enough scans across the peak had to be obtained for statistical significance. Sample injection volume and flow rate were optimized for this analysis. Samples were analyzed in triplicate, typically in order of decreasing levels of ACN, but were later run in reverse and random order. The phenomenon persisted for TATP through 5 separate analyses (excluding the initial infusion experiments) over several months (Appendix 1: Supporting Information Table S1-1).

Previous work with the cyclic peroxide, HMTD showed very little response in ESI, so analysis was performed in APCI. Since MeOH showed reactivity toward HMTD in the APCI source, ACN had been chosen as the solvent for subsequent APCI analyses.[4] With this work still being in an area of active investigation in our lab, HMTD was examined in the same fashion as described for TATP above. With APCI or ESI, the HMTD signal was significantly more intense when no ACN was present. Irrespective of the ion source, HMTD showed as much as 47% signal suppression with as little as 2% ACN present in the solvent (**Figure 1-1** and **Figure 1-2**). With the solubility of HMTD being much greater in ACN, this precludes any notion that the compounds analyzed were simply more soluble in MeOH compared to ACN.

Hexamine, the starting material for HMTD synthesis, was also analyzed by this method with no suppression by ACN observed (**Figure 1-2**).

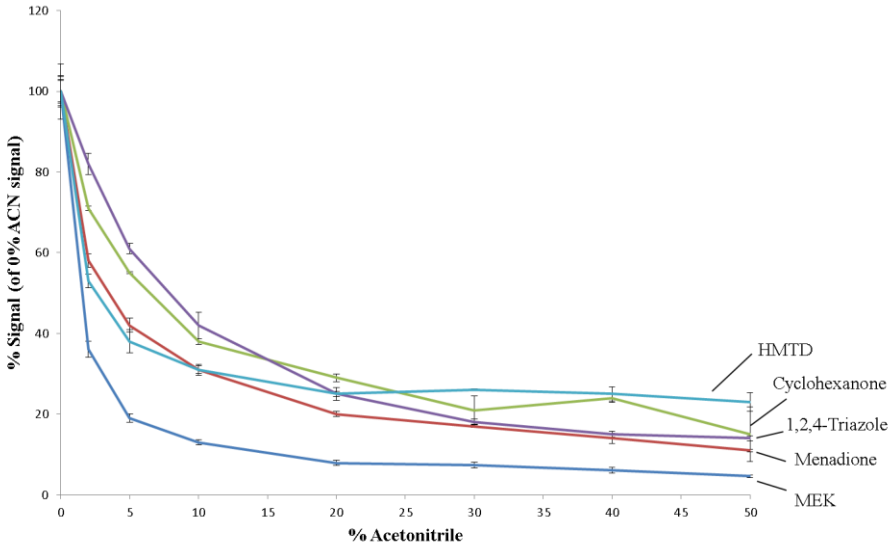

Figure 1-1. *FIA results comparing [M+H]+ relative signal intensity vs. %ACN for 5 compounds in APCI.*

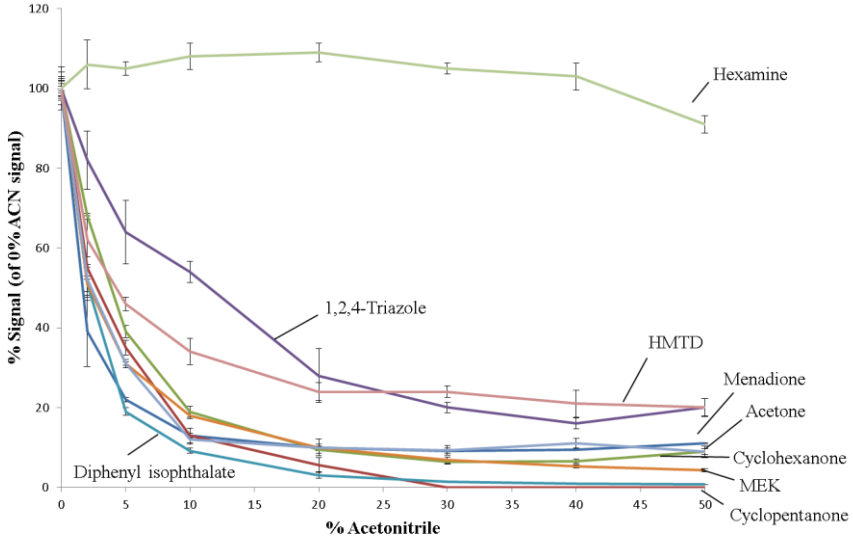

Figure 1-2. *FIA results comparing [M+H]+ relative signal intensity vs. %ACN for 9 compounds in ESI.*

With two major cyclic peroxides exhibiting the suppression effect of ACN, we examined MEKPs in ACN. While TATP is the favored, aqueous-insoluble product of the reaction of acetone and HP, a similar synthetic route using MEK and HP produces a liquid mixture of linear dihydroperoxy peroxides (DHP), hydroxyhydroperoxy peroxides, dihydroxy peroxides (DH) and cyclic peroxides (CP) containing one, two, three and four MEK units. Dissolving freshly made MEKP product mixtures in MeOH for subsequent analysis provided a substantial amount of data in one run. While the moderately sized (300 < MW < 400 Da) MEKP products were only minimally affected by the presence of ACN, products over MW 400 Da (DHP4) showed no effect at all. However, some of the smaller (< MW 300 Da) MEKP products were significantly affected. Only data for the 10 µg/mL solution is presented since the signal was completely suppressed for some MEKPs in the 1 µg/mL solution with merely 10% ACN present. All peroxides were detected as adduct ions of either NH_4^+ or Na^+; with the exception of HMTD (only the $[M+H]^+$ observed). The starting materials, MEK and acetone, both showed the ACN suppression effect as well (**Figure 1-2**). Analysis of MEKP in the presence of ACN using the TSQ Quantiva with the HESI source (vaporizer temperature at 200ºC) exhibited an even greater suppression effect than had been observed for the ESI source. This was particularly true for the CP3 and DHP3 products that appeared minimally affected under ESI conditions. **Figure 1-3** shows the relative signal loss for the $[M+NH_4]^+$ ions of the peroxide compounds in the ESI source.

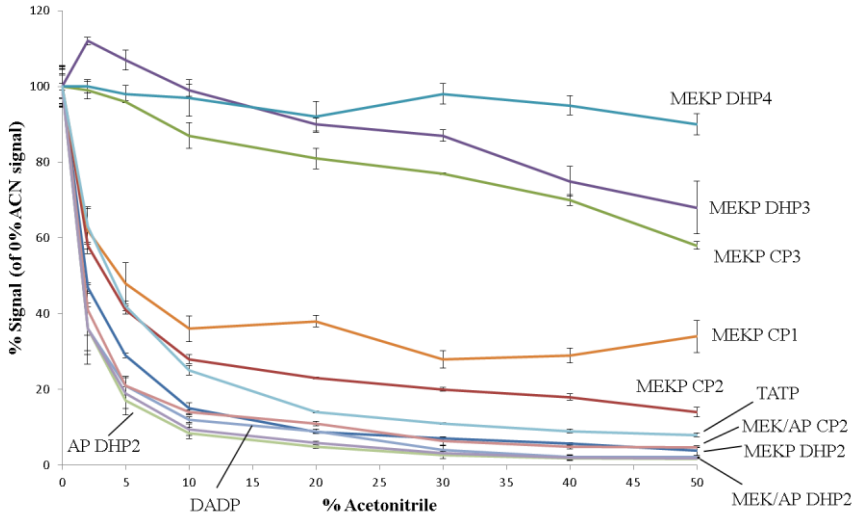

Figure 1-3. *FIA analysis results comparing the [M+NH4]+ relative signal intensity vs. %ACN for 11 peroxide compounds in the ESI Source.*

To investigate the generality of the ACN ionization suppression effect other ketones were examined. Significant ACN ion suppression was observed for acetone, cyclohexanone, cyclopentanone, and diphenyl isophthalate (**Figure 1-2**) but not for Michler's ketone. Menadione, a vitamin K analog with significant biological roles, has proven to be a difficult molecule to detect by LC/MS.[20–22] The FIA procedure showed that the addition of 2% ACN suppressed menadione ionization by as much as 40 to 60% for APCI and ESI, respectively. All the ketones, except Michler's, showed both $[M+NH_4]^+$ and $[M+H]^+$ responses affected by ACN with both ESI and APCI. Additional experiments using cyclohexanone and diphenyl isophthalate with no NH_4OAc added to either the mobile phase or the sample, showed consistent ACN-dependent signal reduction (no $[M+NH_4]^+$ ion was observed for cyclohexanone in APCI under these conditions).

Cyclohexanone was chosen for additional testing since it was readily available, showed a stronger response than the other ketones tested, was safer and more stable than the peroxides, and showed good response for both $[M+H]^+$ and $[M+NH_4]^+$ ions. The signal for cyclohexanone was considerably more intense by APCI, and the concentration had to be lowered from 1.02 mM to 10.2 µM or signal saturation occurred. Most additional experiments were conducted under ESI conditions unless otherwise stated. The standard 50% aqueous NH_4OAc portion was changed to 0%, 5%, 20% or 80%, and the remaining percentage was made up with varying ACN/MeOH ratios. The signal response was insensitive to the aqueous environment, but highly dependent on the ACN concentration (Appendix 1: Supporting Information Figure S1-1 and **Table 1-1**). To further test the effects of the aqueous environment, an acidified aqueous NH_4OAc solution (~pH 3 with 0.1% formic acid) was used in both the sample and the mobile phase, which showed ion suppression was still ACN dependent.

To evaluate the sensitivity effects of ACN ion suppression for the $[M+H]^+$ and $[M+NH_4]^+$ ions, calibration curves were produced and analyzed on the TSQ Quantiva for cyclohexanone and diphenyl isophthalate. Calibration curve slopes (sensitivity) were determined over each compound's dynamic range at four ACN concentrations (0%, 2%, 5% and 10 %) keeping a constant 50% 10 mM NH_4OAc and varying the levels of MeOH. The dynamic range with no acetonitrile present was between 81.5 and 2.55 mM for cyclohexanone and between 1.26 and 0.0393 mM for diphenyl isophthalate. The reduction in sensitivity caused by the ACN addition is expressed as the percent of the slope of each curve to the slope of the curve without ACN. Data for

the calibration curves is shown in **Table 1-1** (with 0% ACN added being 100% signal). All correlation coefficients were between 0.974 and 0.999. Single concentration response data (**Figure 1-2** above, Appendix 1: Supporting Information Table S1-1), which shows a consistent decrease in ion response as ACN concentration is increased, is mirrored over the entire calibration curve dynamic range from 0 to 10% ACN concentration.

Table 1-1. Relative (to 0% ACN) sensitivities of cyclohexanone and diphenyl isophthalate using HESI source.

Compound	Ion	%ACN		
		10	5	2
Diphenyl isophthalate	$[M+NH_4]^+$	19	30	58
Diphenyl isophthalate	$[M+H]^+$	22	37	63
Cyclohexanone	$[M+NH_4]^+$	41	52	69
Cyclohexanone	$[M+H]^+$	36	47	66

With the small molecules being used for this study, we considered the ion evaporation model for ESI. Both ACN and MeOH have comparable surface tension and relative permittivity making them excellent solvents to overcome the Rayleigh charge condition for solution ions to escape into the gas phase.[8] It may be that the ACN is preventing the neutral analyte molecules from forming ions prior to ejection from the charged droplets. However, considering that the ion suppression effect of ACN is observed in APCI as well as ESI, it appears that this phenomenon must be occurring in

the gas phase. It may be that certain analytes are emitted from the charged droplets as neutral molecules which can then undergo gas phase reactions with other charged reagent molecules similar to APCI. This would suggest that, for some molecules, there is a convergence of theories for APCI and ESI, where ultimately, gas phase conditions prevail prior to charged ions being detected. If the cause is high volatility, it may explain the reason TATP was affected (since it is known to sublime).[23] However, this idea falls short when considering HMTD has such a low vapor pressure that it cannot be accurately measured and must be estimated.[24]

To explain the source of ion suppression observed for some analytes with ACN, the theory applied in APCI was considered. For the volatilized analyte to be ionized, it must have a higher proton affinity than the reagent molecules.[7] Literature values for the proton affinity (PA) and gas phase basicity (GPB) data for some of the solvents and analytes used are readily available online (Appendix 1: Table S1-2, Supporting Information).[25] Both values for ACN (PA 779.2 kJ/mole, GPB 748 kJ/mole) are considerably lower than those of the analytes presented. With PA being defined as the $-\Delta H°(T)$ at temperature (T) for reaction (1), protonation of the analytes (MH^+) should be favorable over ACN protonation (m/z 42, $ACNH^+$).[25] Furthermore, with proton transfer from the analyte to ACN being an endothermic process;[12] it might be possible that the heat from the HESI source could allow this endothermic reaction to occur, but this has yet to be clearly demonstrated. Analytes may be within a temperature range that is thermodynamically insignificant since the perceived temperature of the ion/molecule under these conditions can only be estimated. The PA data for the ACN dimer (m/z 83, $(ACN)_2H^+$) is unknown, but analogous methyl-

substituted imidazole and pyrazole compounds suggest this PA value may be considerably higher (900-960 kJ/mol) than the ACN monomer or the analytes.[12] Although minimal $(ACN)_2H^+$ ion was detected in the presence of NH_4OAc, we did detect high levels (1.1×10^{-7} height counts--comparable to the $[M+H]^+$ of cyclohexanone without ACN present for that analysis) of m/z 59 ($ACN\text{-}NH_4^+$), which decreased in parallel with decreasing levels of ACN. This could explain the reason ammonium adduct levels were affected, but it is unclear why the proton adduct would also be suppressed. With no ammonium present, the levels of ACN dimer were significant (6.7×10^{-7} height counts--just under the $[M+H]^+$ of cyclohexanone without ACN present for that analysis). It may be that the dimer or the ammonium adduct of ACN scavenged the positive charge, reducing the formation of analyte ions. However, this does not explain the reason the ammonium adduct was reduced proportionally to the proton adduct. With the understanding that solvated molecules will increase the proton affinity for the analyte,[12] it may be that the analyte-solvent cluster for these compounds increased the proton affinity for ACN and therefore did not form analyte ions (reaction 2 and 3). The charged, intermediate ACN adducts (in brackets) were not detected in any of the analyses, suggesting that this may not be the case.

$$M_{(g)} + H^+_{(g)} \rightarrow MH^+_{(g)} \qquad (1)$$

$$M_{(g)} + ACN_{(g)} \rightarrow M{\cdot}ACN_{(g)} + H^+_{(g)} \rightarrow [M{\cdot}ACN{\cdot}H^+_{(g)}] \rightarrow M(g) + ACNH^+_{(g)} \qquad (2)$$

$$M_{(g)} + ACN_{(g)} \rightarrow M{\cdot}ACN_{(g)} + NH_4^+{}_{(g)} \rightarrow [M{\cdot}ACN{\cdot}NH_4^+{}_{(g)}] \rightarrow M(g) + ACNNH_4^+{}_{(g)} \qquad (3)$$

With PA/GPB failing to fully explain the suppression phenomenon, determining the mechanism of ACN ion suppression was attempted by substituting ACN with pivalonitrile (TMACN), cyanamide or bromoacetonitrile (BrACN). These nitriles were tested against cyclohexanone to determine if they would behave similarly to ACN with regards to ion suppression. Since TMACN and BrACN were immiscible in water, the aqueous portion was replaced with MeOH (also tested against ACN). The electron donating properties of cyanamide were expected to exacerbate the ion suppression, while the electron-withdrawing Br on ACN was expected to improve analyte signal. Both cyanamide and BrACN performed as expected as can be seen in **Figure 1-4**. However, it should be noted that cyanamide produced multiple, intense ion clusters up to 4 units with multiple adducts, but none were associated with cyclohexanone. TMACN extensively diminished the analyte signal, consistent with its higher PA (810.9 kJ/mole) compared to other nitriles tested. However, the TMACN proton affinity was still 30 kJ/mol lower than that of cyclohexanone (841 kJ/mole).

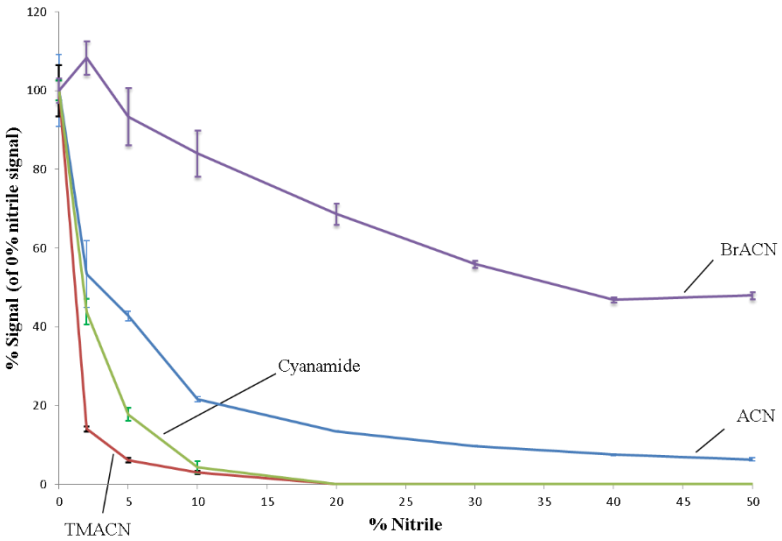

Figure 1-4. *FIA analysis results comparing the cyclohexanone [M+H]+ relative signal intensity vs. %nitrile for 4 different nitrile compounds tested in the ESI Source.*

Since the majority of molecules in this study contained carbonyl or peroxide groups, 1, 2, 4-triazole was examined. Although it has a PA of about 100 kJ/mol higher than ACN, it was significantly affected by ACN in all three sources used (APCI, ESI, HESI, Appendix 1: Supporting Information Table S1-1). We initiated a study of other molecules frequently analyzed in our lab. Nitroarenes and nitrate esters examined in negative ion mode MS exhibited no ion suppression with ACN. However, initial indications for nitramines suggest ACN may be inhibiting ionization and further investigation into this continues. As noted previously, only hexamine, DHP4, and Michler's ketone were completely unaffected by ACN. TBAH, a quaternary ammonium, was tested to determine if ACN could affect a charged species. As expected, the signal for TBAH was not affected. **Figure 1-5** summarizes the species

tested, grouping by adducts formed (hydronium and/or ammonium) and the effect of ACN on their ionization.

Nitrile and carbonyl groups have large dipole moments[26] with the electron densities primarily around the nitrogen and oxygen. The electron configuration of nitrile can be arranged to mimic a carbonyl, i.e. they become isosteres.[27] When polarization occurs with a significant excess of nitrile present (compared to the analyte), a neutral clustering of molecules may form, as shown in **Scheme 1-1**. Once clustering occurs, the site of analyte ionization is blocked by the functional group attached to the nitrile. Furthermore, the excess electrons of the nitrile are not accessible for charge formation while occupied with the carbonyl. With a neutral aggregate formed, the mass spectrometer has no ability to break these clusters as it would with a charged analyte. Formation of this type of aggregate could explain the occurrence of steric, electron-donating and electron-withdrawing nitriles. Peroxides have small dipole moments in the trans configuration but quite large in the cis configuration.[28] Cyclic peroxides are forced into a cis configuration; thus, making them susceptible to acetonitrile suppression. Linear peroxides are free to rotate, though energy input via heat may favor the cis configuration. Large linear peroxides would be forced into self-interaction, allowing some trans configuration, making them available for ionization. The cyclic MEKP CP3 may have been less affected by ACN than TATP due to the steric interaction of the additional methyl group. Heating may alter the molecular conformation of MEKP CP3 and DPH3 allowing nitrile interaction which could explain their increased suppression in the HESI source. All data results including

comments on analysis can be found in the Appendix 1: Supporting Information Table S1-1 (Online Resource 1).

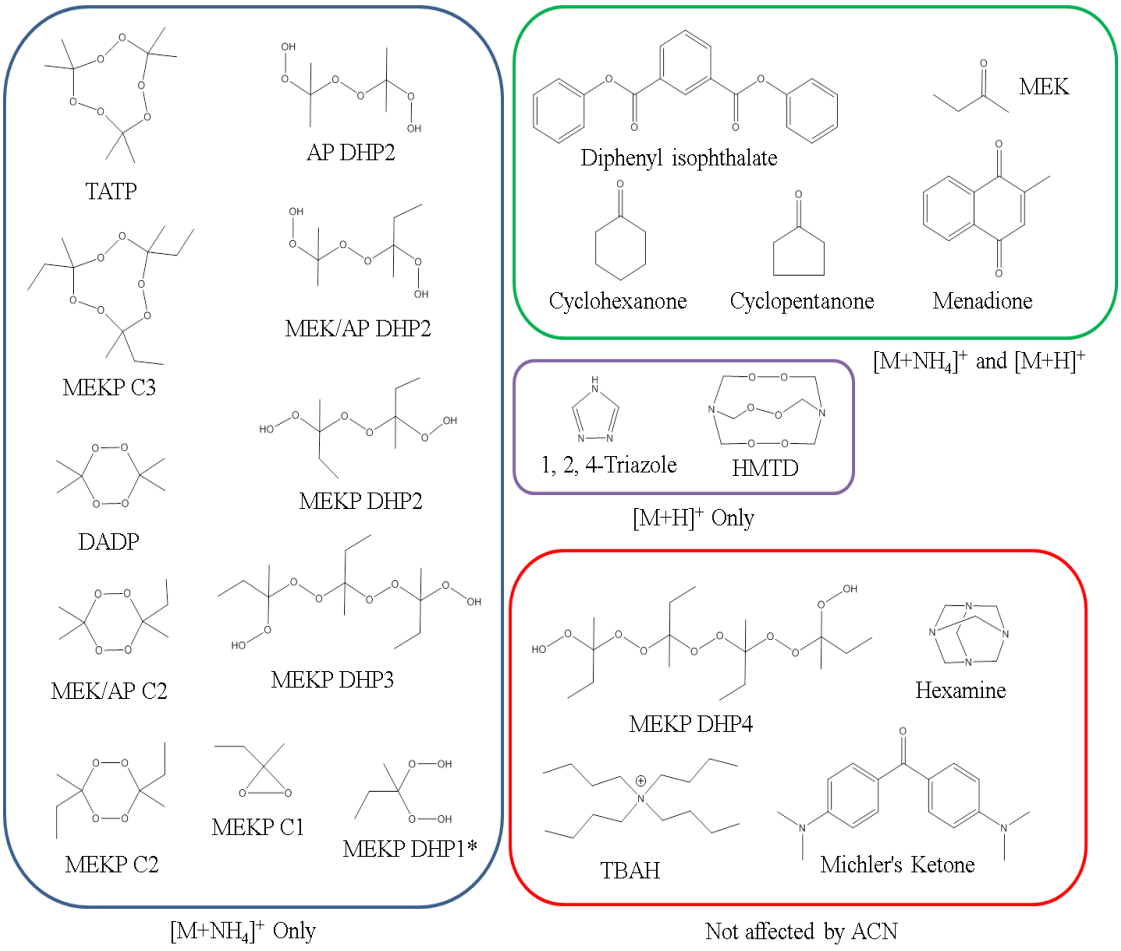

Figure 1-5. *Structures tested for ACN ion suppression (*only one compound produced a sodium adduct).*

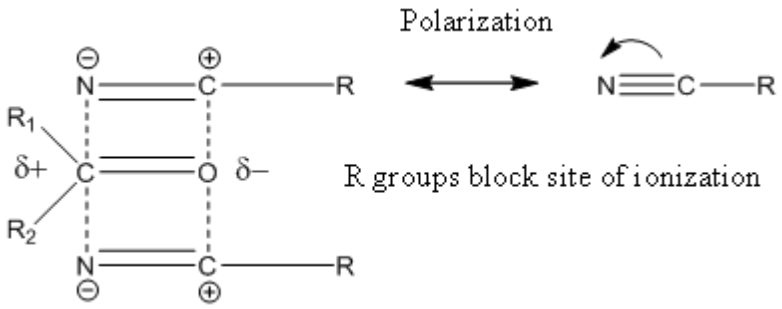

Scheme 1-1

Conclusions

With little success we attempted to correlate the ACN suppression effect to ion size and shape, functionality, volatility, gas phase energy and solvation. This has been rigorously tested in multiple mass spectrometers with different ionization sources. Currently accepted mechanisms for ion formation fail to fully explain the phenomenon. Although the mechanism is still unclear, we have tentatively proposed a polarity aggregation model involving nitriles and carbonyls, peroxides or other polar molecules that may inhibit ionization. An important objective to this work is alerting the LC/MS community to the significant ion suppression that may be caused by the presence of ACN. Chemical analysis/trace detection of peroxides, ketones, and related compounds would be particularly impacted fields.

Associated Content:

Appendix 1: Supporting Information

Acknowledgements: The authors thank the U.S. Department of Homeland Security (DHS) for funding. However, the views and conclusions contained are those of the authors and should not be interpreted as necessarily representing the official policies, either expressed or implied, of the DHS.

References

1. Annesley, T.M.: Ion suppression in mass spectrometry. Clin. Chem. 49, 1041–1044 (2003).
2. Furey, A., Moriarty, M., Bane, V., Kinsella, B., Lehane, M.: Ion suppression; A critical review on causes, evaluation, prevention and applications. Talanta. 115, 104–122 (2013).
3. Gosetti, F., Mazzucco, E., Zampieri, D., Gennaro, M.C.: Signal suppression/enhancement in high-performance liquid chromatography tandem mass spectrometry. J. Chromatogr. A. 1217, 3929–3937 (2010).
4. Colizza, K., Porter, M., Smith, J.L., Oxley, J.C.: Gas-phase reactions of alcohols with hexamethylene triperoxide diamine (HMTD) under atmospheric pressure chemical ionization conditions. Rapid Commun. Mass Spectrom. 29, 74–80 (2015).
5. Vieno, N.M., Tuhkanen, T., Kronberg, L.: Analysis of neutral and basic pharmaceuticals in sewage treatment plants and in recipient rivers using solid phase extraction and liquid chromatography-tandem mass spectrometry detection. J. Chromatogr. A. 1134, 101–111 (2006).
6. Kamel, A., Jeanville, P., Colizza, K., J-Rivera, L.E.: Mechanism of [m+h]+

formation in atmospheric pressure photoionization mass spectrometry: identification of propionitrile in acetonitrile with high mass accuracy measurement and tandem mass spectrometry and evidence for its involvement in the protonation p. J. Am. Soc. Mass Spectrom. 19, 1579–89 (2008).

7. Covey, T.R., Thomson, B.A., Schneider, B.B.: ATMOSPHERIC PRESSURE ION SOURCES. Mass Spectrom. Rev. 28, 870–897 (2009).
8. Kebarle, P., Tang, L.: From Ions in Solution to Ions in the Gas Phase. Anal. Chem. 65, 972–986 (1993).
9. Konermann, L., Ahadi, E., Rodriguez, A.D., Vahidi, S.: Unraveling the mechanism of electrospray ionization. Anal. Chem. 85, 2–9 (2013).
10. Bruins, A.P.: Mass spectrometry with ion sources operating at atmospheric pressure. Mass Spectrom. Rev. 53–77 (1991).
11. Duderstadt, R.E., Fischer, S.M.: Effect of organic mobile phase composition on signal responses for selected polyalkene additive compounds by liquid chromatography-mass spectrometry. J. Chromatogr. A. 1193, 70–78 (2008).
12. Jarvis, M.J.Y., Koyanagi, G.K., Zhao, X., Covey, T.R., Bohme, D.K.: Scrubbing ions with molecules: Kinetic studies of chemical noise reduction in mass spectrometry using ion-molecule reactions with dimethyl disulfide. Anal. Chem. 79, 4006–4012 (2007).
13. Annesley, T.M.: Methanol-associated matrix effects in electrospray ionization tandem mass spectrometry. Clin. Chem. 53, 1827–1834 (2007).
14. Hewavitharana, A.K., Shaw, P.N.: Enhancing the ratio of molecular ions to non-covalent compounds in the electrospray interface of LC-MS in quantitative

analysis. Anal. Bioanal. Chem. 382, 1055–1059 (2005).

15. Oxley, J., Zhang, J., Smith, J., Ciof, E.: Mass Spectra of Unlabeled and Isotopically Labeled Hexamethylene Triperoxide Diamine (HMTD). Propellants, Explos. Pyrotech. 25, 284–287 (2000).
16. Oxley, J.C., Smith, J.L., Shinde, K., Moran, J.: Determination of the Vapor Density of Triacetone Triperoxide (TATP) Using a Gas Chromatography Headspace Technique. Propellants, Explos. Pyrotech. 30, 127–130 (2005).
17. Tzanavaras, P.D., Themelis, D.G.: Review of recent applications of flow injection spectrophotometry to pharmaceutical analysis. Anal. Chim. Acta. 588, 1–9 (2007).
18. Bellamy, A.J.: Triacetone Triperoxide : Its Chemical Destruction. J. Forensic Sci. 44, 603–608 (1999).
19. Widmer, L., Watson, S., Schlatter, K., Crowson, A.: Development of an LC/MS method for the trace analysis of triacetone triperoxide (TATP). Analyst. 127, 1627–1632 (2002).
20. Loughlin, A.F., Skiles, G.L., Alberts, D.W., Schaefer, W.H.: An ion exchange liquid chromatography/mass spectrometry method for the determination of reduced and oxidized glutathione and glutathione conjugates in hepatocytes. J. Pharm. Biomed. Anal. 26, 131–142 (2001).
21. Liu, R., Wang, M., Ding, L.: A novel liquid chromatography-tandem mass spectrometry method for determination of menadione in human plasma after derivatization with 3-mercaptopropionic acid. Talanta. 128, 51–57 (2014).
22. Hirota, Y., Tsugawa, N., Nakagawa, K., Suhara, Y., Tanaka, K., Uchino, Y.,

Takeuchi, A., Sawada, N., Kamao, M., Wada, A., Okitsu, T., Okano, T.: Menadione (vitamin K3) is a catabolic product of oral phylloquinone (vitamin K1) in the intestine and a circulating precursor of tissue menaquinone-4 (vitamin K2) in rats. J. Biol. Chem. 288, 33071–33080 (2013).

23. Brady, J.E., Smith, J.L., Hart, C.E., Oxley, J.: Estimating Ambient Vapor Pressures of Low Volatility Explosives by Rising-Temperature Thermogravimetry. Propellants, Explos. Pyrotech. 37, 215–222 (2012).
24. Aernecke, M.J., Mendum, T., Geurtsen, G., Ostrinskaya, A., Kunz, R.R.: Vapor Pressure of Hexamethylene Triperoxide Diamine (HMTD) Estimated Using Secondary Electrospray Ionization Mass Spectrometry. J. Phys. Chem. A. 119, 11514–11522 (2015).
25. Hunter, E.P.L., Lias, S.G.: Evaluated Gas Phase Basicities and Proton Affinities of Molecules: An Update. J. Phys. Chem. Ref. data. 27, (1998).
26. Hammer, N.I., Diri, K., Jordan, K.D., Desfrançois, C., Compton, R.N., Hammer, N.I.: Dipole-bound anions of carbonyl , nitrile , and sulfoxide containing molecules Dipole-bound anions of carbonyl , nitrile , and sulfoxide containing molecules. J. Chem. Phys. 119, 3650–3660 (2003).
27. Fleming, F.F., Yao, L., Ravikumar, P.C., Funk, L., Shook, B.C.: Nitrile-Containing Pharmaceuticals: Efficacious Roles of the Nitrile Pharmacophore. J. Med. Chem. 53, 7902–7917 (2010).
28. Maciel, G.S., Bitencourt, A.N.A.C.P., Ragni, M., Aquilanti, V.: Alkyl Peroxides : Effect of Substituent Groups on the Torsional Mode Around the O O bond. J. Quantum Chem. 107, 2697–2707 (2007).

Chapter 2 : Reactions of Organic Peroxides with Alcohols in Atmospheric Pressure Chemical Ionization—the Pitfalls of Quantifying Triacetone Triperoxide (TATP)

Status: Published

Journal of the American Society of Mass Spectometry, 2018 Feb;29(2):393-404

Abstract

Over the last several decades, mass spectrometry has become one of the principle methods for compound identification and quantification. While for analytical purposes, fragments which are not fully characterized in terms of origin and intensity as a function of experimental conditions have been used, understanding the nature of those species is very important. Herein we discuss such issues relative to TATP and its frequently observed fragment at m/z 89. This "fragment" has been identified as the gas phase reaction product of TATP with one or two methanol molecules/ions. Additionally, the origin and conditions of other fragments at m/z 91, 75 and 74 associated with TATP will be addressed. Similar analytical issues associated with other multi-peroxide organics compounds (HMTD, MEKP) will also be discussed. Solution storage conditions for TATP, HMTD and TMDDD have been determined.

Introduction

Terrorist incidents and resulting government focus on so-called "homemade" explosives have resulted in a number of researchers examining the organic peroxides--triacetone triperoxide (TATP)[1], hexamethylene triperoxide diamine (HMTD)[2], and methyl ethyl ketone peroxides (MEKP)[3] (**Figure 2-1**). With attention being on rapid detection and analysis, traditional analytical tools, infrared[4], Raman[4, 5], and x-ray[5] have been applied. However, screening usually employs ion mobility mass spectrometry (IMS)[6–8]. Spectroscopy, which offers no possibility of separation from interferences, has reported limits of detection (LOD) ranging between 1[9] and 5 ppm[10] in standoff mode. IMS, which has some ability to separate interferences, has

a reported LOD of 23.3 ng for TATP and 0.2 ng for HMTD.[8] For unequivocal identification and quantification some type of separation is essential prior to detection.

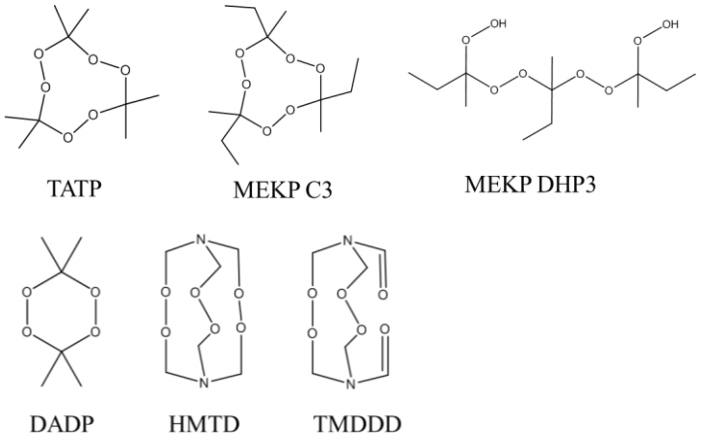

Figure 2-1. *Structures of peroxides analyzed.*

Volatile organic compounds have traditionally relied on separation by gas chromatography (GC) coupled to either a mass spectrometer (MS)[11–15] or electron capture detector (ECD).[13, 16]. In one of the earliest reports of TATP detection in a criminal case study, both GC/MS electron impact (EI) and chemicals ionization (CI) techniques were used.[17] Since that time, the number of GC/MS applications for TATP and HMTD have grown exponentially; today it is one of the prominent techniques for their detection. The reported LODs for TATP in a condensed phase range between 0.05 and 2 ng,[18] depending on the mode of ionization and type of mass spectrometer used; even lower LODs (<0.1 ng) are recorded for headspace analysis.[19] Low nanograms levels were reported by DART™-time-of-flight-MS[20] for HMTD analysis. The major drawback using GC is the potential for thermal degradation of explosives in the inlet or ion source. For this reason, liquid

chromatography mass spectrometry (LC/MS) is becoming a predominant technique for unequivocal structural elucidation and quantification of most organic molecules. The benefits over GC include room temperature sample introduction, availability of soft ionization techniques, and high resolution accurate mass capability.[21, 22] Selected LC methods with monitored ions and LODs are presented in **Table 2-1**.

Table 2-1. LC/MS Methods with Reported LOD for Peroxide Explosives

Peroxide	LOD (ng)	Monitored Ions (m/z)	Ionization Mode	Ref
TATP				
	62.5	[245], 215, 81	APCI	[23]
	20	[229]	EESI	[24]
	15	[240], 242, 224, 223, 210	DBDI	[25]
	10	[245], 240, 223, 215, 91, 74	DESI	[26]
	25	252, 240, 194, 107, 102, 91, [89], 90, 75	APCI	[21]
	1-50	[240], 245, 223	DESI	[22]
	0.8-148	[223], 240, 132, 91, 74	APCI	[27]
	0.88	240.1441, 89.0597	APCI	[28]
	1	89.0597	APCI	[29]
	0.1	348.1869	APCI	[30]
HMTD				
	3	[229], 209, 191, 145, 104	APCI	[31]
	1	[231], 247, 209	DESI	[26]
	10,000	[224], 177, 207, 209	APCI	[32]
	0.08-12	[118], 207, 191, 147, 72, 58	APCI	[27]
	-	[209], 224, 207, 179, 145, 88	DART	[33]
	0.43	[207.0975], 209.0768, 179.0666, 145.0606	APCI	[28]

2.5	207.0976	APCI	[29]
1	[209], 207, 179, 106, 90, 62	APCI	[34]
0.2-0.5	207.0615, 177.0861	APCI	[30]

LOD – limit of detection, [m/z] – most abundant observed ion, *APCI* – atmospheric pressure chemical ionization, *ESI* – electrospray ionization, *DESI* – desorption electrospray ionization, *DART* – direct analysis real time, *DBDI* – dielectric barrier discharge ionization, *EESI* - extractive electrospray ionization.

Much of the reported research utilizing LC/MS was performed on nominal mass instruments making some assignments and fragment origins questionable.[25] For example, though many researchers identify or quantify TATP using m/z 89,[6, 7, 21, 29] exact mass MS shows this fragment contains four carbons, which cannot readily be explained from the structure of TATP (**Figure 2-1**). Our work investigates the origin of that fragment and addresses chromatographic and mass spectrometric parameters (e.g. solvents,[35] temperatures, gas flows and voltage differentials) that can affect ion production.

Materials and Methods

Chemicals and Reagents

Caution: The sensitive organic peroxides mentioned below are powerful explosives. Take all necessary precautions when working with these compounds.

Water, acetonitrile, methanol, 2-propanol (all Optima HPLC grade), ammonium acetate (NH_4OAc), sodium acetate, lithium acetate, n-butanol (all HPLC grade), n-propanol (sequencing grade), tert-butanol, methyl ethyl ketone (MEK) and acetone

(ACS grade) were purchased from Fisher Chemical. Stable isotope labelled material was purchased from Cambridge Isotope Labs. Hexamethylenetetramine (hexamine) was purchased from Acros Organics. Hydrogen peroxide (HP, 50%) was purchased from Univar. All mobile phase used for chromatography consisted of aqueous 10 mM NH_4OAc prepared at neutral pH with methanol (MeOH) as the organic modifier unless otherwise stated.

TATP, DADP, TMDDD and MEKP Synthesis:

Triacetone triperoxide (TATP) and diacetone diperoxide (DADP) were synthesized according to literature methods.[13] TATP was purified by recrystallizing once with 80/20 (w/w) MeOH/H_2O and then with pentane [melting point (mp) 94-96 °C]. Deuterated TATP (d_{18}-TATP) was synthesized as above[13] using d_6-acetone. DADP was recrystallized in hot methanol (mp: 131-133 °C).

For hexamethylene triperoxide diamine (HMTD) synthesis, a round-bottom flask equipped with magnetic stir bar was used to dissolve hexamine (2.43 g, 17.3 mmol) in 50% hydrogen peroxide (9.88 g, 145 mmol) and chilled in an ice bath. Anhydrous citric acid (3.61 g, 18.9 mmol) was added in small portions so the temperature did not exceed 10 °C. The reaction mixture was left in the ice bath and stirred for 15-18 hours. Product was collected by vacuum filtration, washed with deionized water and room temperature methanol and allowed to dry. This HMTD was used to produce trimethylene diperoxide diamine dialdehyde (TMDDD), which was synthesized according to Wierbeczki et al.[36] This crude product (mp: 156-157°C) was used for all TMDDD testing.

Methyl ethyl ketone peroxides were synthesized by a modified literature method.[37] In a test tube containing a micro stir bar, hydrogen peroxide (50-wt%, 1.4 mL) was mixed with methyl ethyl ketone (0.82 mL, 9.49 mmol). The solution was chilled in an ice bath and concentrated H_2SO_4 (0.5 mL, 9.38 mmol) was added slowly so that the temperature did not exceed 20 °C. Stirring continued for 15-18 hours before the solution was extracted with pentane, washed with saturated ammonium sulfate (3x3 mL), deionized water (3x3 mL) and dried with sodium sulfate. The product was stored as a solution in pentane and was pipetted into tared vials for immediate dilution with MeOH to desired concentrations.

Instrumentation

Using a Thermo Electron LTQ Orbitrap XL or Exactive mass spectrometer equipped with an atmospheric pressure chemical ionization (APCI) interface, ions were generated and introduced into the ion transfer tube set between 180 to 275 ºC (depending on the experimental conditions being tested). All work was performed using positive ion mode. Tune conditions for APCI infusion experiments were varied depending on the parameters being tested: discharge current, 2500-6000 µA; N_2 sheath gas, 8-50 arbitrary units (AU); N_2 auxiliary gas, 5-40 AU; vaporizer temperature 180-350 ºC; ion transfer tube, 14 V; tube lens, 35-70 V; and skimmer offset (Exactive), 0 V. Minor voltage changes were made at times to improve signal intensity for some compounds. Mass resolution was set to 30000 (LTQ Orbitrap) and 50000 (Exactive) for all experiments. Solvent delivery was performed using either Thermo infusion syringe pumps or Thermo Electron Accela quaternary pumps. A CTC Analytics HTS

PAL autosampler injected directly from either amber, glass LC vials with PTFE septa (Agilent Technologies) or polypropylene, 1 mL 96-well plates with pre-slit silicone plate covers (Analytical Sales and Service). Data collection and analysis was performed with Thermo Xcalibur software version 2.2, SP 1.48. All data collected within this work is APCI full scan MS unless otherwise noted. Chromatographic traces are all extracted ion chromatograms (XIC) with a mass window of 15 ppm of the expected exact mass. *Note: All masses reported below are exact mass values within ±15 ppm for species less than 130 m/z and ±7.5 ppm for species over m/z 130*.

Methods

TATP Analysis

The mass spectrometry gas flows and temperature were originally optimized using a constant flow of 50% 10 mM NH_4OAc in pump channel B and 50% MeOH in channel A at 230 µL/min flow and directly infusing 20 µL/min TATP standard (20 µg/mL/90.1 µM in MeOH) into the flow. Monitoring the $[M+NH_4]^+$ ion at m/z 240.1442, the vaporizer temperature was set to 250 °C, with the sheath gas at 40 AU and auxiliary gas at 20 AU. Using this optimized system, 40 µL sample volumes of TATP in 50/50 ACN/water were injected into a LC flow of 250 µL/min with 5% MeOH (channel A) and 95% aqueous 10 mM NH_4OAc (channel B) for introduction onto a Thermo Syncronis C18 column (2.1 x 50 mm, 5 µm). Initial conditions were held for 1.5 minute before a linear ramp to 35% A/65% B over 1.5 minutes followed immediately by a linear ramp to 95%A/5% B over the next minute. This concentration was held for 2 minutes before a 30 second transition to initial conditions with a hold of 1.5 minutes.

As an internal standard (IS), d_{18}-TATP at 10 μg/mL (41.7 μM) in ACN was added 1:1 to aqueous TATP samples with a final concentration of 5000 ng/mL (20.8 uM). XIC were integrated using the Genesis peak detection algorithm in Thermo Xcalibur Quan Browser. Linear dynamic range comparing concentration to peak area response ratio, relative to the IS, extended from 25 ng/mL (112.6 nM) to 20000 ng/mL (90.1 μM) using 10 points and 1/x weighting of the calibration curve. Identical procedures were followed for the calibration curve of DADP (discussed later). Stability determination for TATP did not use an IS and calibration was determined by peak area response vs. concentration (external calibration). Linear range and curve conditions were the same as above. All dilutions were made in 50/50 ACN/water. Stability was determined by comparing quality control (QC) samples made on day 1 to freshly prepared standards made on the day of stability determination.

TATP Volatility

Volatility of TATP was interrogated by 2 methods. The first involved incubating aqueous TATP at 37 °C in 1.5 mL Eppendorf tubes both open and closed. For this analysis, 995 μL of water was brought to 37 °C before addition of 5 μL of 20 mM TATP in ACN (final concentration 100 μM) to initiate the study (time 0). At time 0, 15, 30, 45 and 60 minutes, 100 μL aliquots were removed and placed in 100 μL of ACN containing IS. Analysis were performed in duplicate and average values are displayed with RSD values less than 0.5%. The second method involved placing 100 mg of TATP powder in two separate 1L vessels (screw top) and two separate 500mL vessels (screw top). Each vessel was covered with aluminum foil, capped and allowed

to sit at room temperature (~20 °C) for ~4 hours. For each vessel, 3 labelled GC vials were filled with 500 µL of 50/50 ACN/water and capped with PTFE septa seals. At 4 hours, the cap was removed from the first vessel; a 2.5 mL, gas-tight hypodermic syringe penetrated the foil to withdraw 2.5 mL of vapor; and the cap was immediately replaced. The vapor was transferred into the GC vial ensuring the needle tip was well under the liquid while the plunger was slowly depressed and the vial gently swirled. This was repeated 3 times for each vessel before sample solutions were injected onto the HPLC/MS system described above (without IS). Samples were injected in duplicate; average TATP vapor concentration is reported.

HMTD/TMDDD Analysis

Stability determination of HMTD ($[M+H]^+$ ion of m/z 209.0768) and TMDDD ($[M+NH_4]^+$ ion of m/z 224.0877) were performed by the same method used for TATP to keep analysis consistent for these 3 compounds. All dilutions were made in 50/50 ACN/water. The HMTD 9-point external calibration curve was linear from 50 ng/mL (240 nM) to 20000 ng/mL (96.2 µM). TMDDD was linear over a 10-point external calibration from 25 ng/mL (121 nM) to 20000 ng/mL (97.1 µM). Stability was determined by comparing QC samples made on day 1 to freshly prepared standards made on the day of stability determination.

MEKP Analysis

With the MEKP's lacking any true "standard", stability determination or quantitative analysis of any specific one of these was not possible. Purification of these

compounds, particularly the cyclic trimer (MEKP C3), was attempted using a CombiFlash Rf+ PurIon (Teledyne Isco, Lincoln, NE) system with C18 cartridges. HPLC methods developed for this system are as follows. A 25 µL sample containing an estimated 20 µg/mL (by weight) of total MEKP was injected onto the Syncronis C18 column into 250 µL/min flow of mobile phase 65% A/35% B. Initial conditions were held for 1 minute followed by a linear ramp to 80% A/20% B over 3 minutes and a 6-minute isocratic hold. Conditions were then changed to 98% A/2% B over 30 seconds and held for 1.5 minutes before dropping to initial conditions over 30 seconds with a 2-minute hold. Using this method, we were able to achieve baseline separation of what we believe to be the MEKP C3 ($[M+NH_4]^+$ m/z 282.1911) from other linear peroxides.

Isotope Incorporation Studies

To examine the origin of certain products/fragments observed in the LC/MS experiments, isotope incorporation studies were performed as follows. Hydrogen/deuterium exchanged (HDX) began with concentrated (20 µg/mL), 0.5 mL samples of TATP and d_{18}-TATP prepared in deuterium labeled methanol/water (CD_3OD/D_2O) and unlabeled ($MeOH/H_2O$) solvents, respectively. An ammonium source was provided by the addition of 5 µL of 500 mM NH_4OAC. Solutions were individually infused at 20 µL/min. Two samples containing an estimated 30 µg/mL of total MEKP and 20 µg/mL of both TATP and d_{18}-TATP were produced from highly concentrated standards prepared in MeOH. These samples were briefly placed under a light stream of N_2 gas to evaporate the solvents but prevent significant evaporation of

TATP. One sample was reconstituted in 100 µL of MeOH and 20 µL of water before infusion onto the optimized APCI-MS conditions for in-source fragment production (discussed later). Once this sample was successfully observed, the second sample was reconstituted in 100 µL of $Me^{18}OH$ and 20 µL of water and infused.

Alcohol Incorporation and Infusion Experiments

A 25 µL sample containing an estimated 20 µg/mL of total MEKP and 10 µg/mL of both TATP and d_{18}-TATP was injected onto the LC/MS system developed for MEKP (above). Mobile phase transition from MeOH to isopropanol (IPA) or n-propanol (PrOH) required significant change due to the higher solvent strength and column back pressure of the larger alcohols. The same sample (25 µL) was injected into a mobile phase of 20% PrOH/80% B flowing at 200 µL/min onto the C18 column. Conditions were held for 1 minute followed by a linear ramp to 90% PrOH/20% B over 8 minutes. This was held for 1 minute before ramping to initial conditions over 30 seconds and holding for 2 minutes.

Infusion of TATP into the APCI source was performed by two methods. To generally optimize MS voltages, TATP (20 µg/mL in 90/10 MeOH/10 mM NH_4OAc) was directly infused onto the ACPI source at 20 µL/min. We termed this "direct infusion." To assess the effects of temperature and gas flow, TATP (20 µg/mL in 90/10 MeOH/10 mM NH_4OAc) was infused at 20 µL/min into a 230 µL/min flow of 95% MeOH/5% 10 mM NH4OAc (total flow was 250 µL/min, the environment of TATP eluting from a C18 column). This we termed "MP infusion." An additional MP infusion study was performed but using the TATP gradient program (described

above). Full scan data was collected from m/z 70 to 500, and the XIC data for TATP $[M+NH_4]^+$ and m/z 89.0597 were exported to Microsoft Excel for data analysis. Additional studies to show incorporation of various alcohols were performed by directly infusing 20 μg/mL samples of TATP and d_{18}-TATP in 20% 10 mM NH_4OAC/80% alcohol. Alcohols (other than MeOH) tested were ethanol (EtOH), PrOH, n-butanol (BuOH) and tert-butanol (t-BuOH).

Results and Discussion

Stability and Volatility of Analytes

Many unexpected challenges and unusual findings were encountered during the development of LC/MS analysis methods for the peroxide explosives TATP, DADP, HMTD, TMDDD and MEKP. Samples can be prepared and stored in ACN without issue as long as MeOH is used as the organic mobile phase modifier for reverse phase LC/MS and the compound is not eluting in the void volume. The peroxides described in this work are generally well-retained and free of can, which is washed away in the sample plug. However, if ACN is present in the source using either ESI or APCI, the signal will be significantly reduced or almost completely eradicated.[35]

Individually synthesized products of TATP, HMTD and TMDDD were treated separately for stability analysis. While attempts were made to purify HMTD, it always contained a small amount of TMDDD and vice versa. Solutions of each peroxide were prepared and stored in acetonitrile. Autosampler stability (for the 10000 and 5000 ng/mL samples), is presented in the Online Resource for the first reanalysis (day 7) since concentrations were changing rapidly once the container seal was compromised.

Samples were run at N=2 (RSD <5%). Calibration curve values were within ±15% of nominal concentrations with R^2 values > 0.98 for 1/x or $1/x^2$ weighted curves. TATP showed ~9% recovery after 7 days storage in the refrigerated autosampler (in a 96-well plate, Appendix 2: Table S2-1). This loss of TATP is attributed to its high volatility and the fact that the 96-well mat was no longer sealed; subsequent data supports this conclusion.

The peak shape of HMTD on a C18 column was strongly dependent on the organic concentration in the sample plug. As the organic concentration increased, the peak fronting became severe, with optimal peak shape occurring at low organic content. By placing the samples in 50/50 ACN/water, peak shape and limit of detection for HMTD was compromised to keep sample processing consistent with the previously developed method for TATP analysis. Despite this compromise, HMTD curve and QC data was within acceptable criteria of ±15% accuracy. As ACN evaporated from the 96-well plate, concentration of HMTD and TMDDD increased significantly. Evidence of ACN evaporation was observed by the greatly improved peak shape of the HMTD sample after sitting in the autosampler for 7 days (Appendix2: Table S2-1, Figure S2-1). In fact, due to the change in concentration of HMTD or TATP over a relatively short period of time, separate curves using the same vial or well-plate position could not be used to bookend analyses greater than 3 or 4 hours apart.

TATP concentration was relatively unchanged over 60 days under conditions where the storage vessel was airtight. HMTD degraded ~15% in 40 days at room temperature and about 7% in the refrigerator or freezer in 60 days (Appendix2: Table S2-1). This loss corresponds to a similar increase in TMDDD levels in the HMTD samples. This

suggests that in ACN, HMTD oxidizes into TMDDD. QC concentrations were kept intentionally high (10000 to 1000 ng/mL) compared to the curve limits in order to identify degradation products (if possible) and to quantify the conversion of HMTD to TMDDD or vice versa. Concentrations of TMDDD did not appear to decrease, suggesting that this compound did not decompose under the experimental conditions. Storage in methanol or water was not attempted due to the lack of solubility of one or more of the compounds in these solvents.

The vapor pressure of TATP is known to be extremely high for a solid. When aqueous solutions of TATP (concentration 100 µM) were incubated at 37 °C for 60 minutes in an open 1.5 mL, polypropylene Eppendorf tube, the concentration of TATP dropped ~ 40% every 15 minutes. To assure that the compound was not degrading under these conditions, the same experiment was performed simultaneously with the snap-cap lid closed. **Figure 2-2** clearly shows that evaporation, not degradation, is the problem that must be overcome during quantitative analysis. This effect is exaggerated at lower TATP concentration samples (<10 µM kept in closed 1.5 mL Eppendorf tubes) where periodic opening of the tube to remove aliquots resulted in significant evaporative loss up to 3% per tube sampling.

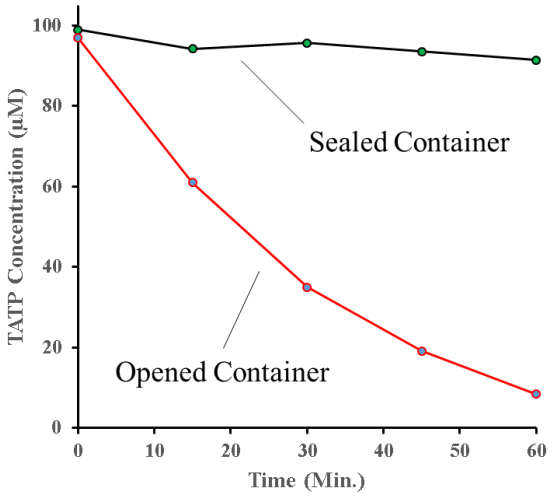

Figure 2-2. *Evaporative loss of TATP (aqueous 100 µM sample) held at 37 °C in a shaking dry bath.*

By directly extracting the TATP vapor from the headspace of pure TATP in sealed containers, bubbling that vapor into a solvent system, and quantifying by LC/MS, the concentration of TATP in the headspace was determined to be 376 ng TATP/mL, based on 12 individual trials analyzed in duplicate (Appendix2: Table S2-2). Using the ideal gas law, with a temperature of 20 °C (293K), the partial pressure of TATP was calculated to be 4.1 ± 0.1 Pa. This is in excellent agreement with the determined partial pressure by headspace GC of 7 Pa in 2005.[16] It is quite possible that some of the TATP was not fully trapped by the solvent, resulting in a slightly lower partial pressure by this technique.

TATP and MEKP In-Source Fragmentation/Reaction

During the LC optimization of TATP and its fully deuterated analog, d_{18}-TATP (used as an IS), several unexpected "fragment" peaks were observed. Coeluting with the TATP $[M+NH_4]^+$ XIC at m/z 240.1442 was an apparent fragment of m/z 89.0597 corresponding to molecular formula $C_4H_9O_2^+$. Since each TATP ring is comprised of three C_3H_6 units separated by peroxide linkages, making a 4 carbon fragment is rather unlikely. When observing the deuterated analog of the $[M+NH_4]^+$ ion at m/z 258.2571, the major fragment observed switched from m/z 89.0597 to m/z 95.0974, associated with the molecular formula $C_4H_3D_6O_2^+$. We speculated that the source of the non-deuterated methyl group was derived from the addition of the solvent methanol into TATP, as we had observed for HMTD[38] and proposed by Rondeau, et al for dialkyl mono-peroxides.[14] In order to determine the extent of methanol dependence for the m/z 89 signal, TATP was infused post-column into the normal LC gradient used for TATP analysis. Initially, m/z 240 increased with increasing methanol (as would be expected with increased organic modifier), but that signal quickly leveled off and began to diminish while m/z 89 continued to increase. To clearly illustrate the effect of methanol on the m/z 89 fragment, the ratio of m/z 89 to m/z 240 was plotted against time and compared to the methanol concentration of the gradient (**Figure 2-3**). There was a significant increase in m/z 89 when increasing from 5% to 95% methanol in the gradient. This accounted for some of the previously unexplained variations between the levels of m/z 89 and m/z 240 we had experienced.

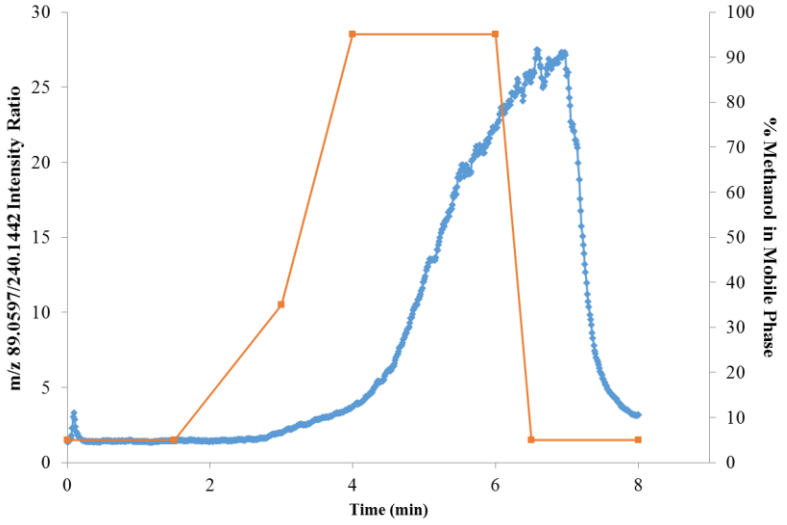

Figure 2-3. *TATP MP infusion into linear gradient of methanol (right) and m/z 89/240 ratio (left).*

It was noted that under similar LC/MS conditions as used for TATP, each of the MEKP peaks had fragments of m/z 89.0597. This is a reasonable fragment for MEKP since each subunit consists of 4 carbons. A far more abundant ion at m/z 103.0754, associated with the formula $C_5H_{11}O_2^+$, was also present for each MEKP chromatographic peak. This "fragment" could be explained readily by the incorporation of methanol. To support the hypothesis of methanol incorporation into TATP and MEKP, the mobile phase was changed from methanol to n-propanol or isopropanol. The results (**Figure 2-4**) demonstrate the concept of alcohol incorporation into one of the polymer units for each of these compounds. All fragments associated with methanol disappeared with incorporation of propanol (***Table 2-2*** and **Figure 2-4**). Note that for MEKP C3, an additional m/z 282.1911 peak was detected but presumed to be the in-source fragment of the major linear MEKP

dihydroperoxy trimer (DHP3, $[M+NH_4]^+$ m/z 316.1966) since their XIC peak shapes matched (**Figure 2-4**). Furthermore, fragments other than m/z 95.0975 related to d_{18}-TATP MeOH incorporation were consistently observed at m/z 97.0766 ($C_3HD_6O_3^+$) and m/z 92.0785 ($C_4H_6D_3O_2^+$). To probe these findings, complete HDX experiments were performed on TATP and d_{18}-TATP. Multiple fragments were observed (***Table 2-2***). **Figure 2-5** shows the full scan spectrum (from m/z 50 to 125 for resolution purposes) of the infusion of d_{18}-TATP and the proposed assignments. The fragment m/z 92.0785 corresponds to the incorporation of 2 alcohols. Importantly, for non-deuterated TATP, this peak would also be m/z 89.0975. This is critical since every molecule of TATP present may react with either 1 or 2 molecules of alcohol depending on the conditions of the method. Slight variations in the method generally result in vastly different results when monitoring m/z 89.

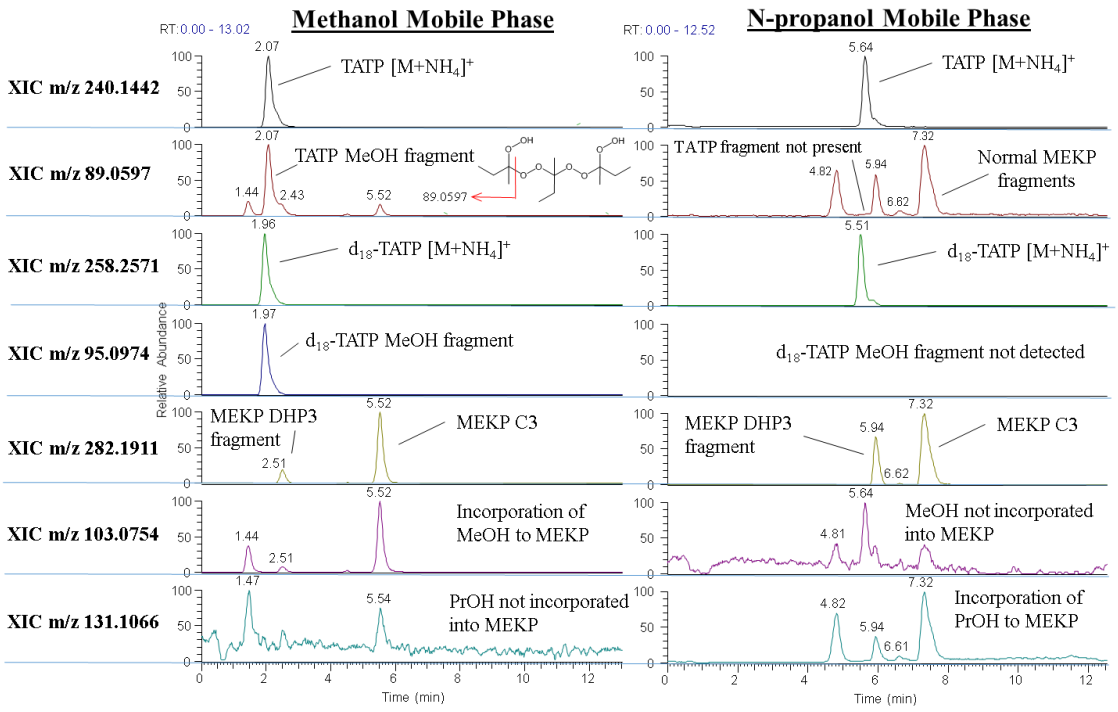

Figure 2-4. *Chromatogram of mixture of TATP, d18-TATP, and MEKP with mobile phase of MeOH or PrOH. Peak locations varied due to need to accommodate stronger solvent properties of PrOH vs MeOH.*

Table 2-2. *Products ions associated with TATP and MEKP with and without incorporation of alcohols.*

TATP only

Proposed Structure	Product	Material/solvent	Exact Mass	Molecular formula	Observed Mass	ΔPPM	Comments
	**1**	U/CH3OH	89.0597	C4H9O2+	89.0587	-11.2	Infusion experiment
		D18/CH3OH	95.0974	C4H3D6O2+	95.0964	-10.5	Infusion experiment
		U/CD3OD	92.0785	C4H6D3O2+	92.0776	-9.8	Infusion experiment
		U/PrOH	117.091	C6H13O2+	na	na	Contaminant present in solvent
		D18/PrOH	123.1287	C6H7D6O2+	123.1298	8.9	Observed in chromatogram
		U/CH3^{18}OH	91.0639	C4H9O^{18}O+	91.0651	13.2	Infusion experiment
		D18/CH3^{18}OH	97.1016	C4H3D6O^{18}O+	97.1027	11.3	Infusion experiment
	**2**	U/CH3OH	91.0390	C3H7O3+	91.038	-11.0	Infusion experiment
		D18/CH3OH	94.0578	C3H4D3O3+	94.0568	-10.6	Infusion experiment
		U/CD3OD	95.0641	C3H3D4O3+	95.0631	-10.5	Infusion experiment
		U/PrOH	119.0703	C5H11O3+	119.0715	10.1	Weak signal, Observed in chromatogram
		D18/PrOH	122.0891	C5H8D3O3+	122.0903	9.8	Weak signal, Observed in chromatogram
		U/CH3^{18}OH	93.0432	C3H7O2^{18}O+	93.0443	11.8	Infusion experiment
		D18/CH3^{18}OH	96.0620	C3H4D3O2^{18}O+	96.0632	12.5	Infusion experiment
	**3**	U/CH3OH	89.0597	C4H9O2+	89.0588	-10.1	Infusion experiment
		D18/CH3OH	92.0785	C4H6D3O2+	92.0776	-9.8	Infusion experiment
		U/CD3OD	95.0974	C4H3D6O2+	95.0964	-10.5	Infusion experiment
		U/PrOH	145.1223	C8H17O2+	145.1226	2.1	Observed in chromatogram
		D18/PrOH	148.1411	C8H14D3O2+	148.1415	2.7	Observed in chromatogram
		U/CH3^{18}OH	93.0682	C4H9^{18}O2+	93.0693	11.8	Infusion experiment
		D18/CH3^{18}OH	96.0870	C4H6D3^{18}O2+	96.0881	11.4	Infusion experiment
	**4**	U/CH3OH	91.0390	C3H7O3+	91.0380	-11.0	Infusion experiment
		D18/CH3OH	97.0766	C3HD6O3+	97.0757	-9.3	Infusion experiment
		U/CD3OD	92.0452	C3H6DO3+	92.0443	-9.8	Infusion experiment
		U/PrOH	na	na	na	na	No alcohol incorporated
		D18/PrOH	na	na	na	na	No alcohol incorporated
	**5**	U/CH3OH	75.0441	C3H7O2+	75.0431	-13.3	Infusion experiment
		D18/CH3OH	81.0817	C3HD6O2+	81.0808	-11.1	Infusion experiment
		U/CD3OD	76.0503	C3H6DO2+	76.0494	-11.8	Infusion experiment
		U/PrOH	na	na	na	na	No alcohol incorporated
		D18/PrOH	na	na	na	na	No alcohol incorporated
	**6**	U/CH3OH	74.0362	C3H6O2•+	74.0353	-12.2	Infusion experiment
		D18/CH3OH	80.0739	C3D6O2•+	80.0730	-11.2	Infusion experiment
		U/CD3OD	74.0362	C3H6O2•+	74.0353	-12.2	Infusion experiment
		U/PrOH	na	na	na	na	No alcohol incorporated
		D18/PrOH	na	na	na	na	No alcohol incorporated

MEKP only (Deuterated material not available)

Proposed Structure	Product	Material/solvent	Exact Mass	Molecular formula	Observed Mass	ΔPPM	Comments
	**7**	U/CH3OH	103.0754	C5H11O2+	103.0765	10.7	Not present when using PrOH
		U/PrOH	131.1067	C7H15O2+	131.1078	8.4	Not present when using MeOH
		U/CH3^{18}OH	105.0796	C5H11O^{18}O+	105.0807	10.5	Infusion experiment
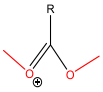	**8**	U/CH3OH, R=Me	89.0597	C4H9O2+	89.0609	13.5	Also from MEKP fragment similar to Product E
		U/CH3OH, R=Et	103.0754	C5H11O2+	103.0765	10.7	May also be from Product G
		U/PrOH, R=Me	145.1223	C8H17O2+	145.1226	2.1	Observed in chromatogram
		U/PrOH, R=Et	159.13796	C9H19O2+	na	na	Contaminant present in solvent
		U/CH3^{18}OH, R=Me	93.0682	C4H9^{18}O2+	93.0693	11.8	Infusion experiment
		U/CH3^{18}OH, R=Et	107.0839	C5H11^{18}O2+	107.0849	9.3	Infusion experiment
	**9**	U/CH3OH	88.0519	C4H8O2•+	88.0531	13.6	Cyclic Trimer only

U/CH3OH = Unlabled material/Methanol solvent
D18/CH3OH = D18-Material/Methanol solvent
U/CD3OD = Unlabled material/D-labled solvent
U/PrOH = Unlabled material/Propyl alcohol solvent
D18/PrOH = D18-Material/Propyl alcohol solvent
U/CH3^{18}OH = Unlabled material/^{18}O-labled Methanol
D18/CH3^{18}OH = D18-Material/^{18}O-labled Methanol
Red structural components suggest incorporation of solvent alcohol

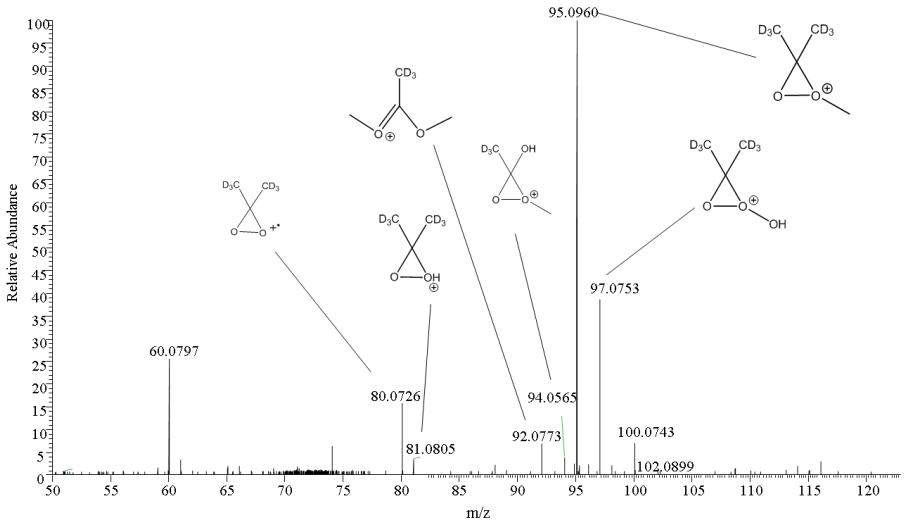

Figure 2-5. *MP infusion of d18-TATP in CH3OH showing low mass range and proposed assignments.*

To test the conditions which contribute to fragment formation, 20 µg/mL of the d_{18}-TATP (90% MeOH/10% 10 mM NH_4OAc) was infused post column at 20 µL/min into 230 µL/min of LC flow (90% MeOH/10% 10 mM NH_4OAc— high concentration to ensure observation). The m/z values of 258, 97, 95 and 92, correspond to the parent d_{18}-TATP and products **4**, **1** and **3**, (***Table 2-2***), respectively. At a vaporizer temperature of 250 ºC, the signal for all ions seemed to be optimized, with **3** being the most intense ion followed closely by **1**. As gas flow from the auxiliary/sheath gas was increased, **1** began to dominate over **3** with little change in either parent or **4** (which was only marginally detected). However, when the LC flow was removed and the same d_{18}-TATP solution was directly infused at 20 uL/min into the high gas flow at 250 ºC, product **4** became the most intense ion with nearly the same intensity as the parent. As gas flow was pushed even higher, parent and product **4** were nearly all that

could be seen, with no **3** present at all. As gas flow was dropped to minimal values (sheath 8 AU and aux 5 AU), product **1** dominated the spectrum, and **3** became slightly more intense than **4**, which had dropped significantly. This suggests that at higher gas flows, ions are pushed into the MS more rapidly with either less time in the corona region or less time exposed to the vaporizer temperature to react with the solvent to form alcohol-incorporated products. Additionally, when infused into the mobile phase (vs. direct infusion) which contains a significantly higher population of MeOH ions/molecules, far more of the alcohol incorporated products are observed (**Figure 2-6**).

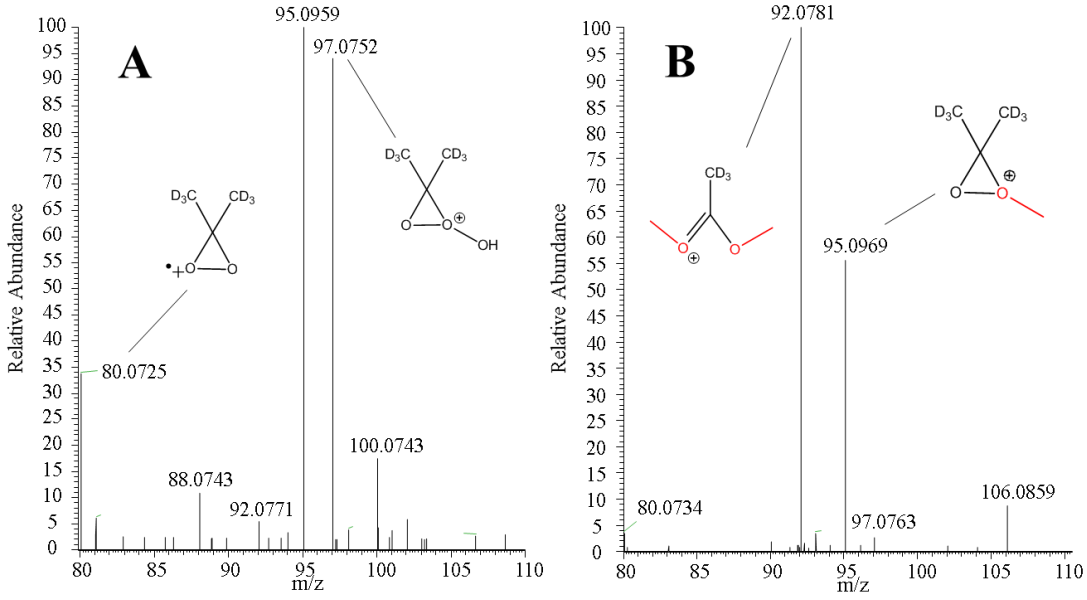

Figure 2-6. *APCI source data from A) direct infusion of 20 µL/min d18-TATP vs. B) 20 µL/min d18-TATP infused into a mobile phase containing 90% MeOH/10 % 10 mM NH4OAc at 230 L/min.*

To assure that the incorporation of the alcohol is completed, a study with the infusion of TATP, d_{18}-TATP and MEKP in $Me^{18}OH$ was performed. Complete incorporation of both the carbon and the oxygen from MeOH into each of the proposed products was observed (Appendix2: Figure S2-2). For this analysis, source conditions that favored the formation of the alcohol incorporated products were used. Due to the cost of the ^{18}O solvents, we were unable to attempt this at mobile phase levels; therefore, doubly incorporated products at m/z 93.0693and 96.0881 were not as significant as shown in **Figure 2-6**(B). **Scheme 2-1** shows the proposed mechanism for the formation of Product **1**, ***Table 2-2***. Note that an interfering component at m/z 117.0920 was present in either PrOH or IPA that obscured detection of the PrOH-TATP product.

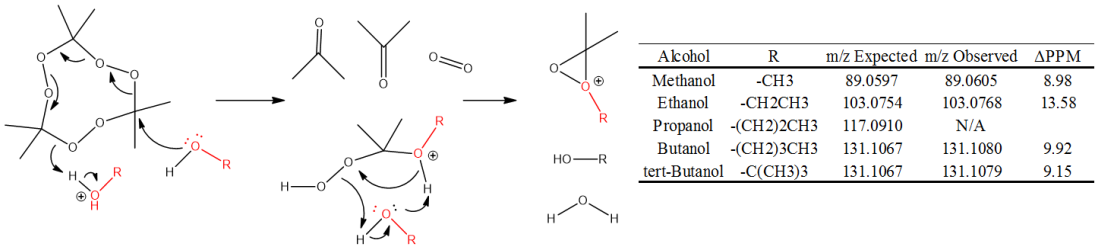

Alcohol	R	m/z Expected	m/z Observed	ΔPPM
Methanol	-CH3	89.0597	89.0605	8.98
Ethanol	-CH2CH3	103.0754	103.0768	13.58
Propanol	-(CH2)2CH3	117.0910	N/A	
Butanol	-(CH2)3CH3	131.1067	131.1080	9.92
tert-Butanol	-C(CH3)3	131.1067	131.1079	9.15

Scheme 2-1

Scheme 2-2 shows the proposed mechanism for the addition of the second alcohol from the product of **Scheme 2-1**. With the abundance of this fragment (depending on conditions used) it may transform by a more concerted mechanism than proposed. It should be noted that as the alcohol chain length increased, the addition of two alcohols seemed to became more significant that the addition of one alcohol. Also, formation of the tert-BuOH product for either 1 or 2 additions of alcohol was nearly non-

existent. This supports the proposed mechanisms since steric interactions would prevent this reaction.

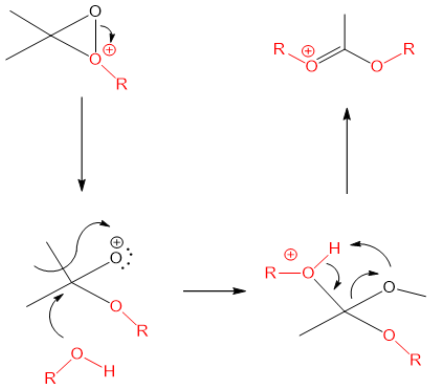

Alcohol	R	m/z Expected	m/z Observed	ΔPPM
Methanol	-CH3	89.0597	89.0605	8.98
Ethanol	-CH2CH3	117.091	117.0924	11.96
Propanol	-(CH2)2CH3	145.1223	145.1228	3.45
Butanol	-(CH2)3CH3	173.1536	173.1541	2.89
tert-Butanol	-C(CH3)3	173.1536	173.1542	3.47

Scheme 2-2

Cyclic peroxides appear to have several analytical nuances that separate them from their linear counterparts. The structure of TATP has, of course, been confirmed by X-ray diffraction and other spectroscopic techniques with subsequent DFT calculations to corroborate this data.[39],[40],[5] However, there has been no definitive identification of the cyclic MEKP species. MEKP product **9** (m/z 88.0519) in ***Table 2-2*** was only produced by the presumed cyclic MEKP C3 trimer. Because TATP also forms this analog (product **6**, ***Table 2-2***) this suggests that the species we are calling MEKP C3 is indeed the cyclic trimer. No other observed MEKP species (all presumably linear) formed product **9**, suggesting that the cis configuration of the cyclic species is required to form this product. The mechanism is proposed in Scheme 3. It is also notable that while the linear MEKP ionized quite well by electrospray ionization (ESI), the cyclic peroxides (TATP, MEKP C3 and HMTD) prefer APCI. Attempts to isolate MEKP on the CombiFlash system using a C18 column gave

inconclusive results for collection of the cyclic trimer using the ESI source for MS collection triggering. When the APCI source was applied, a strong signal at nominal mass m/z 282 dominated the spectrum. This suggests that the structure of this compound is fundamentally different from other components in the MEKP mixture and is most likely cyclic in nature.

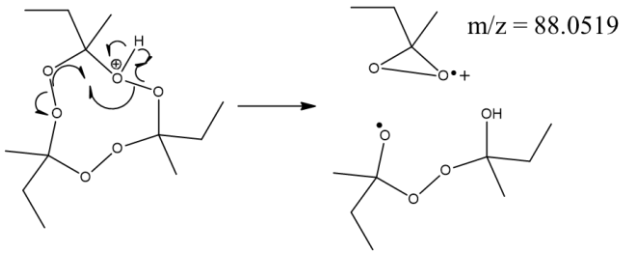

Scheme 2-3

Attempts to Enhance Signal Intensity

Although the sodium adduct of TATP has been used by Desorption ESI (DESI)[26], Extractive ESI (EESI)[24] and LC-ESI[23] to produce abundant ions at m/z 245.0996, our attempts at adding controlled amounts of very low concentrations of sodium to the mobile phase for quantitative analysis ended with plugged electrospray capillaries. However, even using sodium we have been unable to approach the level of quantification provided by APCI for TATP (currently, 1 ng on column for m/z 240.1442 and 200 pg on column for m/z 89.0597). TATP (and all the peroxides associated with MEKP) have historically been observed only as ammonium or sodium adducts in our lab. While in ESI, the TATP sodium adduct is rather intense, the addition of lithium and potassium did not produce a significant signal compared to

either sodium or ammonium, suggesting the size of these ions is optimal for gas phase adduction.

As mentioned above, variation in gas flow affected the intensity and abundance of each ion associated with TATP. To optimized APCI conditions for either the TATP $[M+NH_4]^+$ or the m/z 89 signal, injections (N=3) were made on the C18 column at various conditions of temperature, gas flow and mobile phase modifier (the LC flow was kept at 250 μL/min). At a vaporizer temperature of 250 °C, gas flows ranged from (sheath/aux 1:1) 30 to 70 AU with the most intense $[M+NH_4]^+$ at 70 AU and for m/z 89, 30 AU (nearly 1:1 signal for the d_{18}-TATP m/z 95:92 fragments). Temperature was then varied from 210 °C to 450 °C with the gas flow set to 30 AU. At 210 °C, TATP $[M+NH_4]^+$ was the most intense signal with the m/z 89 peak optimized at 300 °C (nearly 2.5:1 signal for the d_{18}-TATP m/z 95:92 fragments). Temperatures higher than this began to dramatically reduce the total signal. Removal of the ammonium source (mobile phase of water/MeOH) came with the expected reduction of the $[M+NH_4]^+$ signal (less than 1% of the total TATP signal). Surprisingly, the signal for the m/z 89 peak increased nearly 40% over the optimized conditions using 10 mM NH_4OAc (m/z 95 was 70 % of the total signal and m/z 92 was 30% for the d_{18}-TATP sample). Based on this work, we have developed two methods for preferential detection of m/z 89 or m/z 240 for TATP. For the analysis of intact TATP or related compounds, we use the method optimized for $[M+NH_4]^+$ where the mobile phase has 10 mM NH_4OAc and MS conditions favoring m/z 240 production. For low level quantification, we use the method favoring the m/z 89 fragment with the aqueous mobile phase containing only 200 μM NH_4OAc (a concentration that is comparable to

no ammonium addition). Since the mobile phase flow rate would likely alter these conditions, and minor changes seem to correspond to significant ionization variability, each LC/MS instrument being used for the detection of peroxide explosives should be optimized for gas flow and temperature in addition to the instrument automatic signal optimization procedure.

In our lab, DADP has not been observed as the adduct of hydrogen (m/z 149.0808), ammonium (m/z 166.1074), sodium (m/z 171.0628) nor lithium (m/z 155.0890) at reasonable levels (<500 µM) for LC/MS analysis in ESI or APCI. At the level of 100 µg/mL (675 µM), m/z 166.1074 did begin to appear above the background noise. It is important to know that low concentrations of DADP can be observed as the alcohol incorporated fragment at m/z 89.0597 using APCI. On the LC system describe above for TATP analysis, DADP elutes about 40 seconds earlier than TATP. Using the d_{18}-TATP as an IS, a dynamic range for DADP analysis was established between 20000 and 100 ng/mL with a LOD of 50 ng/mL. Inadequate separation of TATP from other peroxides could provide significantly skewed results.

Conclusions

Two cautionary notes come from this research. First, while researchers have long been aware that TATP has a rather high vapor pressure for a solid, the fact that it readily volatilizes from solution has not been fully appreciated. Second, while low-levels of TATP may be quantified by LC/MS using the molecular fragment m/z 89, it must be recognized that this fragment has conditions. It represents two different species which are both dependent on the MeOH concentration, mobile phase

modifiers, temperature, gas flow, and flow rate (among the parameters tested). Since the two most common LC/MS solvents for reverse phase chromatography are methanol and acetonitrile, the analyst is faced with a dilemma. If acetonitrile is used as the mobile phase, ionization is suppressed below reasonable levels of analytical detection.[35] If methanol is used, the compound will invariable react with the species in the gas phase. The gas-phase alcohol attack of peroxides (TATP, DADP, MEKP, and HMTD) at the α-carbon is apparently a general phenomenon.[14],[38] This phenomenon can be exploited to lower the limits of detection for these compounds. However, understanding the origins of a particular fragment is very important, and all variables must be considered prior to using these ions for quantification. Proper separation must be achieved to prevent unwanted materials (many small compounds may have a mass associated with $C_4H_9O_2^+$) from providing a false positive response. Also, analytical conditions may significantly affect this particular signal response, making it more susceptible to interference from unknown, coeluting ion suppressors or enhancers. Lastly, other factors outside the scope of this research may influence the formation of peroxide products.[41]

Appendix 2

Supplemental Info_TATP_with_ROH.pdf

Acknowledgements:

This material is based upon work supported by U.S. Department of Homeland Security (DHS), Science & Technology Directorate, Office of University Programs,

under Grant 2013-ST-061-ED0001. Views and conclusions are those of the authors and should not be interpreted as necessarily representing the official policies, either expressed or implied, of DHS.

References

1. Wolffenstein, R.: Ueber die Einwirkung von Wasserstoffsuperoxyd auf Aceton und Mesityloxyd. Chem. Ber. 28, 2265–2269 (1895).
2. Legler, L.: Ueber die sogenannte Aether- oder Lampenaiiare. Chem. Ber. 14, 602–604 (1881).
3. Milas, N.A., Golubovic, A.: Studies in Organic Peroxides. XXV. Preparation, Separation and Identification of Peroxides Derived from Methyl Ethyl Ketone and Hydrogen Peroxide. J. Am. Chem. Soc. 81, 5824–5826 (1959).
4. Oxley, J., Smith, J., Brady, J., Dubnikova, F., Kosloff, R., Zeiri, L., Zeiri, Y.: Raman and infrared fingerprint spectroscopy of peroxide-based explosives. Appl. Spectrosc. 62, 906–15 (2008).
5. Jensen, L., Mortensen, P.M., Trane, R., Harris, P., Berg, R.W.: Reaction kinetics of acetone peroxide formation and structure investigations using Raman spectroscopy and X-ray diffraction. Appl. Spectrosc. 63, 92–97 (2009).
6. Kozole, J., Tomlinson-Phillips, J., Stairs, J.R., Harper, J.D., Lukow, S.R., Lareau, R.T., Boudries, H., Lai, H., Brauer, C.S.: Characterizing the gas phase ion chemistry of an ion trap mobility spectrometry based explosive trace detector using a tandem mass spectrometer. Talanta. 99, 799–810 (2012).
7. Tomlinson-Phillips, J., Wooten, A., Kozole, J., Deline, J., Beresford, P., Stairs,

J.: Characterization of TATP gas phase product ion chemistry via isotope labeling experiments using ion mobility spectrometry interfaced with a triple quadrupole mass spectrometer. Talanta. 127, 152–162 (2014).

8. Jiang, D., Peng, L., Wen, M., Zhou, Q., Chen, C., Wang, X., Chen, W., Li, H.: Dopant-Assisted Positive Photoionization Ion Mobility Spectrometry Coupled with Time-Resolved Thermal Desorption for On-Site Detection of Triacetone Triperoxide and Hexamethylene Trioxide Diamine in Complex Matrices. Anal. Chem. 88, 4391–4399 (2016).
9. Bauer, C., Willer, U., Lewicki, R., Pohlkötter, A., Kosterev, A., Kosynkin, D., Tittel, F.K., Schade, W.: A mid-infrared QEPAS sensor device for TATP detection. J. Phys. Conf. Ser. 157, 1–6 (2009).
10. Hildenbrand, J., Herbst, J., Wöllenstein, J., Lambrecht, A.: Explosive detection using infrared laser spectroscopy. Proc. SPIE - Int. Soc. Opt. Eng. 7222, 72220B1-72220B-12 (2009).
11. Armitt, D., Zimmermann, P., Ellis-Steinborner, S.: Gas chromatography/mass spectrometry analysis of triacetone triperoxide (TATP) degradation products. Rapid Commun. Mass Spectrom. 22, 950958 (2008).
12. Romolo, F.S., Cassioli, L., Grossi, S., Cinelli, G., Russo, M.V.: Surface-sampling and analysis of TATP by swabbing and gas chromatography/mass spectrometry. Forensic Sci. Int. 224, 96–100 (2013).
13. Oxley, J.C., Smith, J.L., Bowden, P.R., Rettinger, R.C.: Factors influencing triacetone triperoxide (TATP) and diacetone diperoxide (DADP) formation: Part 1. Propellants, Explos. Pyrotech. 38, 244–254 (2013).

14. Rondeau, D., Vogel, R., Tabet, J.-C.: Unusual atmospheric pressure chemical ionization conditions for detection of organic peroxides. Sect. Title Org. Anal. Chem. 38, 931–940 (2003).
15. Oxley, J., Zhang, J., Smith, J., Cioffi, E.: Mass Spectra of Unlabeled and Isotopically Labeled Hexamethylene Triperoxide Diamine (HMTD). Propellants, Explos. Pyrotech. 25, 284–287 (2000).
16. Oxley, J., Smith, J., Shinde, K., Moran, J.: Determination of the Vapor Density of Triacetone Triperoxide (TATP) Using a Gas Chromatography Headspace Technique. Propellants, Explos. Pyrotech. 30, 127–130 (2005).
17. Evans, H.K., Tulleners, F. a J., Sanchez, B.L., Rasmussen, C. a: An unusual explosive, triacetonetriperoxide (TATP). J. Forensic Sci. 31, 1119–1125 (1986).
18. Sigman, M.E., Clark, C.D., Fidler, R., Geiger, C.L., Clausen, C.A.: Analysis of triacetone triperoxide by gas chromatography/mass spectrometry and gas chromatography/tandem mass spectrometry by electron and chemical ionization. Rapid Commun. mass Spectrom. 20, 2851–2857 (2006).
19. Burks, R.M., Hage, D.S.: Current trends in the detection of peroxide-based explosives. Anal. Bioanal. Chem. 395, 301–13 (2009).
20. Peña-Quevedo, A.J., Hernández-Rivera, S.P.: Mass Spectrometry Analysis of Hexamethylene Triperoxide Diamine by its Decomposition Products. Proc. SPIE - Int. Soc. Opt. Eng. 7303, 730303-1-730303–11 (2009).
21. Widmer, L., Watson, S., Schlatter, K., Crowson, A.: Development of an LC/MS method for the trace analysis of triacetone triperoxide (TATP). Analyst. 127, 1627–32 (2002).

22. Cotte-Rodríguez, I., Chen, H., Cooks, R.G.: Rapid trace detection of triacetone triperoxide (TATP) by complexation reactions during desorption electrospray ionization. Chem. Commun. 953–955 (2006).

23. Sigman, M.E., Clark, C.D., Caiano, T., Mullen, R.: Analysis of triacetone triperoxide (TATP) and TATP synthetic intermediates by electrospray ionization mass spectrometry. Rapid Commun. mass Spectrom. 22, 84–90 (2008).

24. Hill, A.R., Edgar, M., Chatzigeorgiou, M., Reynolds, J.C., Kelly, P.F., Creaser, C.S.: Analysis of triacetone triperoxide complexes with alkali metal ions by electrospray and extractive electrospray ionisation combined with ion mobility spectrometry and mass spectrometry. Eur. J. Mass Spectrom. 21, 265–274 (2015).

25. Hagenhoff, S., Franzke, J., Hayen, H.: Determination of Peroxide Explosive TATP and Related Compounds by Dielectric Barrier Discharge Ionization-Mass Spectrometry (DBDI-MS). Anal. Chem. 89, 4210–4215 (2017).

26. Cotte-Rodríguez, I., Hernández-Soto, H., Chen, H., Cooks, R.G.: In situ trace detection of peroxide explosives by desorption electrospray ionization and desorption atmospheric pressure chemical ionization. Anal. Chem. 80, 1512–1519 (2008).

27. Xu, X., van de Craats, A.M., Kok, E.M., de Bruyn, P.C.A.M.: Trace Analysis of Peroxide Explosives by High Performance Liquid Chromatography-Atmospheric Pressure Chemical Ionization-Tandem Mass Spectrometry (HPLC-APCI-MS/MS) for Forensic Applications. J. Forensic Sci. 49, 1–7

(2004).

28. Xu, X., Koeberg, M., Kuijpers, C.-J., Kok, E.: Development and validation of highly selective screening and confirmatory methods for the qualitative forensic analysis of organic explosive compounds with high performance liquid chromatography coupled with (photodiode array and) LTQ ion trap/Orbitrap ma. Sci. Justice. 54, 3–21 (2014).

29. Rapp-Wright, H., McEneff, G., Murphy, B., Gamble, S., Morgan, R., Beardah, M., Barron, L.: Suspect screening and quantification of trace organic explosives in wastewater using solid phase extraction and liquid chromatography-high resolution accurate mass spectrometry. J. Hazard. Mater. 329, 11–21 (2017).

30. DeTata, D., Collins, P., McKinley, A.: A fast liquid chromatography quadrupole time-of-flight mass spectrometry (LC-QToF-MS) method for the identification of organic explosives and propellants. Forensic Sci. Int. 233, 63–74 (2013).

31. Krawczyk, T.: Enhanced electrospray ionization mass spectrometric detection of hexamethylene triperoxide diamine (HMTD) after oxidation to tetramethylene diperoxide diamine dialdehyde (TMDDD). Rapid Commun. Mass Spectrom. 29, 2257–2262 (2015).

32. Marsh, C.M., Mothershead, R.F., Miller, M.L.: Post-Blast Analysis of Hexamethylene Triperoxide Diamine using Liquid Chromatography-Atmospheric Pressure Chemical Ionization-Mass Spectrometry. Sci. Justice. 55, 299–306 (2015).

33. Newsome, G.A., Ackerman, L.K., Johnson, K.J.: Humidity Affects Relative Ion

Abundance in Direct Analysis in Real Time Mass Spectrometry of Hexamethylene Triperoxide Diamine. Anal. Chem. 86, 11977–11983 (2014).

34. Crowson, A., Beardah, M.S.: Development of an LC/MS method for the trace analysis of HMTD. Analyst. 126, 1689–1693 (2001).

35. Colizza, K., Mahoney, K.E., Yevdokimov, A.V., Smith, J.L., Oxley, J.C.: Acetonitrile Ion Suppression in Atmospheric Pressure Ionization Mass Spectrometry. J. Am. Soc. Mass Spectrom. 27, 1796–1804 (2016).

36. Wierzbicki, A., Salter, E.A., Cioffi, E. a., Stevens, E.D.: Density Functional Theory and X-ray Investigations of P- and M-Hexamethylene Triperoxide Diamine and Its Dialdehyde Derivative. J. Phys. Chem. A. 105, 8763–8768 (2001).

37. Smith, M.E., Wall, C., Fitzgerald, M.: Characterisation of the major synthetic products of the reactions between butanone and hydrogen peroxide. Propellants, Explos. Pyrotech. 37, 282–287 (2012).

38. Colizza, K., Porter, M., Smith, J.L., Oxley, J.C.: Gas-phase reactions of alcohols with hexamethylene triperoxide diamine (HMTD) under atmospheric pressure chemical ionization conditions. Rapid Commun. Mass Spectrom. 29, 74–80 (2014).

39. Groth, P.: Crystal Structure of 3,3,6,6,9,9-Hexamethyl-1,2,4,5,7,8-hexa-oxacyclononane ("Trimeric Acetone Peroxide"). ACTA Chem. Scand. 23, 1311–1329 (1969).

40. Dubnikova, F., Kosloff, R., Almog, J., Zeiri, Y., Boese, R., Itzhaky, H., Alt, A., Keinan, E.: Decomposition of triacetone triperoxide is an entropic explosion. J.

Am. Chem. Soc. 127, 1146–1159 (2005).

41. Newsome, G.A., Ackerman, L.K., Johnson, K.J.: Humidity Effects on Fragmentation in Plasma-Based Ambient Ionization Sources. J. Am. Soc. Mass Spectrom. 27, 135–143 (2016).

Chapter 3 : Gas Phase Reactions of Alcohols with Hexamethylene triperoxide diamine (HMTD) under Atmospheric Pressure Chemical Ionization Conditions

Status: Published

Rapid Communication in Mass Spectrometry, 2015; 29, 74-80

Abstract

Rationale: Hexamethylene triperoxide diamine (HMTD) is a sensitive peroxide explosive first synthesized in 1885.[1] HMTD exhibits an unusual gas phase phenomenon in the presence of alcohols that has been previously observed,[9] [11] [12] but incorrectly resolved. We are attempting to determine this specific mechanism.

Methods: In this work, we used positive ion mode atmospheric pressure chemical ionization (APCI) as the interface to the mass spectrometer. HMTD was infused with various solvents included ^{18}O and ^{2}H labeled methanol in order to determine gas phase reaction mechanisms.

Results: Based on these labeled experiments, it was determined that under APCI conditions, the alcohol oxygen attacks a methylene carbon of HMTD and releases H_2O_2. This was attempted with 9 different alcohols and in each case, the alcohol is fully incorporated into the molecule with the peroxide release. A mechanism for this reaction has been proposed.

Conclusions: This work appears to have confirmed the gas phase reaction mechanism of HMTD with alcohols. As we continue efforts to characterize this unusual molecule, the information may prove useful in determining formation and degradation mechanism(s). In addition, this property of HMTD my find use in other fields of science.

Key Words: HMTD (hexamethylene triperoxide diamine), APCI (atmospheric pressure chemical ionization), ESI (electrospray ionization), Alcohol reactivity, Gas phase mechanism

Introduction

Hexamethylene triperoxide diamine (HMTD) is a sensitive peroxide explosive that is relatively easy to synthesize from hexamethylenetetramine (hexamine), hydrogen peroxide and catalytic levels of citric acid. Although it has never found use as a military explosives due to poor thermal stability and high sensitivity to impact, friction and electrostatic charge, it has become more commonly used by terrorist.[2] [3] [4] [5] Our efforts to successfully prevent the use or production of HMTD by terrorists require fundamental understanding of mechanistic principles associated with its formation and decomposition.

First synthesized in 1885 by Legler,[1] the structure was not proposed until 1967 by Urbanski[6] and not confirmed until 1985 by Schaefer et al.[7] using X-ray crystallography. Its structure is unusual in that there is a planar 3-fold coordination about the two bridgehead nitrogen atoms rather than a pyramidal structure.[7] Ring strain in HMTD may account for the stability and sensitivity issues mentioned above. Despite a plethora of information on HMTD, a mechanism for formation of this compound has only recently been tentatively proposed.[8]

Development of an analytical method for HMTD was investigated to identify potential, non-volatile decomposition products by liquid chromatography interfaced with a mass spectrometer (LC/MS). Typical optimization for the LC/MS conditions of a new compound is initiated by directly infusing a solution (usually 50/50, v/v, acetonitrile/water at 1 to 10 μg/mL) of purified standard into an electrospray ionization (ESI) or atmospheric pressure chemical ionization (APCI) source. Further signal enhancement may be source or solution specific and is usually investigated in an iterative manner to alter detection limits depending on the analysis requirements.

During solution optimization it is important to take future chromatography conditions into consideration. Though previous separation work reported for HMTD used methanol and water,[9] we preferred to perform initial testing using the aprotic organic solvent, acetonitrile. When HMTD was later infused into the mass spectrometer in a methanol/water solution, the spectrum suggested a gas-phase chemical reaction occurred between a methylene carbon of HMTD and the alcohol. The purpose of this work is to help describe the behavior of HMTD in the gas phase. This information may aid present efforts to elucidate formation and destruction mechanisms of this molecule. Additionally, the ability of HMTD to react with alcohols under chemical ionization conditions may prove useful to other fields of research.

Materials and methods

Chemicals and Reagents

Water, acetonitrile and methanol were all Optima HPLC grade solvents from Fisher Chemical (Fair Lawn, NJ, USA). Isopropanol, isobutanol, 1-butanol, cyclohexanol and anhydrous citric acid were ACS grade, also from Fisher Chemical. Hexamine, xylitol, 1-octanol and *tert*-butyl alcohol were purchased from Acros Organics (Morris Plains, NJ, USA). 2-butanol was purchased from Aldrich Chemical (Milwaukee, WI, USA). D-(+)-glucose was obtained from Sigma-Aldrich (St. Louis, MO, USA). Hydrogen peroxide (50 %) was purchased from Univar (Redmond, WA, USA). Ethanol (200 proof) was ACS grade obtained from Ultrapure (Darien, CT, USA). HMTD was produced in house by standard methods reported in previous work.[10]

Methanol labelled with ^{18}O, d_4-methanol and d_2-water were purchased from Cambridge Isotope Labs (Cambridge, MA, USA).

Instrumentation and Methods

Using a Thermo Electron (Franklin, MA, USA) Exactive Orbitrap mass spectrometer affixed with an APCI interface, positive ions were produced and introduced into the instrument.. Tune conditions for infusion experiments (10-20 μL/min flow) were as follows: spray voltage, 5000 V; capillary temperature, 140 °C; sheath gas (N_2), 25; auxiliary gas (N_2), 3; heater temperature 160 ºC; capillary voltage, 40 V; tube lens, 160 V; and skimmer, 15 V. Units for sheath and auxiliary gas flow are arbitrary. Mass spectrometer source conditions for chromatographic analysis were optimized by increasing the sheath gas to 30 and auxiliary gas to 15 to provide better desolvation at higher liquid flow rates (200-250 μL/min flow). Liquid chromatography was performed using a Thermo Electron Accela quaternary pump. Sample injections were performed by a CTC Analytics (Zwingen, Switzerland) HTS PAL autosampler. Initial reverse phase chromatography used a Thermo Scientific (Franklin, MA, USA) Hypersil C-18 (2.1 x 100 mm, 5 μm) column with binary delivery of a gradient mobile phase. Ultimately, the HPLC system developed for optimum analysis of HMTD and hexamine employed an Analytical Sales and Service (Pompton Plains, NJ, USA) Advantage PFP column (100 x 2.1 mm, 5 μm). In order to gain some retention of hexamine, neutral pH conditions were preferable, but this caused broadening of the HMTD peak shape. To remedy this problem, 3 different mobile phase solvents were used to provide both pH and solvent strength gradients. Initially, 95% solvent A (10 mM ammonium acetate, pH 6.8) and 5% solvent C (acetonitrile) were held for 3

minutes following injection to retain hexamine. The system was then rapidly ramped to 85% solvent B (0.1% acetic acid), 5% solvent A and 10 % solvent C over the next 3 minutes. Organic levels increased slowly for 9 minutes to 35% C, 60% B and 5% A, then rapidly for 3 minutes to 90% C and 5% of both A and B. This was held for 2 minutes before returning to initial conditions and re-equilibrated for 5 minutes prior to the next injection. Data collection and analysis was performed with Thermo Xcalibur software version 2.2, SP 1.48.

Results and Discussion

Infusion of HMTD in 50/50 (v/v) acetonitrile/water into the APCI source operated in positive ion mode produced abundant protonated molecules $[M+H]^+$ at *m/z* 209 (± 5 ppm from theoretical *m/z* 209.0768). Fragment ions of *m/z* 191, 179, 145 and 117 were produced in the source and are depicted in **Figure 3-1** (structures are also consistent with later H/D exchange data, not shown). Initially, acetonitrile was used as the organic phase while the aqueous phase contained pH modifiers of either 0.1% acetic acid (pH ~ 3.2) or 10 mM ammonium acetate (pH ~ 6.8). Due to the lack of retention or reasonable peak shape, even under highly aqueous conditions, it was decided to switch to methanol (MeOH) as the organic phase. This was consistent with literature methods described by Crowson[9] who also used APCI positive ion mode conditions, but with an isocratic method using 5% MeOH. Although retention was improved by this alteration, peak shape was inconsistent and unacceptably broad. Additionally, a new peak at *m/z* 207 was observed in the spectrum obtained for HMTD (also reported by Crowson).[9] To assure that this was not an impurity from MeOH,

additional infusion experiments were performed using various solutions. When 100 % MeOH was infused, presence of impurities was ruled out. Infusion of HMTD in 100% MeOH provided ion signals of both *m/z* 209 and 207 in roughly equal abundances. Using an aqueous solution with 10% MeOH showed only a small amount of *m/z* 207 (roughly 10% relative abundance, **Figure 3-2**). Initially, the assignment of *m/z* 207 was thought to result from protonated HMTD losing two hydrogen atoms (H_2 gas) in the gas phase, as previously reported.[9] [11] [12] Crowson[9], using a nominal mass, quadrupole instrument, attributed the mass at *m/z* 207 as a fragment of HMTD, but did not specifically designate the fragment structure. In 2004, Xu [11] using a ThermoFinnigan (San Jose, CA, USA) TSQ7000 triple quadrupole mass spectrometer (nominal mass instrument) reported *m/z* 207 as being the $[M-1]^+$ ion. Exact mass calculations for the loss of H_2 from the $[M+H]^+$ is *m/z* 207.0611, which was reported by Kinghorn,[12] using an accurate mass time-of-flight (TOF) instrument. Although we did observed this ion, it was at approximately 5% relative abundance. The majority of *m/z* 207 detected in our lab had an exact mass of *m/z* 207.0981, consistent with the unlikely loss of an oxygen and the gain of a methyl group. Since this phenomena occurred using MeOH and not acetonitrile, an alcohol solvent adduct of a fragment appeared to be the likely culprit. To test the theory, additional infusion experiments were performed with ethanol (EtOH) and isopropanol (IPA) compared to acetonitrile. As expected, use of different alcohols resulted in the addition of corresponding mass (EtOH→221 and IPA→235) verified by exact mass (**Figure 3-3**). Cotte-Rodrıguez,[13] used a nominal mass Thermo Electron LTQ ion trap instrument affixed with a variation of the Desorption Electrospray Ionization (DESI) source

called DAPCI, which provides APCI-like results. This direct analysis technique combined with alkali metal (sodium or potassium) doped solvents was able to detect the sodium adduct of the stable HMTD-methanol product $[M+CH_3OH+Na]^+$ at *m/z* 263.. Since the fragmentation pathway was inconsistent with a normal solvent adduct, they proposed a mechanism in which one peroxide bond of HMTD reacts with MeOH by a homolytic mechanism consistent with peroxide reactions, forming a methyl ether with the loss of water and formaldehyde.[13]

The Cotte-Rodrıguez mechanism[13] involves cleavage of the methanol oxygen and subsequent loss of that oxygen as water. If this mechanism is correct, then the oxygen from the alcohol would be lost as water rather than being incorporated into the HMTD molecule upon gas phase ionization. Therefore, we performed the experiment by infusing HMTD in [^{18}O]-methanol/[^{16}O]-water (50/50 v/v). The results (**Figure 3-4**) show the addition of 2 Da (*m/z* 209.1022) to the *m/z* 207.0976 observed with [^{16}O]-methanol, indicating the oxygen from methanol is incorporated into the HMTD. This species, with *m/z* 209.1022, was clearly resolved from the protonated parent at *m/z* 209.0774 using a moderate level of resolution (25,000) for an Orbitrap system. The minute amount of *m/z* 207.0985 observed in this experiment suggests some contamination of unlabeled MeOH and not the operation of multiple mechanisms. To further confirm alkoxy incorporation, infusion of HMTD was performed in a 1-to-1 mix of deuterated aqueous methanol (CD_3OD/D_2O). The results (**Figure 3-5**) suggest the formation of the deuterated molecular ion at *m/z* 210.0834 and the CD_3O adduct with the loss of D_2O_2 at *m/z* 210.1165, not the loss of DOH. These data confirm that the mechanism involves the loss of H_2O_2 (or D_2O_2), with all oxygen atoms originating

from the HMTD peroxide, while the oxygen and carbon from the methanol are completely incorporated into HMTD as an ether. Formation of an ether rather than a primary alcohol is postulated. If an alcohol were formed, a carbon from HMTD would need to attack the methanol carbon, and this species would be subject to a facile loss of water in the source which was not detected.

To determine whether the reaction of HMTD with methanol was occurring in solution at ambient conditions, HMTD was allowed to sit in 100% MeOH and 50/50 (v/v) MeOH/water for five days at room temperature in an amber HPLC vial at a concentration of 5 μg/mL. These samples (10 μL) were then analyzed on the optimized HPLC system. The lack of any significant signal at *m/z* 207.0976 suggests that this phenomenon occurs rapidly in the gas phase and not as a consequence of a chemical reaction in solution (**Figure 3-6**).

Since both protonated HMTD (*m/z* 209.0768) and $[HMTD+H^{+}+CH_3{}^{18}OH\text{-}H_2O_2]^{+}$ (*m/z* 209.1022) were observed in similar abundance in the [^{18}O]-methanol experiment, it suggests that an intermediate is formed that may be converted to either species. The proposed mechanism, depicted in **Figure 3-7**, is consistent with a chemical ionization mechanism where the protonated solvent molecule (MeOH or water) transfers a proton to a compound with more gas phase basicity such as HMTD.[14] [15] The mechanism shows an intermediate (undetected) where either the charged water or alcohol molecule aligns with the solvent oxygen proximal to one of the 6 carbon atoms of HMTD. Two competing mechanisms can then proceed from that point. In pathway A (Fig 7.), the lone pair of electrons from the nitrogen removes a proton from the solvent to produce the $[M+H]^{+}$ and a neutral solvent molecule. Pathway B may proceed by

the abstraction of the solvent proton by a peroxide oxygen allowing these electrons to attack the electron-poor carbon of the HMTD peroxymethyl amine, breaking the carbon-peroxide bond. This intermediate (also not detected) can rapidly lose H_2O_2 as shown in **Figure 3-7**. When water is the solvent, procession by pathway B is not favored since the product of this mechanism (*m/z* 193.0819) is only about 1% of the relative abundance. This mechanism allows six possible intermediates for reaction initiation as opposed to only three intermediates by a homolytic reaction mechanism of the peroxide.[13]

Compared to ESI, the protonated molecule of HMTD was produced in far greater abundance using APCI, but it was still detected by ESI. To determine whether the reported reactions were driven by chemical ionization, the methanol/water solution was infused under positive ESI conditions. Small amounts of *m/z* 209 were observed until the electrospray voltage was increased to 6000 V or higher. At this point, where corona discharge could be physically observed, both *m/z* 209.0786 and 207.0976 (as seen in APCI, **Figure 3-2**A) were observed at very high levels. This is consistent with a chemical ionization mechanism, but not a desirable result for ESI conditions since this can lead to destruction of the electrospray tip.

Infusion of HMTD with 100 % methanol produced positive ions of *m/z* peak 207.0976 $[M+H^+ + CH_3OH - H_2O_2]^+$ in equal or greater abundance than parent $[HMTD+H]^+$ (**Figure 3-2**). When HMTD was added (10 μg/mL) to a mixture containing equal volumes methanol, ethanol, isopropanol and individual isomers of butanol, each alcohol added to HMTD with a general trend of increasing abundance for larger alcohols (with equal signals for ethanol and isopropanol). This was true for n-butanol,

2-butanol and isobutanol, each producing a large signal at *m/z* 249.1445. Interestingly, in the case of n-butanol, the abundance of the methanol adduct dropped below the $[M\text{-}H_2+H]^+$ ion (*m/z* 207.0612). However, for the *tert*-butanol, the signal intensity of *m/z* 249.1445 was below 20% relative abundance (**Figure 3-8**, 2-butanol not shown due to large impurities in this solvent). This is consistent with the proposed mechanism since steric effects of the tertiary butyl group would prevent the alcohol from reacting with HMTD. Steric effects may also account for the similar abundance displayed between ethanol and isopropanol. Both 1-octanol and cyclohexanol were also infused with HMTD and formed corresponding products associated with each (*m/z* 305.2071 and 275.1601, respectively). Additionally, xylitol and glucose (10 μM) were both added to solutions of HMTD (10 μg/mL in acetonitrile or methanol) and infused on the same system. Neither sugar reacted with HMTD in the manner of other alcohols. This may be caused by the electron-rich HMTD peroxides repelling the many oxygen atoms of these sugar molecules to prevent proximity to the methylene groups. Alternatively, the sugars, which are generally poorly ionized under APCI in positive ion mode, may resist reacting with HMTD. Additional work on other alcohols is ongoing research.

Conclusions

Despite the considerable body of work performed on HMTD over the years, it still possesses many secrets. The work presented here shows that a gas phase chemical reaction occurs with HMTD in the presence of alcohols to produce a hemiaminal ether under APCI conditions. We are hoping that this unusual behavior may be exploited to

provide insight into the formation and degradation mechanism(s) of HMTD, neat, in solution and in gas phase. The idea that the methylene groups of HMTD may be more reactive than the peroxides is an interesting prospect when considering the behavior of this molecule. An added benefit of this study is that it provides a method for quick characterization of various alcohols in solution; a property of HMTD that may find use in other fields of science, possibly as a probe substrate. Research efforts into HMTD mechanisms are ongoing in our lab.

Acknowledgement

The authors thank the U.S. Department of Homeland Security (DHS) for funding. However, the views and conclusions contained are those of the authors and should not be interpreted as necessarily representing the official policies, either expressed or implied, of the DHS.

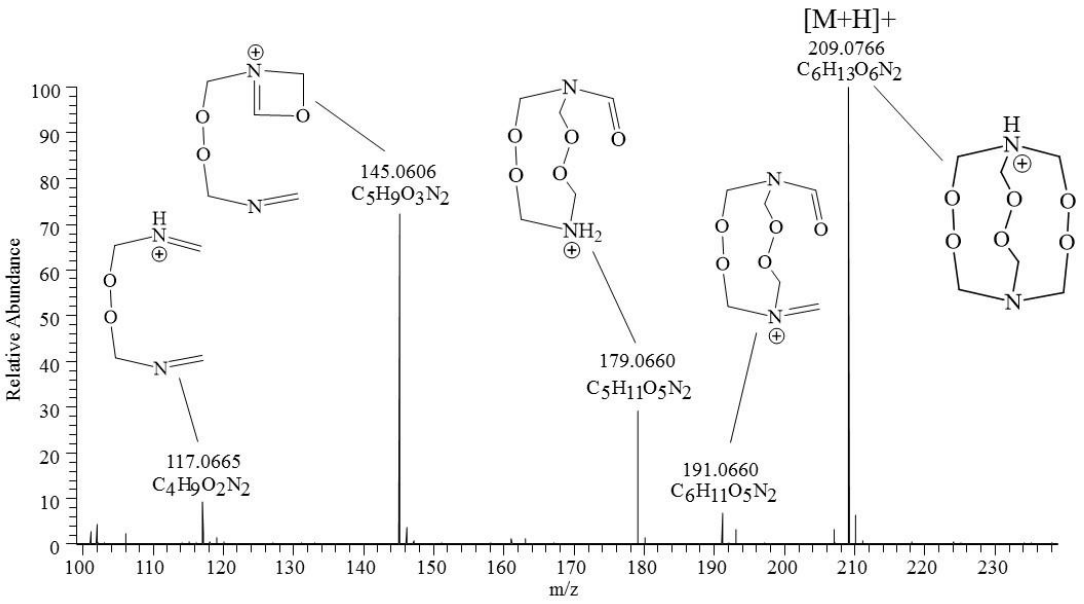

Figure 3-1. *HMTD and tentatively identified fragments produced in the source using APCI+ with acetonitrile/water with 0.1% acetic acid mobile phase..*

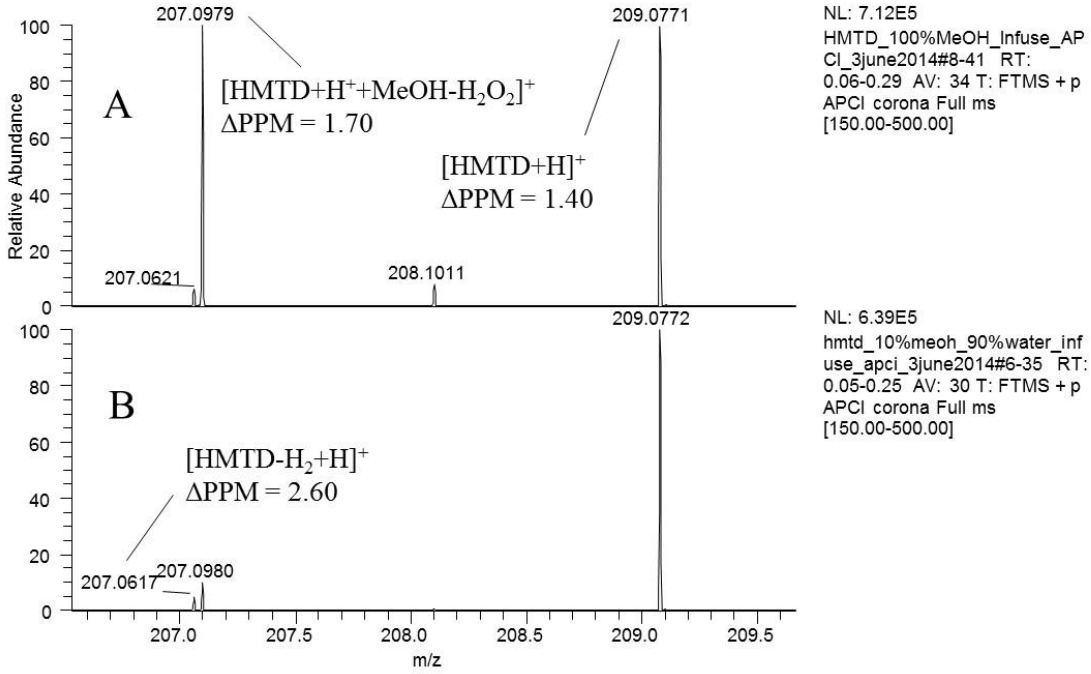

Figure 3-2. *Infusion of HMTD standard solutions (5 µg/mL) in (A) 100 % methanol and (B) 10 % methanol/90 % water. Note that with the 10 % methanol solution, the peak associated with* $[HMTD\text{-}H_2+H]^+$ *is ~50 % of the* $[HMTD+H^+ +MeOH\text{-}H_2O_2]^+$ *peak, but only 5% relative abundance in both spectra.*

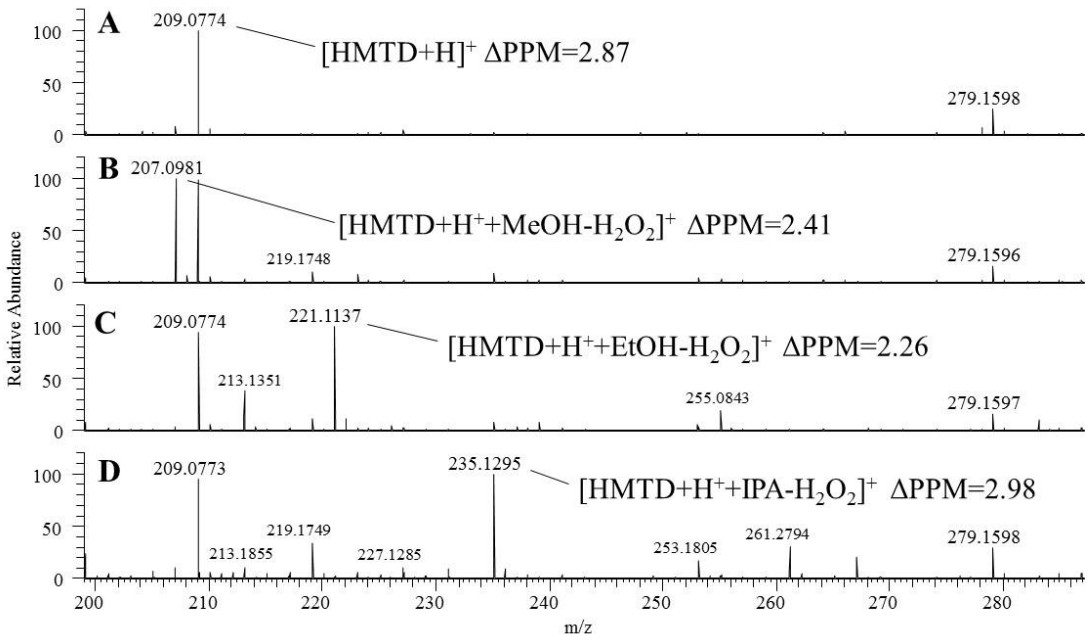

Figure 3-3. *Infusion of HMTD standard solutions (5 µg/mL, 50/50 v/v) in (A) acteonitrile/water, (B) methanol/water, (C) ethanol/water and (D) isopropanol/water.*

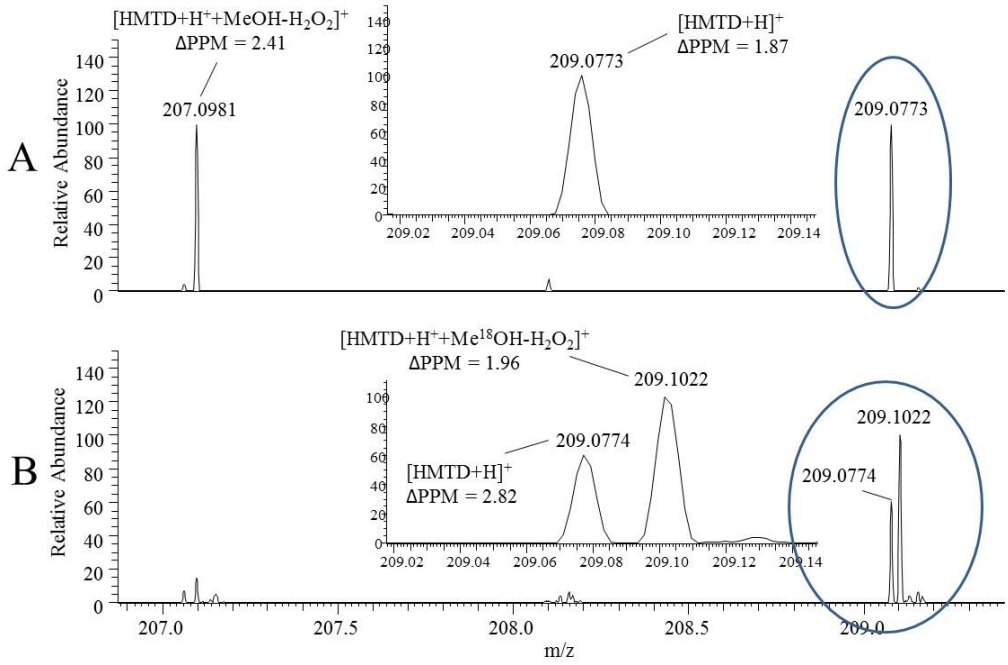

Figure 3-4. *Infusion of HMTD standard solutions (5 µg/mL, 50/50 v/v) in (A) methanol/water and (B) [^{18}O]-methanol/water. Circled areas are expanded insets within each spectrum.*

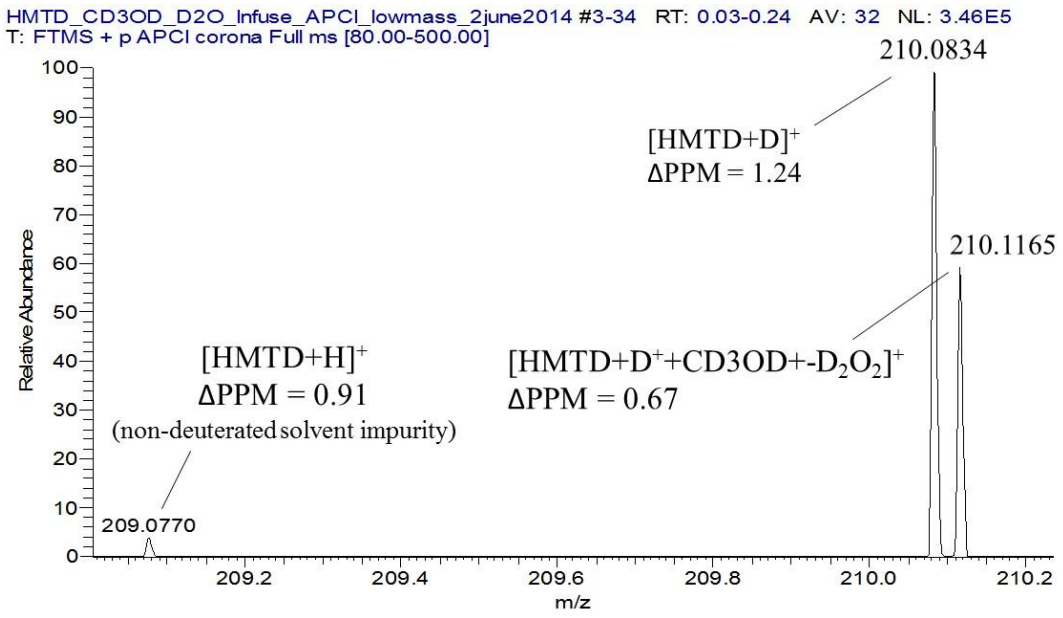

Figure 3-5. *Infusion of HMTD standard (5 µg/mL, 50/50 v/v) in d4-methanol/D2O.*

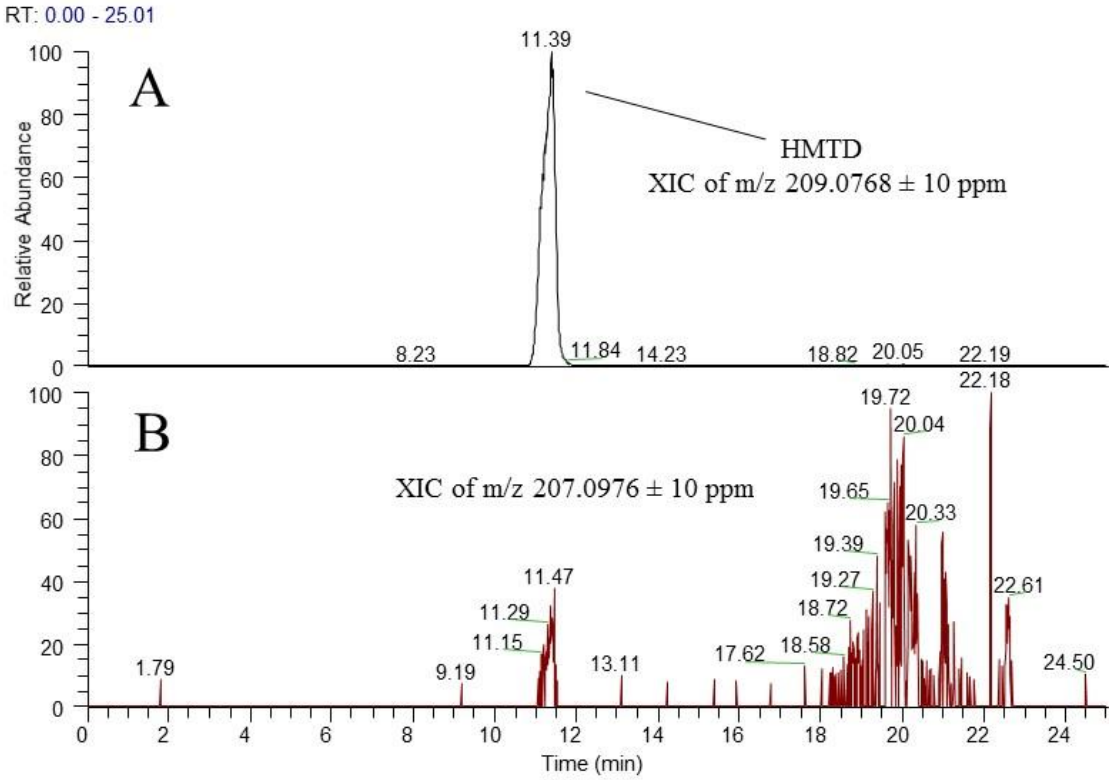

Figure 3-6. *HPLC analysis of HMTD stored in methanol/water (50/50 v/v) at ambient conditions for 5 days. Trace A is the extracted ion chromatogram (XIC) for HMTD (~3x10^6 height counts) and B is the XIC for the methanol adduct (m/z 207.0976, ~4x10^3 height counts)*

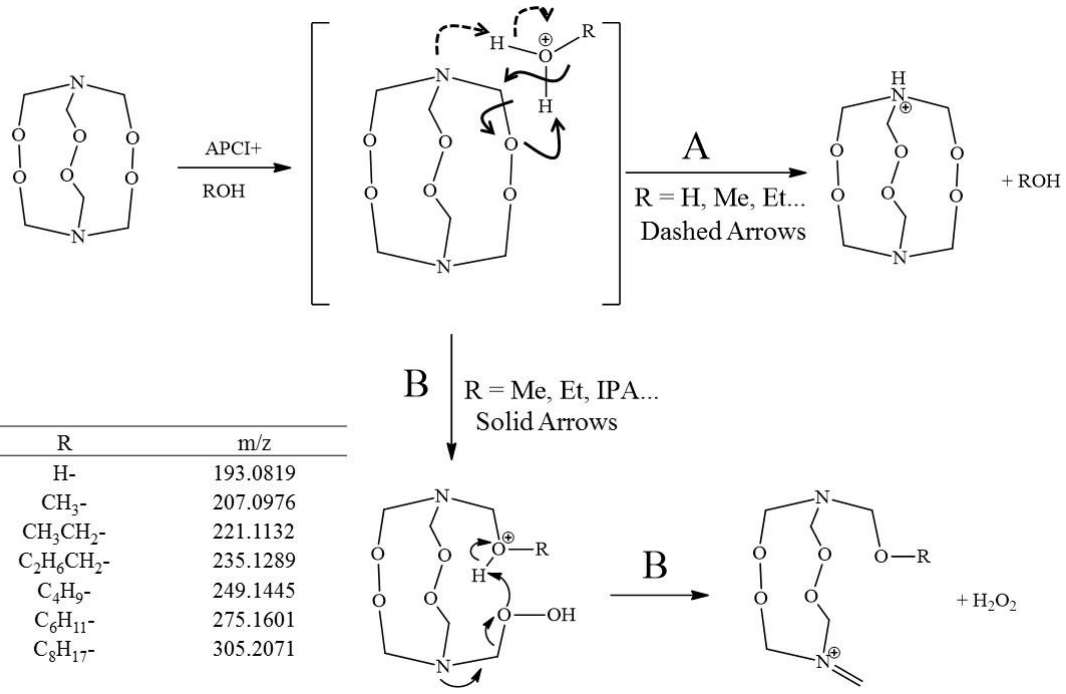

R	m/z
H-	193.0819
CH_3-	207.0976
CH_3CH_2-	221.1132
$C_2H_6CH_2$-	235.1289
C_4H_9-	249.1445
C_6H_{11}-	275.1601
C_8H_{17}-	305.2071

Figure 3-7. *Proposed mechanism for the formation of (A) the protonated molecule and (B) the various alcohol adducts.*

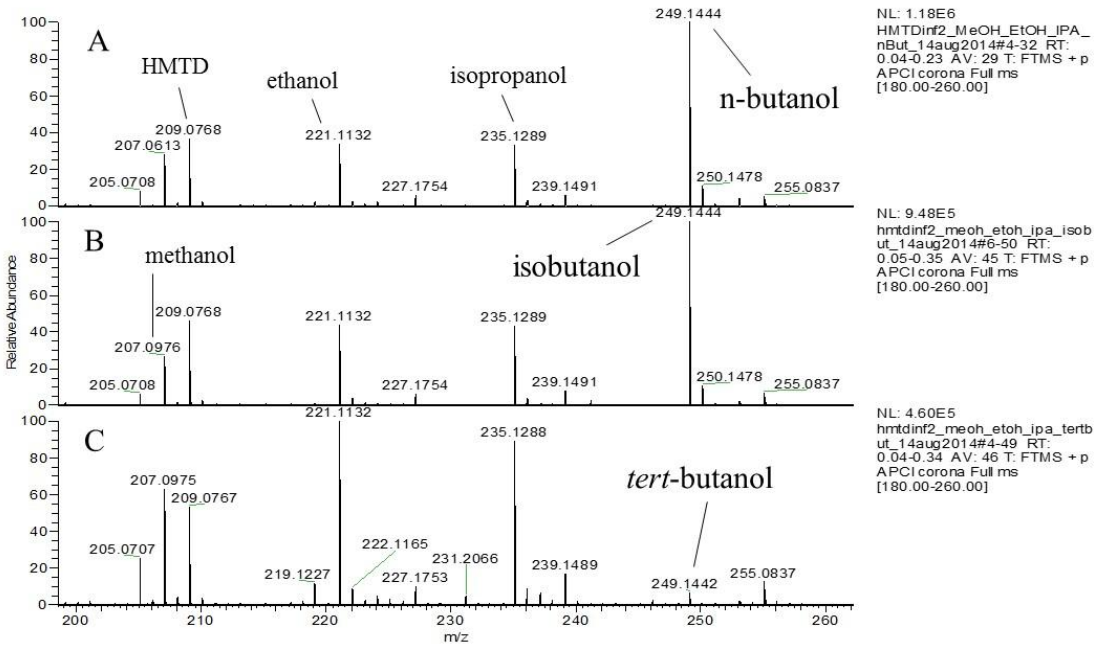

Figure 3-8. *HMTD infused with alcohol mixtures of methanol, ethanol, isopropanol and A) n-butanol, B) isobutanol and C) tert-butanol. 2-butanol was not included due to large impurities found in this alcohol, but the trend for HMTD adducts was similar to N-butanol and isobutanol.*

References

[1] L. Legler, Ueber Producte der langsamen Verbrennung des Aethyläthers, *Berichte der deutschen chemischen Gesellschaft*, **1885**, 18, 3343.

[2] J.C Oxley, J.L. Smith, H. Chen; E. Cioffi, Decomposition of Multi-Peroxidic Compounds: Part II: Hexamethylene Triperoxide Diamine (HMTD), *Thermochemica Acta*, **2002**, 388, 215.

[3] D. Van Natta, Jr., E. Sciolino, S. Grey, "Details Emerge in British Terror Case", *The New York Times*, 28 August **2006**.

[4] S. Morris, Terror suspect student 'had suicide vest and explosives', *The Guardian*, 4 June **2009**.

[5] K. Johnson, New Sentence Imposed in Bomb Plot from 1999, *The New York Times*, October **2012**.

[6] T. Urbanski, *Chemistry and Technology of Explosives*, Vol. 3, Pergamon Press, Oxford, **1967**, pp. 225

[7] W. P. Schaefer, J. T. Fourkas, B. G. Tiemann, Structure of Hexamethylene Triperoxide Diamine, *J. Am. Chem. Soc*., **1985**, 107, 2461.

[8] C. M. Lock, H. Brust, M. van Breukelen, J. Dalmolen, M. Koeberg, D. A. Stoker, Investigation of Isotopic Linkages between Precursor Materials and the Improvised High Explosive Product Hexamethylene Triperoxide Diamine, *Anal. Chem*, **2012**, 84, 4984.

[9] A. Crowson, M. S. Beardah, Development of an LC/MS method for the trace analysis of hexamethylenetriperoxidediamine (HMTD)**,** *Analyst*, **2001,** 126, 1689.

[10] J.C. Oxley, J. Zhang; J.L. Smith; E. Cioffi, Mass Spectra of Unlabeled and Isotopically Labeled Hexamethylene Triperoxide Diamine (HMTD), *Propellants, Explosives, Pyrotechnics*, **2000**, *25*, 1.

[11] X. Xu, A. M van de Craats, E. M Kok, P. C A M de Bruyn, Trace Analysis of Peroxide Explosives by High Performance Liquid Chromatography-Atmospheric Pressure Chemical Ionization-Tandem Mass Spectrometry (HPLC-APCI-MS/MS) for Forensic Applications, *J. of Forensic Sci.*, **2004**, 49, 1.

[12] R. Kinghorn, C. Milner, J. Zweigenbaum, Analysis of Trace Residues of Explosive Materials by Time-of-Flight LC/MS, *Agilent Technologies, Application, Forensics*, **2005**, 1.

[13] I. Cotte-Rodrıguez, H. Hernandez-Soto, H. Chen, R. G. Cooks, In Situ Trace Detection of Peroxide Explosives by Desorption Electrospray Ionization and Desorption Atmospheric Pressure Chemical Ionization, *Anal. Chem*. **2008,** 80, 1512.

[14] M. S. B. Munson, F. H. Field, Chemical Ionization Mass Spectrometry. I. General Introduction, *J. Am. Chem. Soc.*, **1966**, 88, 2621.

[15] D. I. Carroll, I. Dzidic, R. N. Stillwell, M. G. Horning, E. C. Horning, Subpicogram Detection System for Gas Phase Analysis Based upon Atmospheric Pressure Ionization (API) Mass Spectrometry, *Anal. Chem.*, **1974**, 46, 706.

Chapter 4 : Using Gas Phase Reactions of Hexamethylene Triperoxide Diamine (HMTD) to Improve Detection in Mass Spectrometry

Status: Published online

Journal of the American Society of Mass Spectometry, online version:

https://doi.org/10.1007/s1336

Abstract

Our efforts to lower the detection limits of hexamethylene triperoxide diamine (HMTD) have uncovered previously unreported gas-phase reactions of primary and secondary amines with one of the six methylene carbons. The reaction occurs primarily in the atmospheric pressure chemical ionization (APCI) source and is similar to the behavior of alcohols with HMTD[1]. However, unlike alcohols, the amine reaction conserves the hydrogen peroxide on the intact product. Furthermore, with or without amines, HMTD is oxidized to tetramethylene diperoxide diamine dialdehyde (TMDDD) in a temperature-dependent fashion in the APCI source. Synthesized TMDDD forms very strong adducts (not products) to ammonium and amine ions in the electrospray ionization (ESI) source. Attempts to improve HMTD detection by generating TMDDD in the APCI source with post-column addition of amines were not successful. Signal intensity of the solvent related HMTD product in methanol, $[HMTD+MeOH_2\text{-}H_2O_2]^+$ (m/z 207.0975), was understandably related to the amount of methanol in the HMTD environment as it elutes into the source. With conditions optimized for this product, the robust analysis of 300 pg (1.44 pmol) on column were routinely accomplished using Orbitrap mass spectrometers.

Introduction

Among organic peroxides, hexamethylene triperoxide diamine (HMTD) is an unusual nitrogen-containing molecule with three peroxide functionalities (**Figure 4-1**). Combined with its ease of formation, the native sensitivity of this peroxide has facilitated use in illicit explosive devices.[2][3][4][5] As part of our research in counterterrorism programs, the quantification of minor amounts of this material by liquid chromatography coupled to high resolution mass spectrometric detectors (LC/HRMS or LC/MS) has become necessary. These systems offer fast and sensitive detection of the intact molecules for unequivocal identification. We have already found that choice of mobile phase and ionization source are crucial. In both electrospray ionization (ESI) and atmospheric pressure chemical ionization (APCI) use of acetonitrile (ACN) in the mobile phase extensively reduces the ionization of most peroxides.[6] However, the use of ACN as a storage solvent is not a problem since this solvent can be easily separated from the analytes prior to ionization.[7] Using APCI and a mobile phase of ammonium acetate/methanol, detection limits of 1 ng on-column were achieved for the $[M+H]^+$ (m/z 209.0768) ion. Use of methanol or any alcohol requires attention as HMTD and other cyclic peroxides create gas-phase products with solvent alcohols.[1,7] HMTD reacts with MeOH in the APCI source to produce the alcohol incorporated product $[HMTD+MeOH_2\text{-}H_2O_2]^+$ with m/z 207.0975 ($C_7H_{15}N_2O_5^+$).[1] This does not appear to negatively affect the HMTD signal intensity. In fact, this product can be used as confirmation of the presence of HMTD along with other in-source fragments frequently observed, including 191.0662, 179.0662,

145.0608 and 88.0393, depending on source conditions.[8] In this paper we consider LC/MS parameters which can greatly effect detection limits of HMTD.

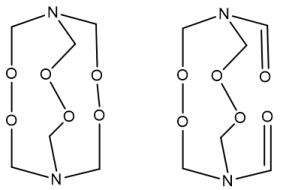

HMTD TMDDD

Figure 4-1. *Structure of HMTD and TMDDD.*

Materials and methods

Chemicals and Reagents

Caution: HMTD is a powerful explosive, and organic peroxides, in general, are sensitive compounds. Take necessary precautions when working with these compounds.

Water, acetonitrile, methanol, (all Optima HPLC grade), ammonium acetate (NH_4OAc, HPLC grade), triethylamine and aniline were purchased from Fisher Chemical (Fair Lawn, NJ) . Methylamine, ethylamine, dimethylamine, 2-nitroaniline, (2-aminoethyl)trimethylammonium were purchased from Sigma-Aldrich (St. Louis, MO). Deuterated formaldehyde (D2), water (D2) and methanol (D4) were purchased from Cambridge Isotope Labs (Cambridge, MA). Isopropylamine, cyclohexlyamine, choline and hexamethylenetetramine (hexamine) were purchased from Acros Organics (Morris Plains, NJ). Hydrogen peroxide (HP, 50%) was obtained from Univar (Redmond, WA). Unless otherwise stated, the mobile phase used for chromatography consisted of aqueous 10 mM NH_4OAc prepared at neutral pH with methanol (MeOH) as the organic modifier.

HMTD and TMDDD Synthesis

To synthesize hexamethylene triperoxide diamine (HMTD), hexamine (2.43 g, 17.3 mmol) was placed in a round-bottom flask, immersed in an ice bath, and dissolved in 50% hydrogen peroxide (9.88 g, 145 mmol). Anhydrous citric acid (3.61 g, 18.9 mmol) was added in small portions so that the temperature did not exceed 10 °C. The reaction mixture was left in the ice bath and allowed to warm with stirring over 15-18 hours. Product was collected by vacuum filtration, washed with deionized water and room temperature methanol and allowed to dry. A similar procedure was used to produce the d_{12}-HMTD by using d_2-formaldehyde. HMTD was used to produce tetramethylene diperoxide diamine dialdehyde (TMDDD), which was synthesized according to Wierbeczki et al.[9] This crude product (mp: 156-157°C) was used for all TMDDD testing.

Instrumentation

Using a ThermoElectron (San Jose, CA) LTQ Orbitrap XL or Exactive mass spectrometer equipped with an atmospheric pressure chemical ionization (APCI) interface, ions were generated and introduced into the ion transfer tube set between 180 to 275 ºC (depending on the experimental conditions being tested). All work was performed using positive ion mode. Tune conditions for APCI infusion experiments were varied depending on the parameters being tested: discharge current, 2500-6000 µA; N_2 sheath gas, 8-50 arbitrary units (AU); N_2 auxiliary gas, 5-40 AU; vaporizer temperature 180-350 ºC; ion transfer tube, 14 V; tube lens, 35-70 V; and skimmer

offset (Exactive), 0 V. Minor voltage changes were made at times to improve signal intensity for compounds. For electrospray ionization experiments, spray voltages ranged from 3500 to 5000 eV. Other focusing voltages were similar to those used for APCI, with the Tube Lens having the most significant effect on ion abundance. For the LTQ Orbitrap, fragmentation was performed with an isolation width of 1.8 m/z, activation time 30 msec, Q_z value of 0.25, and mass resolution was between 7500 and 100000. For the Exactive MS, mass resolution was 50000 and the AGC setting was balanced. Solvent delivery was performed using either Thermo infusion syringe pumps or ThermoElectron Accela quaternary pumps. A CTC Analytics HTS PAL autosampler injected directly from either amber, glass LC vials with PTFE septa (Agilent Technologies) or polypropylene, 1 mL 96-well plates with pre-slit silicone plate covers (Analytical Sales and Service). Data collection and analysis was performed with Thermo Xcalibur software version 2.2, SP 1.48. Most data reported herein employed full scan MS unless specifically stated. Chromatographic traces are extracted ion chromatograms (XIC) with a mass window of 15 ppm of the expected exact mass. *Note: All masses reported below are exact mass values within ±15 ppm for species less than 130 m/z and ±7.5 ppm for species over m/z 130*.

Methods

HMTD/TMDDD Analysis

Direct infusion of HMTD or TMDDD (10 μg/mL or ~48 μM in MeOH) into either the ESI or APCI source was used to optimize voltages for both compounds. Optimized HMTD values were chosen for all analysis since this is the primary compound of

interest. The MS gas flows and temperature were initially optimized using mobile phase (MP) infusion with a constant flow of 50% 10 mM NH_4OAc in pump channel B and 50% MeOH in channel A at 230 μL/min flow and directly infusing 20 μL/min HMTD standard (10 μg/mL/48.1 μM in MeOH) into the flow. Monitoring the $[M+H]^+$ ion at m/z 209.0768, the vaporizer temperature was set to 250 °C, with the sheath gas at 35 AU and auxiliary gas at 20 AU. Using this optimized system, 40 μL sample volumes of HMTD in 50/50 ACN/water were injected into a LC flow of 250 μL/min with 5% MeOH (channel A) and 95% aqueous 10 mM NH_4OAc (channel B) for introduction onto either a Thermo Syncronis C18 column or an Analytical Sales & Service Advantage Polyfluorinated Phenyl (PFP) column (both 2.1 x 50 mm, 5 μm). Initial conditions were held for 1.5 minute before a linear ramp to 35% A/65% B over 1.5 minutes followed immediately by a linear ramp to 95%A/5% B over the next minute. This concentration was held for 2 minutes before a 30 second transition to initial conditions with a hold of 1.5 minutes. Fully deuterated HMTD (d_{12}-HMTD) was produced to be used as an internal standard (IS). Extracted ion chromatograms (XIC) were integrated using the Genesis peak detection algorithm in Thermo Xcalibur Quan Browser. Linear dynamic range comparing concentration to peak area response ratio, relative to the IS, extended from 25 ng/mL to 20000 ng/mL using 10 points and a weighted calibration curve. Solution stability in ACN was previously determined to be up to 40 days at -20 °C.[7] The analysis of TMDDD $[M+NH_4]^+$ ion of m/z 224.0877 or $[M+H]^+$ ion of m/z 207.0612 were performed by the same method used for HMTD. Separation of TMDDD and HMTD was significant on either the C18 or PFP column.

Solvent Incorporation Studies

To examine the origin of certain products/fragments observed in the LC/MS experiments, HMTD or TMDDD (10 μg/mL) were prepared in solutions containing 1 mM of various amine compounds (see **Table 4-1**). Solutions were directly infused into the ESI or APCI source. Due to the strongly basic nature of the amines, most of the compounds were diluted to neutral pH using a small amount of formic acid. To avoid exposing LC columns to the amines, additional studies were performed with 50 mM solutions of amine infused post-column at 5 μL/min into 250 μL/min of mobile phase (final MP concentration ~ 1 mM). These studies were performed while altering vaporization temperatures and N_2 gas flow. Since alcohol incorporation into HMTD is a known phenomenon, additional studies were performed using MP infusion to determine the gas and temperature conditions in APCI to optimize the methanol incorporated product (m/z 207.0975).[1] Also studies were performed by altering vaporization temperatures and N_2 gas flow while injecting HMTD onto the system using the PFP or the C18 column. Peak area counts were compared to determine optimal, stable analytical conditions.

Results and Discussion

Early efforts to identify all species related to HMTD in the APCI source led to the frequently encountered m/z 224.0877, associated with $C_6H_{14}N_3O_6^+$. When chromatographically separated, two peaks with this same m/z 224 were observed. The first peak eluted early with a major signal of m/z 224 and a minor signal of m/z 207.0611 $[HMTD-2H+H]^+$. We believed this compound to be TMDDD (**Figure 4-1**),

with m/z 224 being the ammonium adduct. The second peak eluted at the same retention time as HMTD and exhibited all other masses associated with HMTD ionization. Although this second peak showing m/z 224 was produced in varying degrees from one analysis to another, we believed this to be TMDDD formed from HMTD in the gas phase under APCI conditions. Marr and Groves had reported that, in the gas phase, a small amount of HMTD is converted to the dialdehyde product (TMDDD).[10] When an authentic sample of TMDDD was prepared and analyzed, it eluted with the same retention time (t_R) and peak shape as the early eluting m/z 224, indicating that our HMTD standard was contaminated with a small amount of TMDDD. Quantification of the TMDDD and HMTD samples showed that HMTD was contaminated with about 1% TMDDD and TMDDD contained about 1.5% of HMTD (Appendix 4: Table S4-1). Collision induced dissociation (CID) of m/z 224 for TMDDD and the m/z 224 under the HMTD peak confirmed that HMTD was being oxidized to TMDDD in the APCI source. Very little, if any, conversion of HMTD to TMDDD is observed using ESI.

TMDDD was found to have a significantly better signal in ESI than APCI and a very high affinity for ammonium or amine adducts. In fact, using our standard mobile phase of ammonium acetate/methanol, the minor contamination of TMDDD in HMTD (~1% depending on the batch) produced a signal for the ammoniated TMDDD in ESI that was nearly comparable to the HMTD signal in APCI. Krawczyk discovered that TMDDD also has a high affinity for metal ions in the ESI source and suggested that purposeful oxidation of HMTD be exploited to improve detection levels. This process

involved off-line oxidation of the HMTD samples prior to analysis by ESI in the presence of metal ions.[11] In contrast, the APCI source produced a significantly better signal for HMTD than ESI with variable amounts of conversion from HMTD to TMDDD. We then began to consider ways of intentionally increasing this in-source conversion to improve detection limits with the addition of an adducting agent. Since the production of TMDDD from HMTD required heat in the presence of O_2, several experimental parameters were examined in both APCI and heated ESI (HESI) to cause in-source conversion. Attempts to convert HMTD to TMDDD using the HESI source did not succeed even at temperatures exceeding 300°C. Experiments using APCI show that TMDDD formation increases with increasing temperatures, up to the point (~350°C) where both HMTD and TMDDD begin to decompose. **Figure 4-2** shows the XIC of products related to HMTD and TMDDD for the same sample analyzed at two different vaporization temperatures in the APCI source (other conditions identical). The signal for ion m/z 224 at the t_R ~4.8 min, where HMTD elutes, was nearly 20 times more intense with the vaporizer temperature at 300°C rather than at 210°C. Note that the signal area for TMDDD (t_R ~2.1 min) was unaffected by temperature. These results can be observed in Tables S-2 and S-3 of the Online Resource. While m/z 224 was increased from 2% to 32% of the total signal by increasing the temperature, the peak at m/z 207.0975 was still 46% of the total signal. By summing the peak areas of all HMTD products over all temperatures, it was evident that the largest response for any product was m/z 207.0975 at 250 °C, corresponding to methanol incorporation $[HMTD+MeOH_2-H_2O_2]^+$.

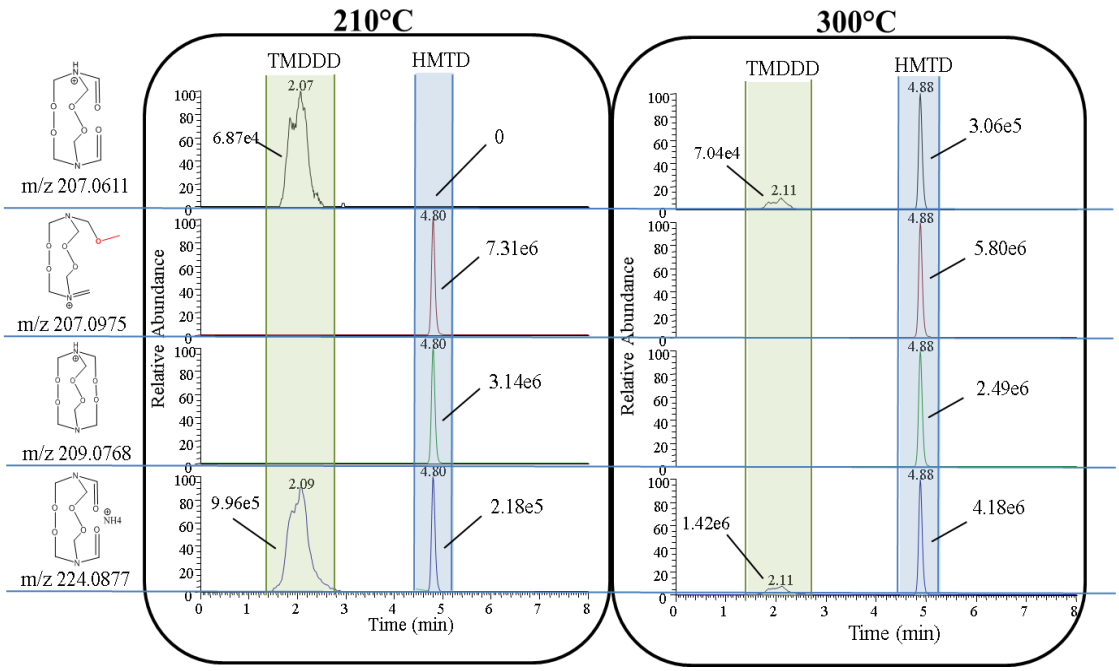

Figure 4-2. *TMDDD and HMTD with 100 ng of HMTD injected onto a 5 cm PFP column with APCI source at 210°C and 300°C (Numbers displayed by each peak is integrated area counts.)*

Since TMDDD formed very strong ammonium adducts, we attempted to enhance the MS response by use of organic amines. A variety of amines at 1 mM concentration were infused with HMTD into either an APCI or ESI source. Methylamine with HMTD produced abundant signal at m/z 238.1034 in ESI and a large signal at m/z 240.1190 in APCI; ethylamine produced similar results at m/z 252.1190 and m/z 254.1347, respectively (**Figure 4-3**). It should be noted that each source produced both the low and high m/z ions to some degree, but the lower m/z, e.g. 238 or 252, clearly dominated in ESI, and the higher m/z, in APCI (**Figure 4-3**). To clarify these results, the same HMTD sample was injected onto the LC-MS system with post-column addition of the same amines using both ESI and APCI (**Figure 4-4**). In ESI, the

intense signal at m/z 252.1190 eluting early with no detectable m/z 254.1347 was the TMDDD contaminant in our HMTD sample. The second peak being HMTD had almost no m/z 252, but a reasonable signal for m/z 254. Results using APCI showed very low intensity for the TMDDD m/z 252 signal (no m/z 254 at all) and a very intense signal of m/z 254 for HMTD with a small amount of m/z 252 present (from TMDDD formed in-source). These results confirm our observations above that TMDDD contaminates HMTD samples. Even HMTD, chromatographically separated from TMDDD, forms TMDDD in the APCI source. Furthermore, it was observed that HMTD produced the strongest signal in APCI, while TMDDD was best observed by ESI. Additionally, both HMTD and TMDDD form products or adducts with amines. At this point, it was not certain whether the amine adduct could be used to improve the APCI signal for TMDDD.

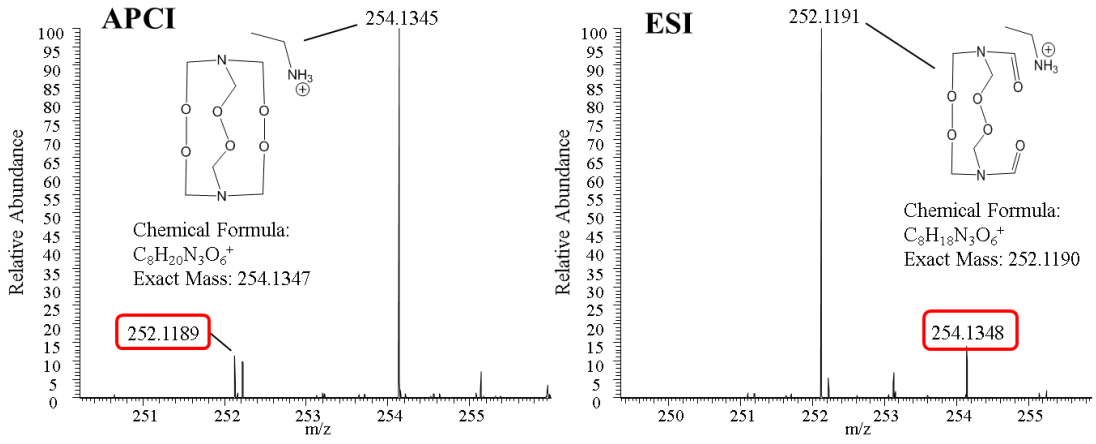

Figure 4-3. *APCI and ESI spectra for the infusion of HMTD with 1 mM ethylamine.*

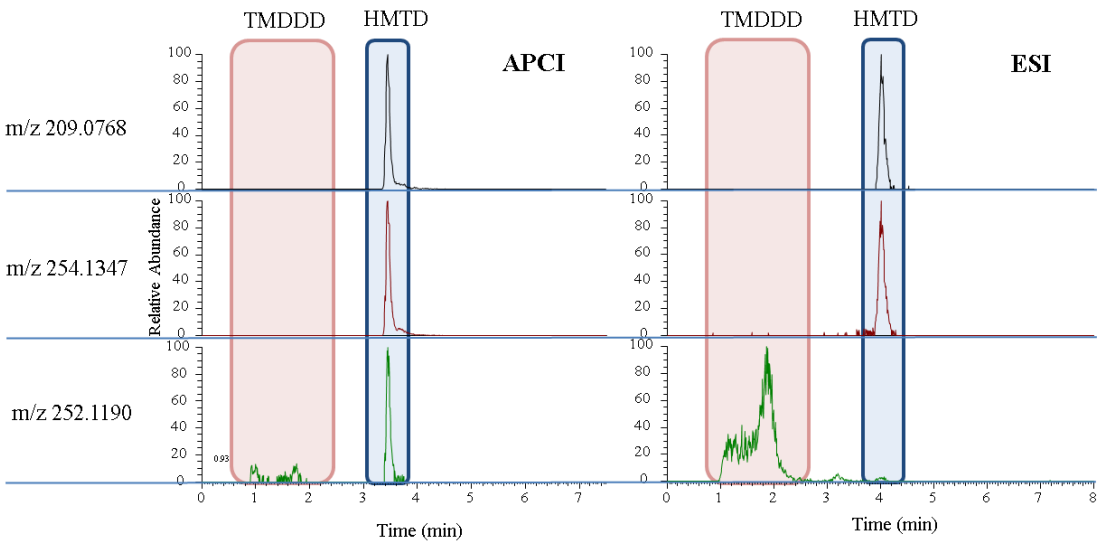

Figure 4-4. *Chromatogram of HMTD in APCI and ESI with post-column addition of ethylamine.*

Attempts to trap and dissociate TMDDD-amine adduct peaks in ESI provided no fragmentation at all, just depletion of the parent ion. Krawczyk also reported that attempting to fragment metal adducts of TMDDD produced no observable fragments.[11] When larger amines (see list in **Table 4-1**) were studied, where the protonated amine had a m/z greater than the 50 Da cut-off of the Orbitrap, we observed only the fragment corresponding to the protonated amine. This suggests that the amine sequestered all charge and explains the reason no fragments were observed during CID of the TMDDD adduct. It appears that the affinity of TMDDD for amines is related to the basicity of the amine, with the more basic amine producing a larger adduct signal. Post-column addition of organic amines indicated that the formation of organic amine adducts with TMDDD are favored over ammonium. Unfortunately, the signal observed for the amine was equivalent in intensity to the ammonium adduct, but not significantly better.

Table 4-1. *Expected and observed masses for HMTD in APCI with fully incorporated amine.*

Organic Amine	Expected mass[†]	Observed mass[†]	ΔPPM	pKa
Methylamine	240.1190	240.1185	-2.1	10.62
Ethylamine	254.1347	254.1342	-2.0	10.87
Dimethylamine	254.1347	254.1341	-2.4	10.73
Triethylamine*	310.1973	310.1963	-3.2	10.78
Isopropylamine	268.1503	268.1489	-5.2	10.63
Cyclohexlyamine	308.1816	308.1813	-1.0	10.63
Ammonia	226.1034	NR		9.25
Aniline	302.1347	302.1338	-3.0	4.6
2-nitroaniline	347.1197	NR		-0.28
(2-aminoethyl)trimethylammonium	311.1925	NR		na
Choline	?	NR		-3.2

*Triethylamine forms a HMTD adduct with no observable chemical reaction;

NR-no reaction:

[†]TMDDD in ESI presented as 2 H reduction of mass for all (ammonium = 224.0877);

na-not available

Unlike TMDDD, trapping and dissociation of the HMTD amine adducts in APCI produced multiple stable fragments (see **Figure 4-5**, **Table 4-2**). CID spectra and proposed fragments for many of the amines tested can be viewed in the Appendix 4: Figures S41-46. Interpretation of the spectra for each of the amines showed that although each exhibited a fragment of 209.0768 (product **4**, **Table 4-2**) suggesting adduct formation, they all lost water (product **2**, **Table 4-2**) and H_2O_2 (product **3**, **Table 4-2**). Notably, in all spectra was the formation of the fragment m/z 197.0768 (product **5**, loss of exactly 12.000 Da from HMTD) and a fragment corresponding to

the parent amine increasing by exactly 1 carbon (product **10**, **Table 4-2**). This suggested that the amine performed a nucleophilic attack on one of the methylene groups of the HMTD molecule, similar to the reaction with alcohols.[1] To confirm this result d_{12}-HMTD was synthesized and full hydrogen/deuterium exchange (HDX) studies were performed using isopropylamine. Results are shown in **Table 4-2** and Appendix 4: Figures S4-7 and S4-8. All fragments produced were in agreement with the proposed structures (within ±5.6 ppm for fragments > 100 m/z and ± 10 ppm for fragments <100 m/z). This nucleophilic attack was observed for both primary and secondary amines. Only triethylamine formed an HMTD adduct, and the dissociation of this product generated only a small protonated HMTD fragment and a large fragment at m/z 102.1277 corresponding to protonated triethylamine. The proposed CID fragmentation mechanism for the HMTD-amine products (confirmed by HDX) is shown in **Scheme 4-1** (arrow colors correspond to formed structure color).

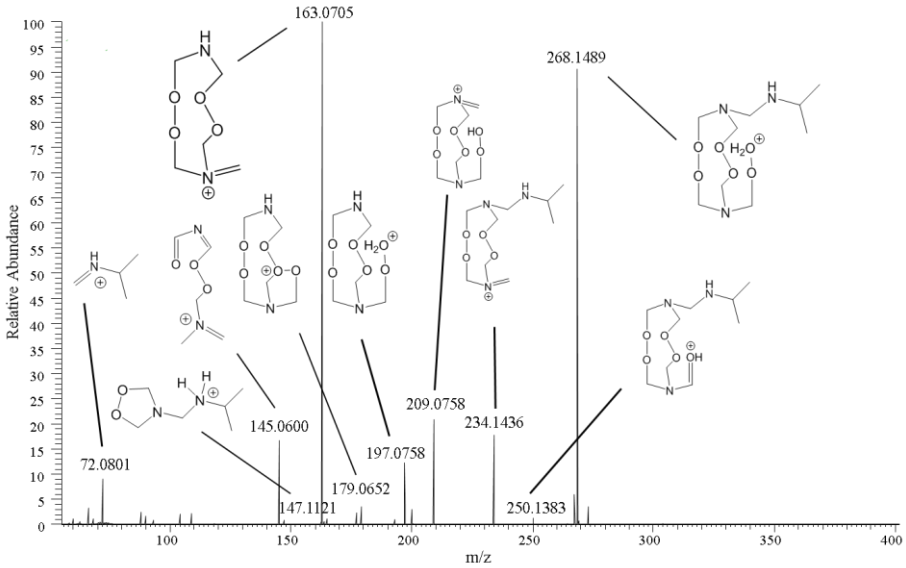

Figure 4-5. *Fragmentation of t HMTD/isopropylamine product formed in APCI at m/z 268.1489.*

Table 4-2. *Fragments associated with HMTD gas-phase reaction (including HDX) with isopropylamine.*

Proposed fragment	Product	Material/solvent	Exact Mass	Molecular formula	Observed Mass	ΔPPM
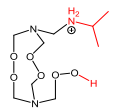	**1**	U/US	268.1503	C9H22N3O6+	268.1489	-5.2
		D18/US	280.2256	C9H10D12N3O6+	280.2247	-3.2
		U/DS	271.1691	C9H19D3N3O6+	271.1686	-1.8
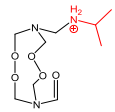	**2**	U/US	250.1397	C9H20N3O5+	250.1383	-5.6
		D18/US	261.2088	C9H9D11N3O5+	261.2091	1.1
		U/DS	252.1523	C9H18D2N3O5+	252.1516	-2.8
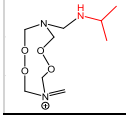	**3**	U/US	234.1448	C9H20N3O4+	234.1436	-5.1
		D18/US	246.2202	C9H8D12N3O4+	246.2194	-3.2
		U/DS	235.1511	C9H19DN3O4+	235.1506	-2.1
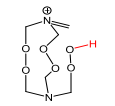	**4**	U/US	209.0768	C6H13N2O6+	209.0758	-4.8
		D18/US	221.1521	C6HD12N2O6+	221.1514	-3.2
		U/DS	210.0831	C6H12DN2O6+	210.0826	-2.4
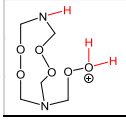	**5**	U/US	197.0768	C5H13N2O6+	197.0758	-5.1
		D18/US	207.1396	C5H3D10N2O6+	207.1389	-3.4
		U/DS	200.0956	C5H10D3N2O6+	200.0951	-2.5
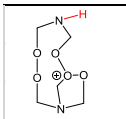	**6**	U/US	179.0662	C5H11N2O5+	179.0652	-5.6
		D18/US	189.1290	C5HD10N2O5+	189.1284	-3.2
		U/DS	180.0725	C5H10DN2O5+	180.0720	-2.8
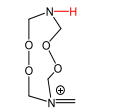	**7**	U/US	163.0713	C5H11N2O4+	163.0705	-4.9
		D18/US	173.1341	C5HD10N2O4+	173.1334	-4.0
		U/DS	164.0776	C5H10DN2O4+	164.0772	-2.4
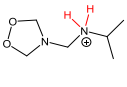	**8**	U/US	147.1128	C6H15N2O2+	147.1121	-4.8
		D18/US	153.1505	C6H9D6N2O2+	153.1498	-4.6
		U/DS	149.1254	C6H13D2N2O2+	149.1249	-3.4
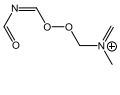	**9**	U/US	145.0608	C5H9N2O3+	145.06	-5.5
		D18/US	154.1173	C5D9N2O3+	154.1167	-3.9
		U/DS	145.0608	C5H9N2O3+	145.0604	-2.8
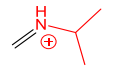	**10**	U/US	72.0808	C4H10N+	72.0801	-9.7
		D18/US	74.0933	C4H8D2N+	74.0927	-8.1
		U/DS	73.0871	C4H9DN+	73.0865	-8.2

U/US = Unlabled material/Unlabled solvent
D18/US = D18-Material/Unlabled solvent
U/DS = Unlabled material/D-labled solvent
Red structural components where H/D exchange can occur or amine is incorporated.

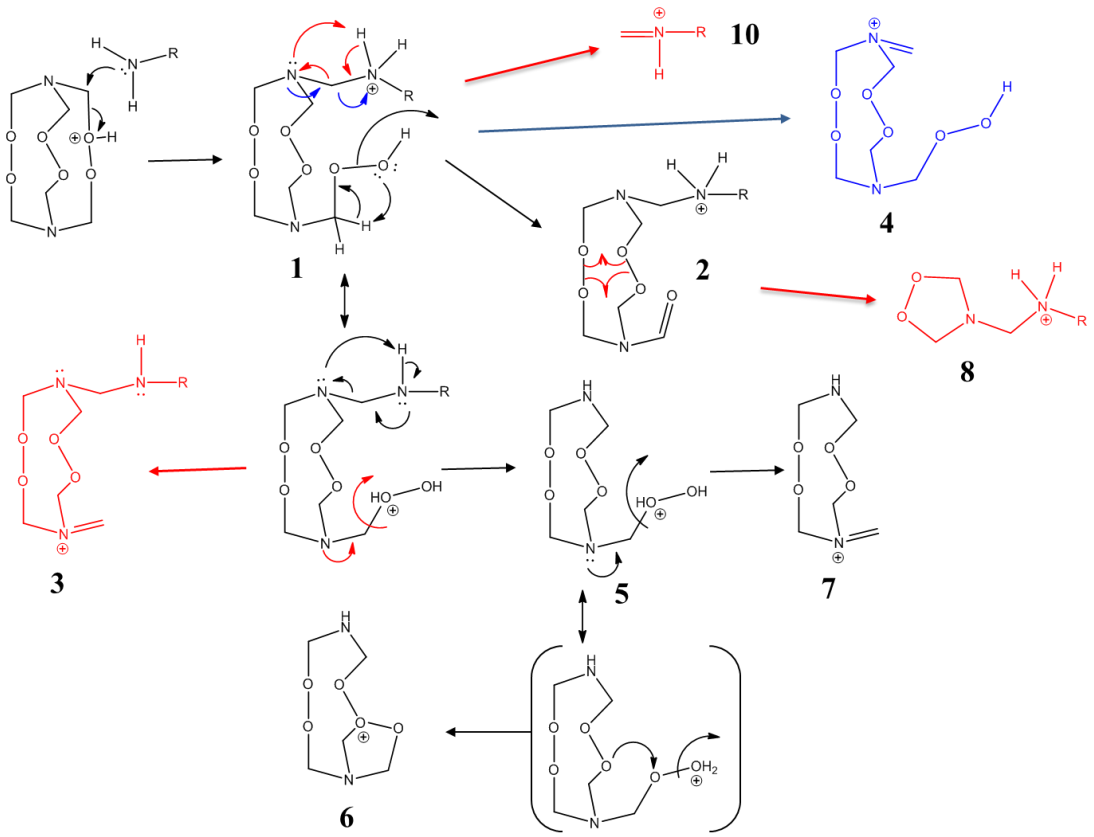

Scheme 4-1 *(arrow colors correspond to formed structure color)*

To improve detection of HMTD, post-column addition of organic amines (with or without neutralization) was examined with increasing temperature in the APCI source. This attempt at in-source conversion of HMTD to TMDDD was successful, but the signal for the TMDDD-amine adduct was not greater than HMTD-methanol product (m/z 207.0975). In another attempt to improve the HMTD signal, we attempted to attach a charged quaternary amine, producing a permanently charged ion. Two organic quaternary amines, one with a pendent primary amine ((2-aminoethyl) trimethylammonium) and the other with a pendent primary alcohol (choline), were infused in a MeOH/H_2O solution of HMTD. No reaction or reaction product (including multiply charged products) was observed in either ESI or APCI. We

speculate that the quaternary amine pulled the electron density from the alcohol or amine tail which created a species that was not a strong enough electrophile to attack the methylene group. Additionally, the electron rich oxygens and nitrogen surrounding the methyl groups can draw the quaternary group toward molecule thus preventing the nucleophilic group from proper approach for reactivity. Similar experiments using amines were attempted with other peroxides including TATP and MEKP. No reaction products were detected in either ESI or APCI for these compounds.[7]

Using the ammonium acetate/methanol mobile phase, chromatographic data frequently showed $[HMTD+MeOH_2\text{-}H_2O_2]^+$ = m/z 207.0975 ion produced the most intense signal under APCI conditions. Inexplicably, the ratio of the $[M+H]^+$ and $[M+MeOH_2\text{-}H_2O_2]^+$ varied from analysis to analysis. In order to use the MeOH incorporated product for HMTD quantification, it was necessary to understand the variability of this signal. Direct infusion of HMTD (10 μg/mL at 20 μL/min) while increasing the N_2 gas flow in the APCI source favored the formation of the parent $[M+H]^+$ over the formation of $[M+MeOH_2\text{-}H_2O_2]^+$. The effect of increased gas flow rate (also observed for TATP[7]) suggests that higher gas flow does not give the alcohol as much time to react with the HMTD ion/molecule in either the corona discharge or the vaporizer region of the source. Direct infusion experiments (even in very high MeOH concentrations) almost always produced more of the $[M+H]^+$ ion. However, MP infusion studies of HMTD show significantly more of the alcohol incorporated product with increasing MeOH concentration. **Figure 4-6** depicts the ratio of m/z 207.0975/209.0768 in the standard LC gradient and demonstrates that this can be

leveraged for column optimization. Use of a PFP column (t_R HMTD ~ 5.1 min.) over the C18 column (t_R HMTD ~ 3.5 min) favors the formation of m/z 207.0975. Optimizing gas flow was performed by injecting the same 10 µg/mL sample onto the PFP column at 250°C vaporizer temperature under various flow conditions (Table S-3, Online Resource). Although a higher sheath than auxiliary gas provided more intense signal, it was also associated with the most variability. The best stability with the most intense signal for the $[M+MeOH_2-H_2O_2]^+$ product was achieved when the sheath and auxiliary gasses were both set to 15 AU. Additionally, HMTD peak shape is strongly affected by the amount of organic in the sample plug. More than 20% ACN in the sample plug can produce sever fronting of the peak, reducing our ability to detect low levels of HMTD (see **Figure 4-7**). Since HMTD is not volatile and we are using a deuterated IS, samples can be evaporated to dryness and reconstituted in 90% water/10% ACN. Although concerns about solubility did arise, the assay linear range spanned from 10 ng/mL (48nM) to 20000 ng/mL (96 µM) demonstrating that this was not an issue. This also allows for the concentration of higher volume samples to push detection limits even lower. Using optimized conditions for HMTD, we have detected HMTD as low as 100 pg on column with a robust analysis of 300 pg on column.

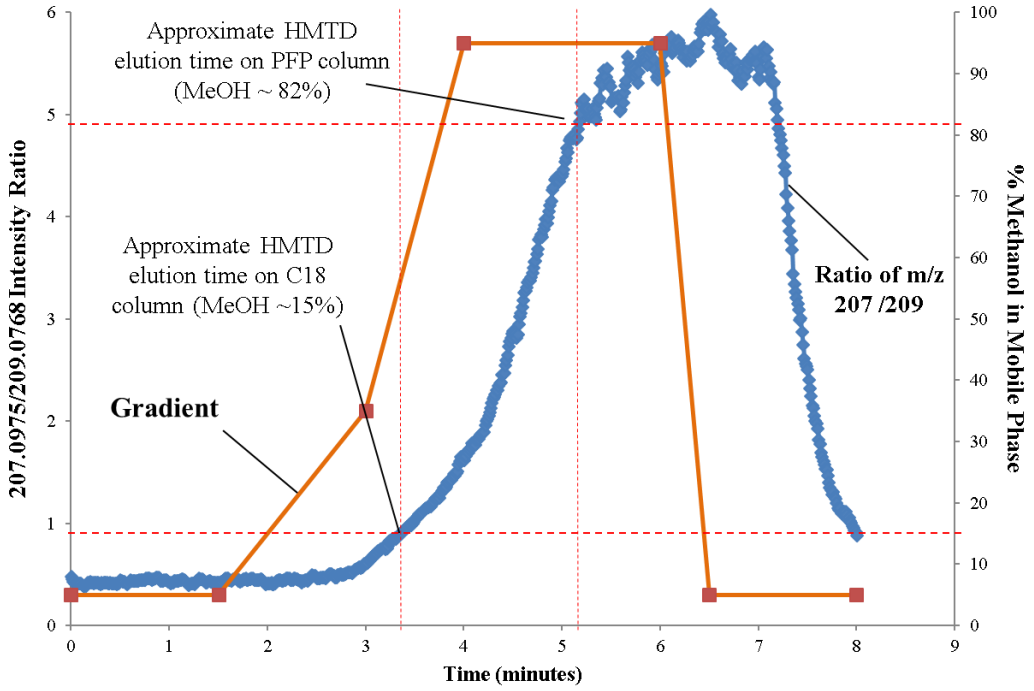

Figure 4-6. *HMTD MP infusion into gradient of methanol (right axis) and observed m/z 207/209 ratio (left axis). Red dotted lines identify the approximate in-source MeOH concentration seen by HMTD on the C18 vs. the PFP column.*

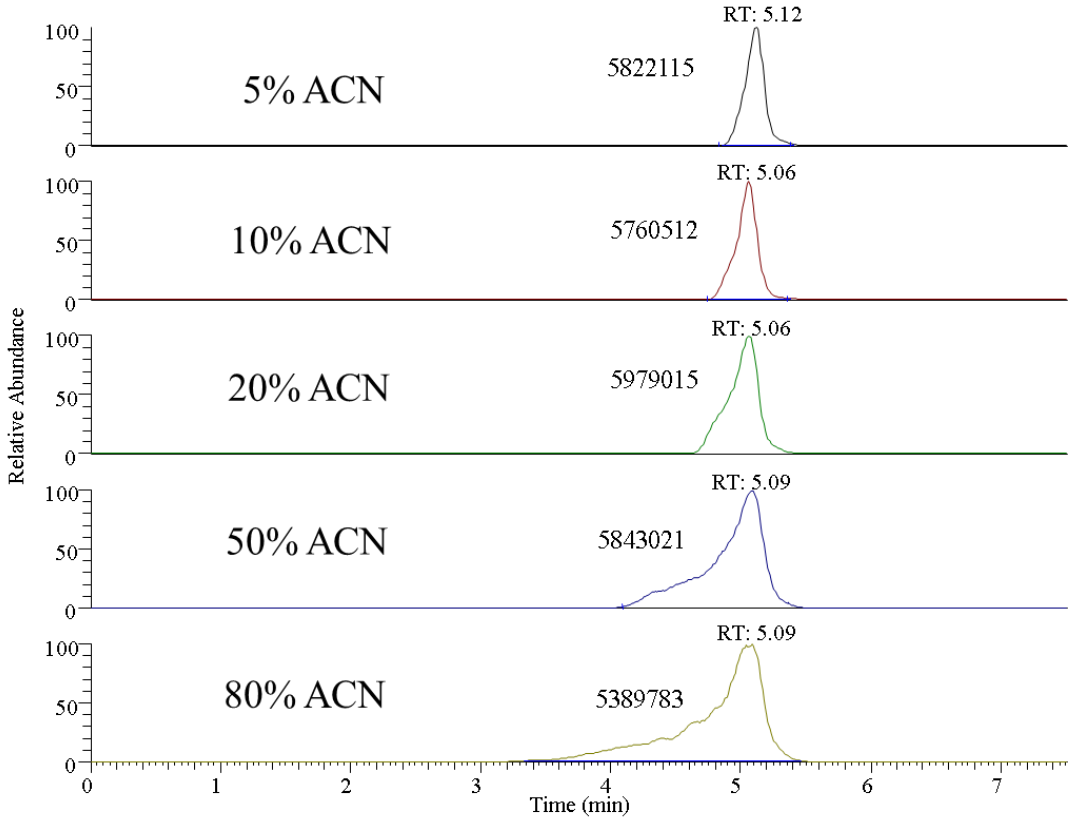

Figure 4-7. *Injection of 20 µL of 10 µg/mL HMTD in various combinations of ACN/water in the sample plug. Peak integration was performed manually, but tR and areas (number left of peak) are quite similar.*

Conclusions

Although TATP and HMTD have been observed to undergo a gas-phase reaction with alcohols[7][1], no corresponding reaction has been observed for TMDDD. While enhancing detection of HMTD we discovered that TMDDD is frequently a contaminant in purified HMTD and can also be formed in the gas phase within the APCI source. TMDDD $[M+H]^+$ (m/z_207.0612) produces a much better signal in ESI than APCI, and has tremendous affinity for ammonium or organic amine ions. HMTD

and cyclic peroxides have exhibited significantly better ionization by APCI, while linear peroxides (MEKP) and TMDDD respond best to ESI.[7] We speculate that the open nature of TMDDD (a 10-membered ring) may allow this to behave more like a linear peroxide. Our attempts to create TMDDD in-situ were a success, in that HMTD is oxidized in a temperature-dependent fashion within the APCI source. Unfortunately, we were unable to exploit the high TMDDD affinity for amines to improve HMTD detection limits. Off-line conversion of HMTD to TMDDD as suggested by Krawczyk[11] might improve detection limits using post-column addition of basic volatile organic amines instead of metals. Additionally, we discovered a direct reaction of organic amines with the methylene carbon of HMTD, analogous to the reaction of alcohols. This behavior may be exploited for other areas of research, but did not appear to enhance detection limits as did the MeOH. Current linear dynamic range for HMTD analysis (using the $[M+MeOH_2-H_2O_2]^+$ product) is 10 ng/mL (48nM) to 20000 ng/mL (96 μM) using APCI with a vaporizer temperature of 250°C and a mobile phase of MeOH/200 μM NH_4OAc on a PFP column. If MeOH is used as the mobile phase organic modifier, there are two different compounds with a nominal mass of m/z 207 being produced. This information combined with the HMTD conversion to TMDDD in storage solution [7] substantiate the need for good separation and high resolution MS for proper identification and quantification.

Acknowledgements

This material is based upon work supported by U.S. Department of Homeland Security (DHS), Science & Technology Directorate, Office of University Programs,

under Grant 2013-ST-061-ED0001. Views and conclusions are those of the authors and should not be interpreted as necessarily representing the official policies, either expressed or implied, of DHS.

References

1. Colizza, K., Porter, M., Smith, J.L., Oxley, J.C.: Gas-phase reactions of alcohols with hexamethylene triperoxide diamine (HMTD) under atmospheric pressure chemical ionization conditions. Rapid Commun. Mass Spectrom. 29, 74–80 (2015).
2. Bradley J. Fikes: REGION: Escondido “bomb house” controlled burn a model for nation, expert says. San Diego Union-Tribune. http://www, (2012).
3. Don Van Natta, J., Sciolino, E., Grey, S.: Details Emerge in British Terror Case. New York Times.
4. Johnson, K.: New Sentence Imposed in Bomb Plot from 1999. New York Times.
5. Morris, S.: Terror suspect student “had suicide vest and explosives.” The Gaurdian.
6. Colizza, K., Mahoney, K.E., Yevdokimov, A.V., Smith, J.L., Oxley, J.C.: Acetonitrile Ion Suppression in Atmospheric Pressure Ionization Mass Spectrometry. J. Am. Soc. Mass Spectrom. 27, 1796–1804 (2016).
7. Colizza, K., Yevdokimov, A., McLennan, L., Smith, J.L., Oxley, J.C.: Reactions of Organic Peroxides with Alcohols in Atmospheric Pressure Chemical Ionization—the Pitfalls of Quantifying Triacetone Triperoxide

(TATP). J. Am. Soc. Mass Spectrom. In Press, (2017).

8. Newsome, G.A., Ackerman, L.K., Johnson, K.J.: Humidity Effects on Fragmentation in Plasma-Based Ambient Ionization Sources. J. Am. Soc. Mass Spectrom. 27, 135–143 (2016).
9. Wierzbicki, A., Salter, E.A., Cioffi, E. a., Stevens, E.D.: Density Functional Theory and X-ray Investigations of P- and M-Hexamethylene Triperoxide Diamine and Its Dialdehyde Derivative. J. Phys. Chem. A. 105, 8763–8768 (2001).
10. Marr, A.J., Groves, D.M.: Ion Mobility Spectrometry of Peroxide Explosives TATP and HMTD. Int. J. Ion Mobil. Spectrom. 6, 59 (2003).
11. Krawczyk, T.: Enhanced electrospray ionization mass spectrometric detection of hexamethylene triperoxide diamine (HMTD) after oxidation to tetramethylene diperoxide diamine dialdehyde (TMDDD). Rapid Commun. Mass Spectrom. 29, 2257–2262 (2015).

Chapter 5 : *In Vitro* Metabolism and Potential Toxicity of Triacetone Triperoxide (TATP) in Canines

Status: Preparing for submission to Chemical Research in Toxicology

Abstract:

Many of the challenging analytical issues surrounding TATP analysis by LC-MS have been addressed in order to quantify *in vitro/in vivo* samples as low as 10 ng/mL (45 nM). Metabolism of TATP was determined in the liver microsomes of male beagle dogs (DLM) with a non-specific K_m of 2.21 μM and a V_{max} of 1.13 nmol/min/mg of protein based on substrate depletion. Only one metabolite, hydroxy-TATP (TATP-OH), was identified. Canine CYP2B11 was the only enzyme specifically determined to catalyze metabolism, but the degree to which it metabolized TATP was insufficient to account for observed DLM metabolism, suggesting more than one enzyme may be functioning. This metabolite disappears over extended incubation times, but no other metabolites were detected. Trapping of either hard or soft electrophilic products was unsuccessful. Similar work performed on MEKP indicated significant metabolism of the hydroperoxides and rapid oxidation of reduced glutathione (GSH). This suggests that TATP does not metabolically form any ring-opened or hydroperoxide product(s). The hydroxy metabolite was synthesized and tested for stability in DLM. At 10 μM concentration, TATP-OH metabolism progressed 3x more rapidly than TATP with no metabolites found or trapped. Chemical degradation of the metabolite, with acetone appearing to be trapped as a byproduct, proceeded in oxygenated pH 7.4 buffer much slower than did its metabolism. The metabolite (TATP-OH) was stable in all organic solvents tested. Data suggests that TATP and TATP-OH may be competitively competing for the same enzyme with TATP dominating this competition. The formation of a second

metabolite(s) that is either undetectable by MS/UV or covalently bound to a protein or polymer in the incubation reaction is very probable. The fate of this second metabolite(s) does not appear to affect TATP metabolism, but is currently still a mystery.

Introduction:

Every drug that is currently on the market has been thoroughly tested in multiple pre-clinical species to predict human exposure, metabolism and toxicity. While it is a common and necessary process to determine the toxicity of many poisons, toxins and toxicants by animal testing [1], alternative *in vitro* methods are constantly being developed or improved to reduce the need for this practice.[2][3] *In vitro* screening techniques have become integral in nearly every research area of the pharmaceutical industry from target identification to metabolism and toxicity.[2][4] Over several decades, a significant body of work correlating *in vitro* testing to *in vivo* results has been published.[5][6] These models are intended to predict what a chemical will do in humans based on the *in vitro*/*in vivo* correlation (IVIVC) with pre-clinical species. Some of these techniques can also be applied to the determination of human or animal hazards arising from environmental and/or occupational exposure to compounds with unknown biological effects. Determination of toxicity from continual exposure to new or different chemical entities is of great concern to the general public. This area of research has implications for both acute, short-term problems as well as long-term, genetic or epigenetic effects.[7][8]

For employees or people living in areas where environmental exposure to explosives may be unavoidable, knowledge of potential toxicity is essential. While some of the more common, older explosives such as trinitrotoluene (TNT) have been fully investigated for metabolism and subsequently found to have toxic metabolites [9][10], many of the newer or peroxide-based explosives have never been tested for toxicity. The peroxide-based explosives are easy to produce, sensitive to initiation, and relatively unstable; therefore, they are not used or produced by the military. However, with the ease of production and power of these explosives, they have become very appealing to those wishing to inflict damage and destruction.[11][12][13] Therefore, research into the formation and safe destruction of these compounds as well as applications for their trace detection must continue. Currently, canines are being trained to detect trace levels of peroxide explosives [14], (triacetone triperoxide, TATP and hexamethylene triperoxide diamine, HMTD) to mitigate terrorist risk in airports, train stations, etc. With that in mind, there may exist some significant risk of toxicity to both humans and canines from exposure to these compounds. No information on the metabolism or potential toxicity of these easy to produce homemade explosives (HME) currently exists.

Hydrogen peroxide is a reactive oxygen species (ROS) that is endogenously produced through many sources including, mitochondrial respiration [15], superoxide dismutase activity [16], and metabolism by P450 [17] or other oxidase enzymes.[18] While ROS are generally thought to be responsible for cellular damage, H_2O_2 is necessary for the redox regulation of many physiological processes.[15] The catabolism of this by catalase and enzymes like glutathione peroxidase are well

studied.[19][20][21] There is also a fair amount of work done on the metabolic fate of hydroperoxides [22][23], which, in the presence of cytochrome P-450 (CYP) and NADPH, react to provide an organic aldehyde and hydrogen gas or a ketone and free alkane (see Figure 5-1).[22]

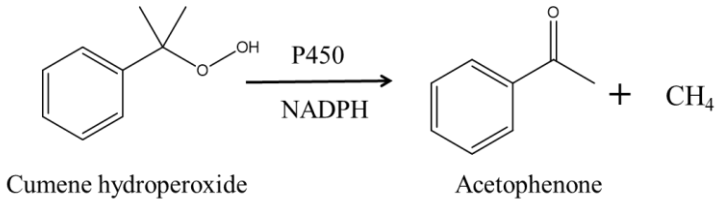

Figure 5-1. *NADPH-dependent P450 metabolism of cumene hyrdoperoxide.*

A significant body of work surrounds peroxidation of fatty acids and their degradation into volatile alkanes and aldehydes.[24][25] There is also much work done on the methylation of DNA from exposure to organic hydroperoxides, particularly in the presence of iron(II).[26][27] Certain oxidation states of selenium are known to be very reactive with hydroperoxides.[28] Selenocysteine (considered the 21st amino acid) integrated into enzymes like glutathione peroxidase are responsible for the anti-oxidizing effects by assisting in the conversion of hydrogen peroxide or lipid hydroperoxides into two water molecules or the lipid alcohol and one water molecule, respectively. This comes at the expense of two reduced glutathione (GSH) molecules being oxidized into GSSG.[29][30]

Whereas organic hydroperoxides are generally far too reactive to be used as forms of medicine [31], cyclic peroxides are used as anti-parasitic drugs, like artemisinin or its analogs.[32][33][34][35] One theory on cyclic peroxide drug

mechanism of action is that they are activated to carbon-centered radicals in the erythrocyte by iron(II) that has been freed by the actions of the parasite.[33][32][35] An alternative to the carbon-centered radical formation premise is a compelling theory involving cyclic peroxide oxidation of flavin cofactors, that disrupt the homeostasis of ROS removal by GSH and NADPH. With the parasites having no natural protection from ROS of their own, they rely on the host for protection. With the host now overburdened by ROS, the parasite is destroyed.[36][37] However, involvement of selenium-containing enzymes may also contribute to this process. Specific mechanisms notwithstanding, literature data would suggest that cyclic peroxides may be stable in the body and available for systemic circulation. When (and if) there is interaction with ferrous iron or some other agent that may initiate radical formation or two-electron reduction, significant toxicity or mutagenicity may occur, depending on where these molecules eventually reside. It should be noted that TATP was shown to be stable in the presence of iron(II) when solvated in tetrahydrofuran, but not in ethanol.[38]

While HMTD is not volatile [39] and is most likely detected by the scent of its degradation products,[40] TATP is quite volatile as an intact molecule and is known to sublime.[41] This would make inhalation the most likely route of exposure. Furthermore, with sensitive explosives, using gloves is generally not an acceptable practice as the static associated with nitrile or latex can cause them to initiate. With these compounds being rather lipophilic (log $P_{o/w}$: TATP = 3.21 and HMTD = 1.99), the risk of exposure due to absorption through the skin is rather high. Investigation of the metabolism of TATP and HMTD may determine if measures should be instituted

to mitigate exposure for both animals and humans working with these compounds. We have previously established that TATP vapor in a closed vessel exists at a concentration of about 375 μg/L[42]. With an average dog lung capacity of about 40 mL/Kg[43], a 30 Kg dog (~65 lbs), has a lung capacity of 1.2 L. A full breath would lead to an exposure of 450 μg. For humans, with a vital lung capacity of 4 to 5 L,[44] exposures in a closed room over a short time could lead to very large doses. As a forensic consideration, if TATP and HMTD are not extensively metabolized and are stable in the body, individuals producing large quantities of these materials for nefarious reasons may be identified by the analysis of small amounts of blood.

The analysis of TATP and HMTD by reverse phase liquid chromatography-mass spectrometry (LC-MS) is the most amenable means of separation and detection for aqueous-based samples of these molecules and their potential metabolites. Development of assays for these compounds have presented significant analytical challenges. For instance, LC-MS analysis of peroxides cannot have acetonitrile in the mobile phase solvent due to severe, direct, gas-phase ion suppression by the solvent.[45] While methanol is a better solvent for ionization, both HMTD[46] and TATP[42] react with alcohols in the gas phase depending on the conditions used. Since concentration of TATP solutions cannot be performed due to the volatility of TATP, it is fortunate that the chromatographic peak shape is relatively unaffected by high levels of strong solvent content in the injection plug. Also fortunate is that HMTD is not affected by solvent evaporation since its peak shape and sensitivity are tremendously altered by small changes to the organic content in the sample plug.[47] The fully deuterated TATP and HMTD molecules have been synthesized for use as an

internal standards (IS) in their analysis[42][47]. The work presented herein focuses strictly on TATP metabolism.

Materials and Methods:

Chemicals and Reagents

Caution: The organic peroxides mentioned below are powerful and sensitive explosives. Take all necessary precautions when working with these compounds. Water, acetonitrile, methanol, (all Optima HPLC grade), potassium phosphate, magnesium chloride ($MgCl_2$), ammonium acetate (NH_4OAc, HPLC grade), methyl ethyl ketone (MEK), semicarbazide (SC), 1-aminobenzotriazole (1-ABT), reduced glutathione (GSH), reduced nicotinamide adenine dinucleotide phosphate (NADPH) and acetone (ACS grade) were purchased from Fisher Chemical (Fair Lawn, NJ, USA). Microsomes, recombinant isoforms and cytochrome b5 were purchased from XenoTech (Kansas City, KS, USA). Deuterated d6-acetone was purchased from Cambridge Isotope Labs (Cambridge, MA, USA). Hydrogen peroxide (HP, 50%) was purchased from Univar (Redmond, WA, USA). All mobile phase used for chromatography consisted of aqueous 10 mM NH_4OAc prepared at neutral pH with methanol (MeOH) as the organic modifier unless otherwise stated.

TATP, TATP-OH and MEKP Synthesis:

Triacetone triperoxide (TATP) was synthesized following the literature methods with the exception that hydrochloric rather than sulfuric acid was used.[48] TATP was purified by recrystallizing once with 80/20 (w/w) MeOH/H_2O and then with pentane [melting point (mp) 94-96 °C]. Deuterated TATP (d_{18}-TATP) was synthesized as above using d_6-acetone. DADP was recrystallized in hot methanol (mp: 131-133 °C). TATP-OH was synthesized by mixing hydrogen peroxide (50% wt), acetone, and hydroxyacetone (2:1:1 mole ratio) at 0 °C. The reaction mixed overnight, warming to room temperature. The white solid was collected by vacuum filtration and rinsed with deionized water (mp: 85-87 °C). The solid contained a mixture of TATP and the hydroxylated TATP. Separation was achieved on a Teledyne Isco CombiFlash system with attached PurIon. The atmospheric pressure chemical ionization (APCI) source must be used for cyclic peroxides.[42] Separation was performed on a C-18 column using the same LC system as described below for TATP analysis with the flow rate at 4 mL/min rather than 250 µL/min. Structures of the synthesized TATP products are shown in Figure 5-2. as the ammonium adducts detected in the LC-MS system.

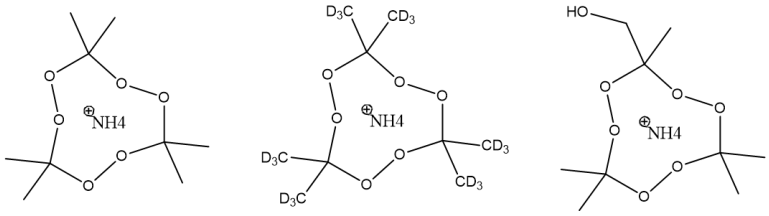

m/z 240.1442 m/z 258.2571 m/z 256.1391

Figure 5-2. *Structures of TATP, D18-TATP and TATP-OH ammonium adducts and their observed exact masses.*

Methyl ethyl ketone peroxides (MEKP) were synthesized by a modified literature method.[49] In a test tube containing a micro stir bar, hydrogen peroxide (50-wt%, 1.4 mL) was mixed with methyl ethyl ketone (0.82 mL, 9.49 mmol). The solution was chilled in an ice bath and concentrated H_2SO_4 (0.5 mL, 9.38 mmol) was added slowly so that the temperature did not exceed 20 °C. Stirring continued for 15-18 hours before the solution was extracted with pentane, washed with saturated ammonium sulfate (3x3 mL), deionized water (3x3 mL) and dried with sodium sulfate. The product was stored as a solution in pentane and was pipetted into tared vials for immediate dilution with MeOH to desired concentrations. Purification of individual MEKP was attempted, but to date has been unsuccessful. With no one specific MEKP structure or concentration, crude MEKP product was weighted and diluted to 10 mg/mL in MeOH. LC-MS detection of the observed products, primarily ammonium adducts of the proposed linear dihydroperoxide (DHP) dimer, trimer, tetramer and pentamer, were used to estimate an average molecular weight based on their relative intensities (346 g/mol, Supporting Information, Appendix 5). This sample was then diluted to the appropriate concentration to prepare incubations at ~30 μM.

Instrumentation

Using a Thermo Electron LTQ Orbitrap XL or Exactive mass spectrometer equipped with an APCI interface, ions were generated and introduced into the ion transfer tube set 275 ºC. All work was performed using positive ion mode. Tune conditions for APCI were as follows: discharge current, 5 μA; N_2 sheath gas, 40 arbitrary units (AU);

N_2 auxiliary gas, 20 AU; vaporizer temperature 250 ºC; ion transfer tube, 14 V; tube lens, 50 V; and skimmer offset (Exactive), 0 V. Minor voltage changes were made at times to improve signal intensity as needed. Mass resolution was set to 30000 (LTQ Orbitrap) and 50000 (Exactive) for all experiments. Solvent delivery was performed using a Thermo Electron Accela quaternary pump. A CTC Analytics HTS PAL autosampler injected directly from either amber, glass LC vials with PTFE septa (Agilent Technologies) or polypropylene, 1 mL 96-well plates with pre-slit silicone plate covers (Analytical Sales and Service). Data collection and analysis was performed with Thermo Xcalibur software version 2.2, SP 1.48. All data collected within this work is APCI full scan MS unless otherwise noted. Chromatographic traces are all extracted ion chromatograms (XIC) with a mass window of 15 ppm of the expected exact mass. *Note: All masses reported below are exact mass values within ±15 ppm for species less than 130 m/z and ±7.5 ppm for species over m/z 130*.

Methods

TATP Analysis

TATP and d18-TATP were monitored within a 15 ppm mass window of the $[M+NH_4]^+$ ions at m/z 240.1442 and m/z 258.2571, respectively. Sample injections of 40 µL in 50/50 ACN/water were injected into a LC flow of 250 µL/min with 5% MeOH (channel A) and 95% aqueous 10 mM NH_4OAc (channel B) for introduction onto a Thermo Syncronis C18 column (2.1 x 50 mm, 5 µm). Initial conditions were held for 1.5 minute before a linear ramp to 35% A/65% B over 1.5 minutes followed

immediately by a linear ramp to 95%A/5% B over the next minute. This concentration was held for 2 minutes before a 30 second transition to initial conditions with a hold of 1.5 minutes. As an internal standard (IS), d_{18}-TATP at 10 μg/mL (41.7 μM) in ACN was added 1:1 to aqueous TATP samples with a final concentration of 5000 ng/mL (20.8 μM). XIC were integrated using the Genesis peak detection algorithm in Thermo Xcalibur Quan Browser. Linear dynamic range comparing concentration to peak area response ratio, relative to the IS, extended from 25 ng/mL (112.6 nM) to 20000 ng/mL (90.1 μM) using 10 points and 1/x weighting of the calibration curve. Quality control (QC) samples were 75, 1500 and 15000 ng/mL. Stability determination for TATP stored in ACN has been previously determined.[42] All necessary dilutions were made in 50/50 ACN/water. An example calibration curve and QC data can be seen in the Supporting Information, Appendix 5. The same analytical procedure for TATP was used to quantify the synthesized TATP-OH. The LLOQ was 50 ng/mL, but linearity extended to only 5000 ng/mL.

TATP Volatility

Aqueous TATP samples at 37 °C in containers open to the atmosphere showed significant loss of compound due to evaporation.[42] Therefore, microsomal incubations had to be performed in closed containers. Oxygen gas was bubbled through the buffer matrix for several minutes prior to incubations to provide the required atmospheric O_2 for enzymatic reactions. Open and closed incubations of verapamil (1 mg/mL DLM protein) were shown to provide identical results using this

method (see Supporting Information, Appendix 5) with half-life of ~28 min and Cl_{int} ~ 25 µL/min/mg protein.

Microsomal Incubations

Samples were run in triplicate with TATP initiating each reaction. Incubations of 1mL were performed in a shaking reaction block at 37 °C in a single, closed, 1.5 mL, polypropylene Eppendorf snap-cap tube containing: 10 mM potassium phosphate buffer (pH 7.4 with oxygen gas bubbled in for 2 minutes); 2 mM magnesium chloride ($MgCl_2$); 1 mM reduced nicotinamide adenine dinucleotide phosphate (NADPH); 0.5mg/mL protein (579 pmol P450/mg protein); and 5 µL of TATP in acetonitrile (concentrations varied to keep organic content at 0.5 %). At time points of 0.5, 2, 4, 6, 8, 10 and 15 minutes for substrate concentrations >10 µM and 0.5, 1, 2, 3, 4, 5 and 6 minutes for concentrations <10 µM, tubes were opened and aliquots of 100 µL were placed into 100 µL of ice cold acetonitrile [containing internal standard (IS) for quantitative assays], vortex-mixed and centrifuged for 2 min at 14000 rpm before being transferred to a 96 well plate for direct injection of 40 µL onto the HPLC-MS system in duplicate. In parallel with each trial, samples of TATP in buffer were incubated and treated identically to account for the headspace evaporative loss associated with opening the tube at each time point (significant at concentration >10 µM). Evaporative loss data was then added to each metabolic loss data point to account for non-metabolic loss. Closed containers of TATP in buffer for up to 60 minutes showed no degradation of TATP when incubated at 37 °C. Verapamil was used as a positive control for microsomal activity.

Results and Discussion:

Initial interrogation of TATP metabolism was limited by poor detection limits for the analysis. With a lower limit of quantification (LLOQ) of only 500 ng/mL, we had to perform preliminary work with a substrate (TATP) incubation concentration of 100 μM in 1 mg/mL [protein] of dog liver microsome (DLM), knowing that this was probably above enzyme saturation. The obtained information was still useful as preliminary data on the Phase I metabolism. Only one metabolite, TATP-OH, was detected and identified as the hydroxylation of one of the primary methyl groups of TATP (Figure 5-2). A significant amount of the TATP remained intact. This product formation was NADPH-dependent and confirmed by incubation of the fully deuterated TATP. To perform any type of enzyme kinetics, incubations would require detection well below 1 μM (222 ng/mL). With that level being diluted in half with ACN/IS addition and our inability to concentrate the samples by evaporation, significant efforts to lower the detection limit were required. The target LLOQ was 10 ng/mL, approximately 10x less than the required 111 ng/mL needed for 1 μM incubations. Achieving this level was possible by adjusting the MS conditions and monitoring m/z 89.0597, the gas phase reaction product of TATP with MeOH.[42] However, to assure that related metabolites could also be detected we chose to look at the intact TATP

ammonium adduct at m/z 240.1442 which could now be detected with an LLOQ of 25 ng/mL.

With adequate assay conditions, incubations were then performed at 5, 10, 20, 30, 40, 50, 75 and 100 μM, initiating the analysis by the addition of NADPH. Due to significant daily variability in the data, closer analysis of the certain aspects of the procedure were investigated. It was considered that the TATP might be insoluble at higher buffer concentrations; therefore, 100 mM potassium phosphate was reduced to 10 mM. This had little effect on the results, but tests were continued with 10 mM concentration. Initiation of the reaction with NADPH was associated with approximately 5 to 15% decrease from the initial TATP concentrations. Additionally, detectable levels of the TATP-OH were present in the time zero samples, suggesting very rapid metabolism (approximately 20 seconds to add substrate, mix and sample). Varying protein concentration from 1 mg/mL to 0.5, 0.2 and 0.1 mg/mL did not account for this initial drop, but it was decided that 0.5 mg/mL provided data that was more manageable with regards to sampling times. Time zero was then specifically changed to 0.5 minutes. Speculations that NADPH or the magnesium ions in the $MgCl_2$ could react with the peroxide were investigated. Performing 10 μM TATP DLM incubations at $MgCl_2$ concentrations of 0, 2 and 5 mM and incubating TATP under three different conditions (in only $MgCl_2$; only NADPH; and $MgCl_2$ with NADPH) showed that neither magnesium nor NADPH were directly associated with TATP depletion. It was, however, observed that the rate of metabolism was higher with $MgCl_2$ present and that there was no difference between 5 and 2 mM $MgCl_2$. It might be possible that the addition of cold NADPH to the reaction causes the TATP to

precipitate. It was also speculated that the TATP might bind tightly in a specific enzyme pocket and addition of the NADPH reducing equivalent caused rapid metabolism that appeared as a drop in initial concentration. This latter speculation was dismissed since the subsequent metabolic rate was not consistent with this behavior and since the TATP-OH metabolite was not detected at levels corresponding to 5-15% production (as was confirmed later following TATP-OH synthesis). To date, this issue has never been resolved but was overcome by initiating reactions with the addition of TATP to the incubations already containing NADPH.

With these issues controlled, day to day variability was still unacceptable. Evaporation in the headspace of the tubes was the prime suspect. On several different days, incubation of two closed, aqueous TATP samples for 1 hour were performed. One sample remained closed the full hour and one was sampled every 15 minutes. Fortunately, there was no detectable substrate degradation, but significant sample loss (frequently > 3% depending on concentration) was observed due to the opening of the tubes for sampling. Attempting to perform separate incubations for each time point in individual tubes provided data with even more inconsistency. With many variables to affect specific evaporation at any given time, it was decided that every incubation would have an identical, parallel incubation performed in buffer alone. The concentration loss at each time point from these buffer-only incubations was added to the TATP concentrations from the metabolic incubation to account for non-metabolic TATP loss due to evaporation. Data for a single incubation trial at 50 μM TATP in DLM is shown in Figure 5-3. For determination of kinetics, three trials were

performed at each concentration. Using this method, results improved to an acceptable consistency.

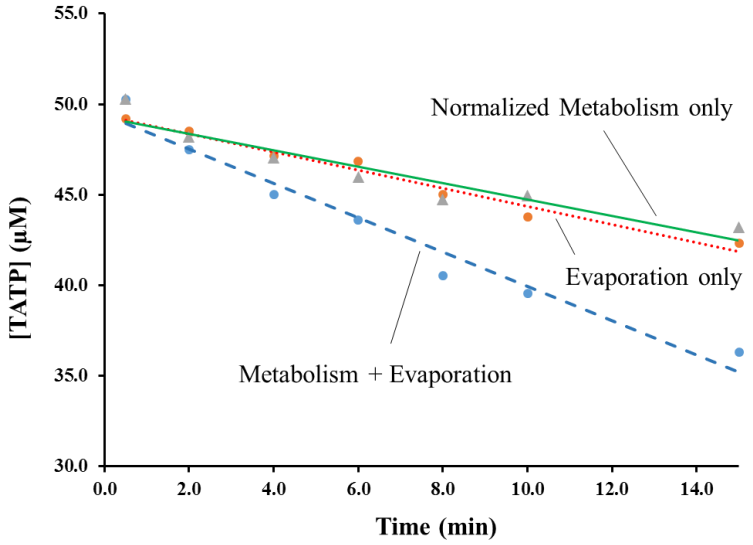

Figure 5-3. *Single trial incubation of 50 µM TATP in DLM showing data normalized for evaporation. Each data point represents the mean of 2 injections.*

Kinetics were assessed on initial substrate depletion at concentrations of 1, 2.5, 5, 10, 20, 30 and 50 µM in DLM. The Michaelis-Menten plot estimation of the non-specific K_m for TATP depletion is 2.21 µM (± 14.8%) with a V_{max} of 1.13 nmol/min/mg protein (± 3.27%) as seen in Figure 5-4. Plotting the kinetics of TATP loss during incubation in Michaelis-Menten, Lineweaver-Burk, and Hanes fashion (Figure 5-4), K_m of 2.21, 2.88, and 1.59 µM and V_{max} 1.13, 1.16 and 1.03 nmol/min/mg protein were obtained, respectively. Closer inspections of the Lineweaver-Burk plot suggested that a two-enzyme system may be functioning. Construction of separate plots for high and low TATP concentrations provided respective K_m values of 3.62 and 1.18 µM and V_{max} 1.19 and 0.89 nmol/min/mg

protein (see Supporting Information, Appendix 5). These values may be too close to definitively state that two enzymes were functioning. Half-life at 2.5 µM (close to K_m) was graphically calculated to be 3.82 minutes with an intrinsic clearance of 363 µL/min/mg protein (Supporting Information, Appendix 5). When sampling time was extended past 15 minutes at concentrations of 10 µM or higher, where TATP metabolism would begin to slow, the mono-oxidation product appeared to be further consumed with no secondary metabolite(s) observed. At concentrations of 50 µM or higher where TATP persisted at high levels past 30 minutes, the TATP-OH product response levels appear to be in a steady state (possible a balance between formation and destruction of the metabolite, see Figure 5-5). Addition of GSH to the reaction at any point in the incubation did not produce any product related to TATP. It was observed that, if anything, the addition of GSH slowed the metabolism of TATP. Considering that further oxidation of TATP-OH to the corresponding aldehyde may occur, SC was added to the reaction when TATP-OH formation appeared to plateau. No TATP-specific reaction products, including acetone, were detected.

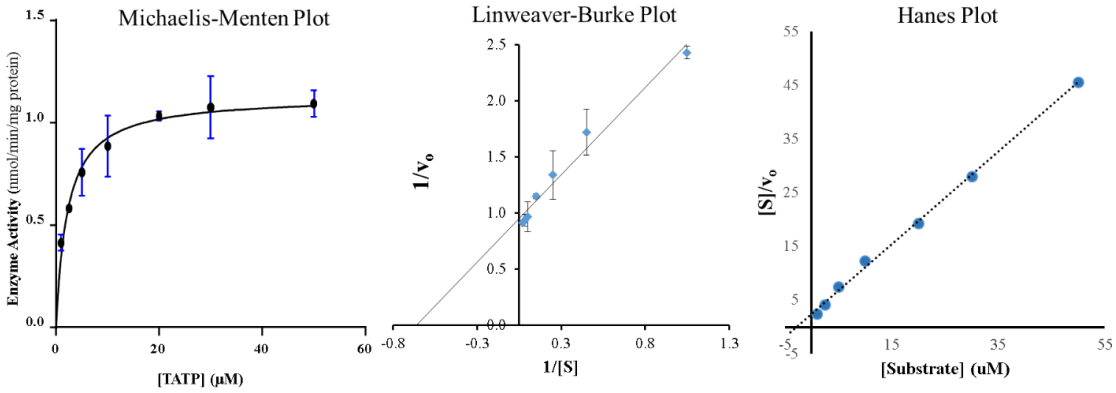

Figure 5-4. *Michaelis-Menten plot (GraphPad Prism (v. 7.03)), Lineweaver-Burk Plot and Hanes Plot (Microsoft Excel) for TATP non-specific metabolism in DLM.*

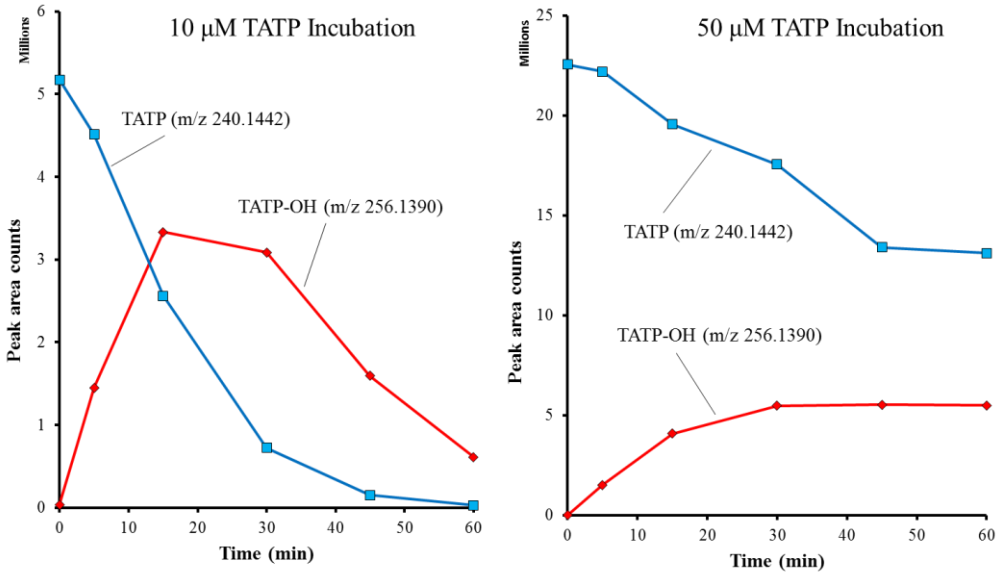

Figure 5-5. *Average peak area counts for TATP and TATP-OH incubated at 10 and 50 µM in DLM for 60 minutes at 37 °C. Area counts are in millions.*

Incubations were then performed with recombinant P450 isoforms for dog (rCYP 3A12, 1A2, 2D15, 2C21 and 2B11) covering ~85% of dog liver P450[50]. A constant P450 concentration of 100 pmol/mL of each rCYP was compared with identical pooled DLM incubations using 200 pmol/mL total [P450]. A constant concentration of 2.5 µM TATP (close to the Km) was incubated for 5 minutes (N=3) in each rCYP as described above. Data (Figure 5-6) suggests that only rCYP2B11 participated in the metabolism of TATP to TATP-OH with only about 15% conversion compared to ~40% turnover in DLM. If we estimate the DLM contain ~18% CYP2B11, this only accounts for about 5-6% of the 40% metabolized. With cytochrome b5 not available in the rCYP's for canines, human CYP b5 was added at

rCYP2B11 at 5x the P450 concentration (as recommended by the vendor) and reanalyzed. The resulting data showed little change from rCYP 2B11 alone at 5 minutes. However, when incubations were carried out to 10 minutes, 30% of the TATP was metabolized in the rCYP2B11 with b5 (compared with little change to rCYP2B11 alone, Figure 5-6). This would support the Lineweaver-Burk kinetic plot suggesting that multiple enzymes may participate in the oxidative metabolism of TATP.

Several experimental conditions were designed in an attempt to identify the actors in TATP metabolism. Although flavin-containing monooxygenase (FMO) enzymes are unlikely to participate in TATP oxidation, their involvement was considered, as cyclic peroxide interaction with flavoenzymes are suspected with anti-parasitics.[36] There was with no evident change to the metabolism when performing the DLM incubation at a temperature (45 °C) known to deactivate FMOs. With the high affinity and low capacity for metabolism, it is possible that the metabolism is perpetrated by a CYP that constitutes a minor portion of the total P450 content in DLM. An attempt was made to deactivate all P450 enzymes by pretreatment with 1-mM ABT, although it has been reported that 1-ABT fails to inhibit all P450.[51] Pretreatment of the microsomes with 1mM 1-ABT did not change the metabolism of TATP.

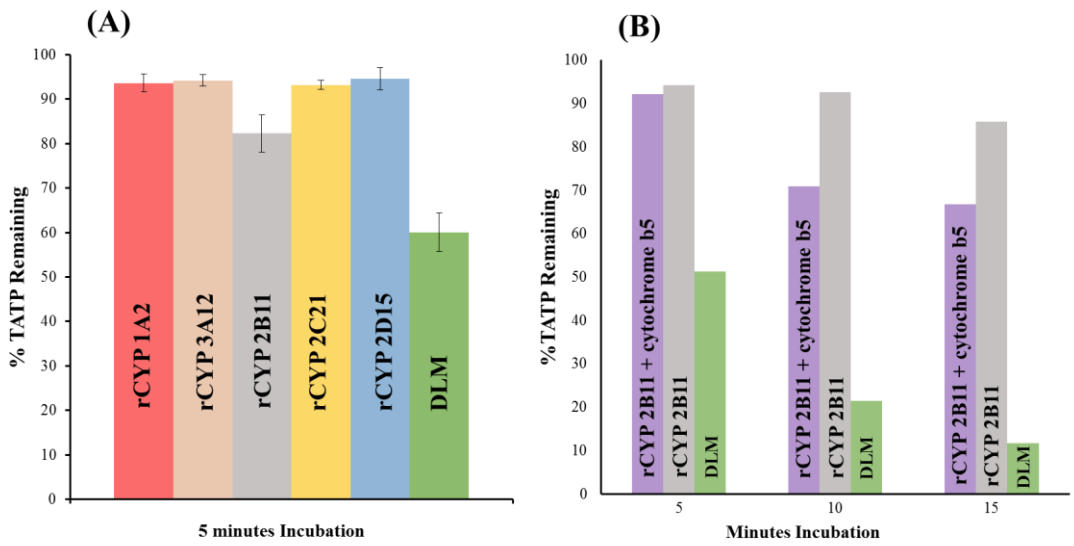

Figure 5-6. *Remaining % TATP following 5 minutes incubation of 2.5μM substrate in 100 pmol/mL rCYP P450 or 200 pmol/mL P450 in DLM (A) and rCYP2B11(50 pmol/mL) run with and without cytochrome b5 (250 pmol/mL) and DLM (200 pmol/mL) for 5, 10 and 15 minutes (B).*

To determine if systemic exposure would been issue, dog lung microsomes (DLgM) were incubated with 2.5 μM TATP. Negligible metabolism was observed compared to DLM. Figure 5-7 compares the formation to the TATP-OH metabolite in dog liver and lung microsomes. The TATP loss is difficult to distinguish from evaporative loss in lung microsomes. This data suggests that TATP could have significant systemic exposure in canines.

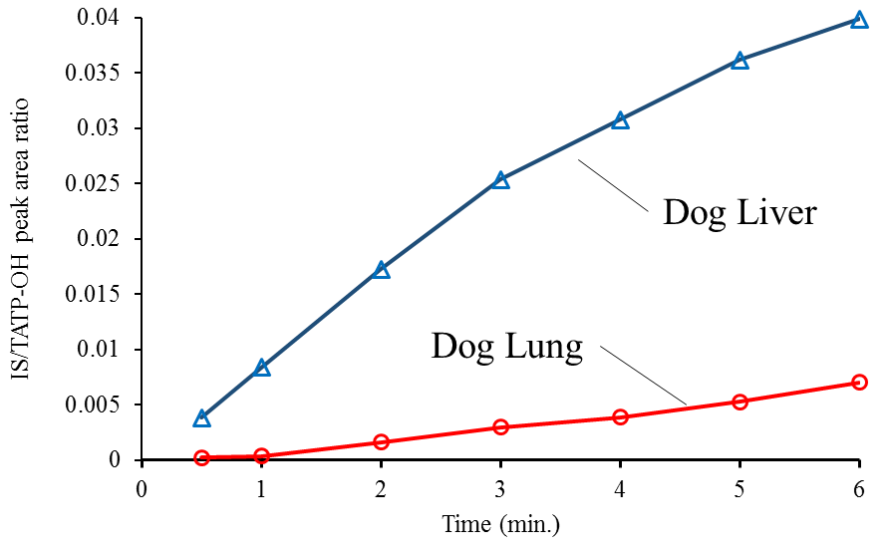

Figure 5-7. *Ratio of TATP-OH/IS peak area ratios from incubation of 2.5 μM TATP in dog liver and lung microsomes.*

It was determined that identifying the fate of the TATP molecule would be a more valuable use of resources than trying to determine specific enzymes. To evaluate the possibility that the TATP ring may open to produce a free hydroperoxide, we began to investigate the effects of MEKP metabolism. Incubations of ~30 μM MEKP in DLM were performed with and without NADPH, and in the presence of both GSH and SC. The metabolism of each polymer showed an NADPH-dependent formation of methyl ketone products suggesting that ethane is exclusively lost (not methane). Addition of SC showed many related products corresponding to this metabolism as well as a large signal for trapped MEK (m/z 130.0975). It may be that either MEK is a direct metabolic product or that metabolism initiates the degradation into MEK. These peaks were not detected with SC added to MEKP crude standard and only to a minor degree without NADPH addition. Glutathione however, was highly reactive with

MEKP with or without the presence of enzymes or NADPH. In each sample, all MEKP products eventually disappeared and the oxidized glutathione (GSSG) was extensively formed (Scheme 5-1). Retrospective analysis of TATP incubations with GSH or SC show no sign of the oxidized GSSG or of SC-trapped acetone. This lack of analogous reactivity with TATP suggests that only linear hydroperoxides participate in these reactions and TATP ring-opening does not occur under the conditions tested.

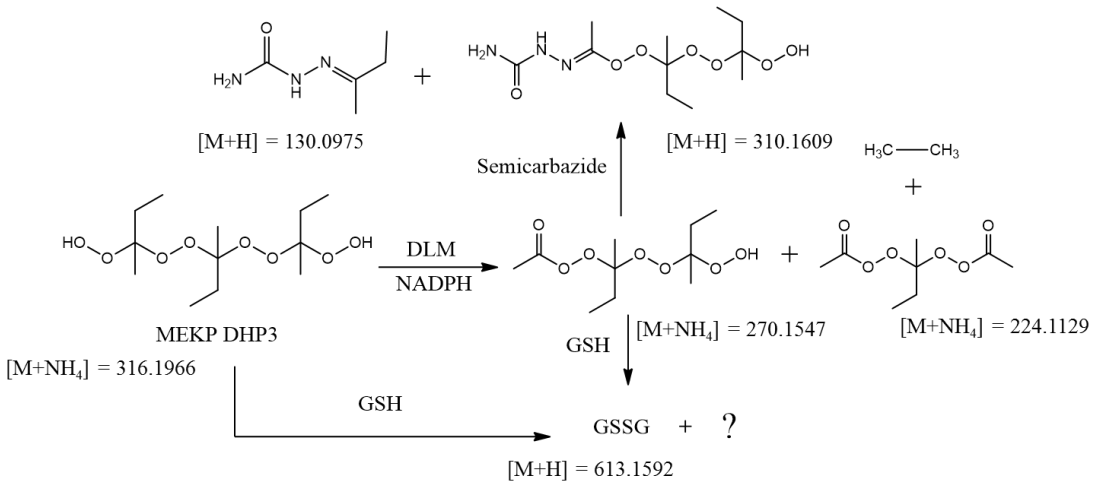

Scheme 5-1. *Reaction pathway of MEKP (dihydroperoxide trimer) under various conditions.*

Attempts to chemically synthesize and purify the metabolite of TATP provided a small quantity of compound with the same exact mass, chromatographic retention time and product ion spectrum as the TATP-OH metabolite. Both this compound and the metabolite react with methanol in the gas phase to produce a large product at m/z 105.0546, the oxidized product corresponding to m/z 89.0597.[42] This was enough supporting evidence to conclude that the synthesis was successful. Initially, we tested

this compound for volatility and found that TATP-OH was not volatile in an aqueous environment, but under certain conditions it was not stable. Upon incubation at 37 °C in oxygenated buffer for one hour, TATP-OH was mostly degraded. To see if this compound was stable in our storage solution (ACN) and other matrices, we incubated it in several solutions—MeOH, ACN, water, buffer and buffer with SC—in closed containers for 60 minutes. The results (Table 5-1) indicated that approximately 50% of the TATP-OH degraded every 15 minutes in the oxygenated buffer solution. Fortunately, it did appear to be more stable in pure water and very stable in organic environments. When SC was added to the oxygenated buffer, at 60 minutes, only 70% of the TATP-OH was gone but an appreciable increase in the amount of SC-trapped acetone (m/z 116.0818) was observed (Table 5-2). While the SC-trapped acetone did significantly increase with TATP-OH incubated for 60 minutes, some m/z 116.0818 was present in all buffer samples with SC added (but not in SC samples placed in water only). This could be the traces of acetone remaining from the synthesis of TATP or TATP-OH, but signal was detected in the oxygenated phosphate buffer with SC added. This cast some doubt on the SC trapping experiments.

Table 5-1. *TATP-OH percent remaining following incubation at 37 °C.*

Incubation Time (min)	Oxygenated Buffer			ACN	MeOH	Water
	Closed	Open	Closed			
0.5	100	100	100	100	100	100
15	57	47				

30	31	25				
45	16	13				
60	8.9	7.3	10	100	99	63

Table 5-2. *TATP-OH acetone trapping with semicarbazide. Data is presented as the ratio of signal to d18-TATP added as an internal standard.*

TATP-OH	SC-trapped Acetone
T0	0.375
T60	1.849

Buffer only	SC-trapped Acetone
T0	0.464
T60	0.483

Although acetone $[M+H]^+$ (m/z 59.0491) had not been detected in our samples (possibly due to the LC/MS conditions), it was now suspected to be a chemical degradant of the primary metabolite (if not a direct metabolite). To probe this issue, metabolism of 10 μM TATP and 20 μM d18-TATP were tested in DLM with attempts to trap the acetone or d6-acetone. Incubations in microsomes (0.5 or 1mg/mL protein concentration, respectively) were performed followed by addition of SC after 30 minutes. In the case of d18-TATP, the indication of d6-acetone formation would be the SC-trapped product at m/z 122.1195. This was confirmed by adding SC to a solution of d6-acetone, which produced a large, early eluting peak at m/z 122.1195. Placing SC in d18-TATP with only buffer produced a strong signal for m/z 122, presumably due to remaining d6-acetone from the synthesis of the deuterated

compound. When d18-TATP was incubated with the microsomes, at 30, 31 (after addition of SC) and 60 minutes, d17-TATP-OH was formed with at very consistent concentrations for all 3 time points. The signal for SC-trapped d6-acetone was observed to be less than that of the buffer only experiment at 31 minutes of incubation. It is likely that the residual acetone was metabolized away, but no other SC-trapped products based on known acetone metabolism (acetol and methyglyoxal) [52][53] were detected. Following an additional 30 minutes of incubation, it appears as though the signal for m/z 122.1195 increased by about 25%, suggesting that acetone may be produced (see Table 5-3). However, this may be due to previously observed chemical degradation and not metabolism. The results for TATP and SC were inconclusive since the m/z 116.0818 was significant in all SC-containing samples tested.

Table 5-3. *Metabolism of d18-TATP to d17-TATP-OH and subsequent trapping with semicarbazide. Data is presented as the ratio of signal to TATP added as an internal standard.*

	Buffer Only	d17-TATP-OH	SC-trapped d6-Acetone
SC added	T0	0	0
	T30	0	0
	T31	0	0.8934
	T60	0	0.6871

	DLM	d17-TATP-OH	SC-trapped d6-Acetone
SC added	T0	0	0
	T30	0.0616	0
	T31	0.0806	0.2428
	T60	0.0680	0.5464

Incubation of TATP-OH was then performed in DLM at a concentration of 10 μM and compared to a similar incubation of TATP. Figure 5-8 indicates that when TATP is incubated, its concentration and that of its metabolite TATP-OH are equivalent in 10 minutes. The profile was consistent with previous data (Figure 5-5). The non-metabolic degradation of TATP-OH matched the metabolism of TATP surprisingly well. While the TATP-OH chemically degrades with a half-life of about 15 minutes in solution, metabolically its half-life is closer to 5 minutes (although probably experiencing non-linear kinetics at this concentration). Despite this rapid metabolism, no metabolites were detected from the TATP-OH incubation in DLM.

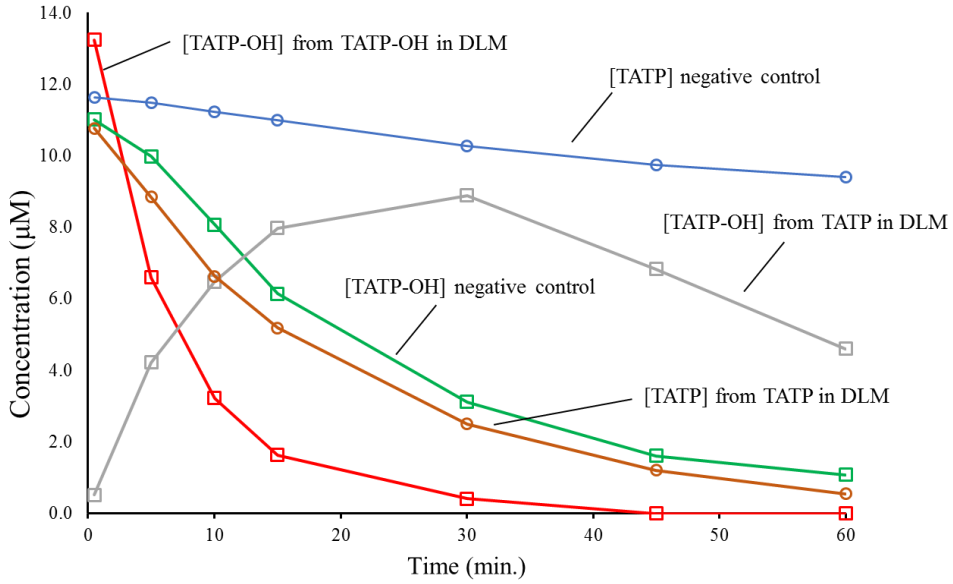

Figure 5-8. *Incubation of 10 μM TATP or TATP-OH in DLM.*

Figure 5-8 allows comparison of the various rates of formation and disappearance of TATP-OH along with loss of TATP. The TATP negative control (evaporation only, blue) and TATP-OH chemical degradation (green) in oxygenated buffer is significantly slower than their corresponding metabolic losses. TATP-OH

metabolic loss (red) appears significantly faster than TATP metabolic loss (brown). This makes the rise in [TATP-OH] in the initial 20 minutes of reaction (grey) puzzling. One explanation is that TATP occupies the same site or blocks the site where TATP-OH is metabolized. Quantification of each species showed that TATP-OH formed as the result of TATP metabolism (grey) could be added to the TATP metabolic loss curve (brown) to achieve a mass balance out to about 15 minutes. At this point, the sum of these two ions no longer totals to initial concentration. The rate of total loss appears much closer to the TATP-OH degradation rate than the metabolic rate, suggesting TATP is metabolized and TATP-OH is chemically degraded. However, with the metabolism of TATP-OH being so rapid, it is unlikely that no metabolism of this metabolite occurs.

To investigate the possibility of any time-dependent inhibition of either TATP or TATP-OH resulting from a second metabolite, the following experiment was performed. An incubation of 10 μM TATP-OH (5 μL ACN organic) and a blank of 5 μL of ACN were incubated in DLM. After 20 minutes, TATP (10 μM) was added to each incubation, and samples were analyzed at 0, 2, 4, 6, 10 and 15 minutes. The rate of TATP loss proceeded identically for both incubations. Also, both pre-treated and non-pre-treated samples produced very similar final concentrations of TATP-OH in 15 minutes. Since there was probably TATP-OH remaining in the pre-incubated samples, the rate of TATP-OH formation in these samples appeared to be nearly half that of the non-pretreated samples (Figure 5-9). This may suggest that the V_{max} for TATP-OH metabolism is constant with and without TATP present. Data indicates that neither TATP-OH nor its undiscovered metabolite(s) interfere with the metabolism of TATP.

Addition of SC after 20 minutes of TATP incubation in DLM showed no SC-trapped products, including the SC-trapped acetone.

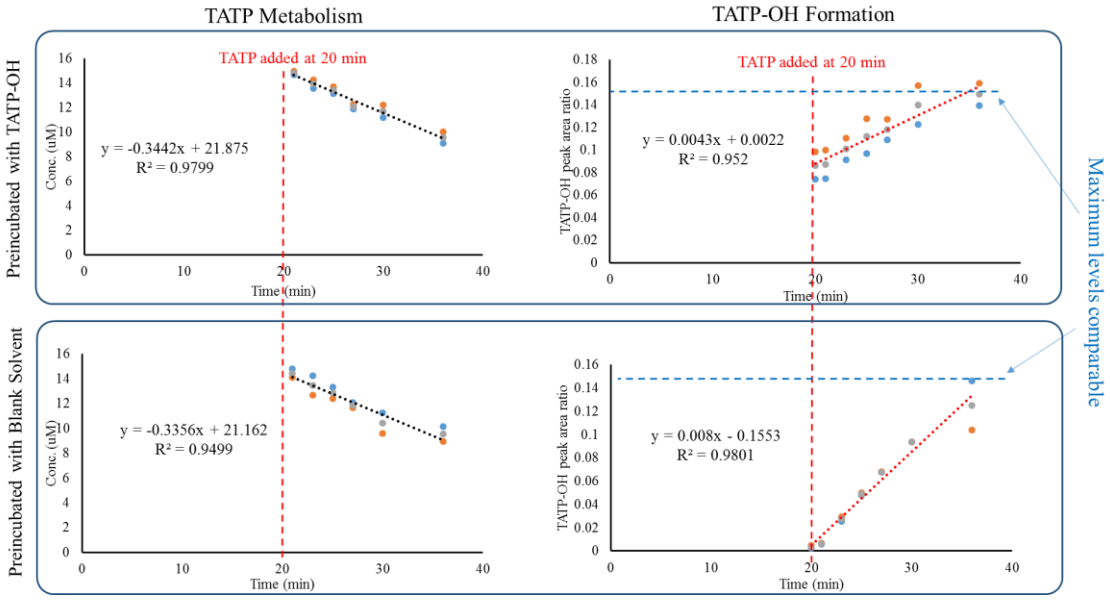

Figure 5-9. *Concentration or signal response for TATP and TATP-OH, respectively, following a 10 μM TATP incubation in DLM with and without preincubation of TATP-OH for 20 minutes.*

While data suggests that TATP-OH degrades into acetone in solution, there appears to be no evidence that it is metabolized into acetone. The loss of the TATP-OH metabolite could be due to complete degradation of the molecule into products smaller than acetone. It could also be due to some non-specific binding of a yet undiscovered, second metabolite to a protein or other material within the system.

With TATP-OH metabolism being considerably more rapid than that of TATP, the question becomes, why is the formation and buildup of TATP-OH observed? Incubations of TATP, TATP-OH and a mixture of TATP plus TATP-OH (all performed with 5 μM concentrations) in DLM provided very interesting results

(Figure 5-10). In both the TATP and TATP+TATP-OH incubations, the rate of TATP depletion was nearly identical. TATP-OH alone showed an initial metabolic depletion rate approximately 1.5 times faster than that of TATP. Mixing TATP with TATP-OH showed an initial formation rate of TATP-OH (exceeding the 5 μM initial concentration) to be nearly identical to the initial formation rate of TATP-OH in the TATP only incubation. This formation of TATP-OH in the mixture plateaued quickly (between 4 and 6 minutes). This data indicates that TATP-OH and TATP are probably metabolized by the same enzyme (if not the same enzymatic pocket), otherwise, buildup of TATP-OH would not be observed due to its faster metabolism that TATP. Reversible competitive inhibition is the most likely mechanism of TATP-OH inhibition as the K_m is clearly increased in the presence of TATP and is also very likely that the V_{max} is unaffected. This study would also support that as TATP is metabolized into TATP-OH, the metabolite does not greatly affect TATP metabolism until concentrations significantly exceed that of TATP.

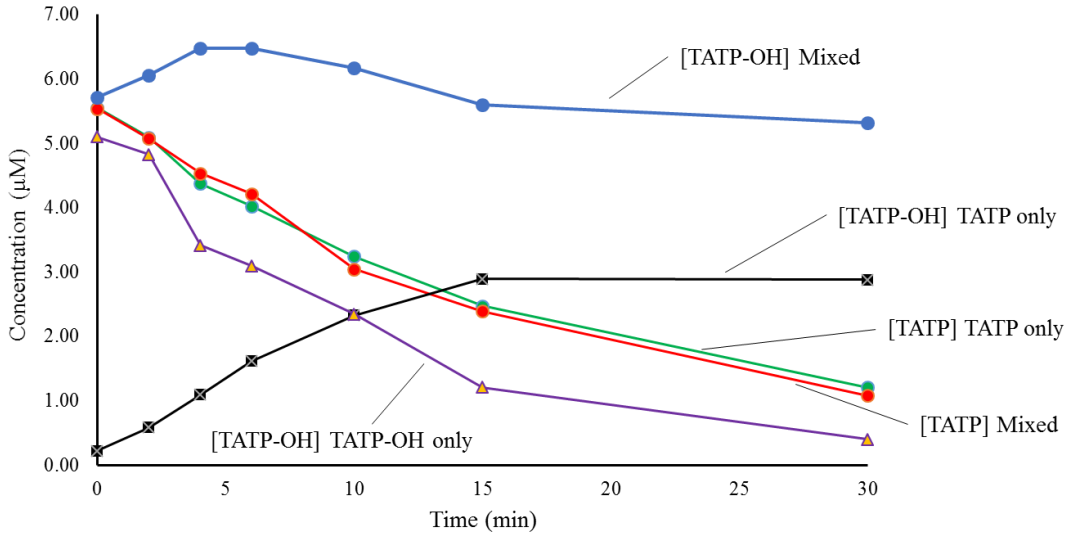

Figure 5-10 *TATP and TATP-OH concentrations following incubations in DLM of TATP, TATP-OH and a mixture of both (termed Mixed, all compounds incubated at 5 µM).*

Alternatively, but less likely, TATP may block TATP-OH from entering a site on a different enzyme. To test this hypothesis, TATP-OH was incubated at 5 µM concentration in each of the five recombinant CYP isoforms along with DLM and buffer only. The results (Figure 5-11) confirm that only rCYP2B11 metabolizes TATP-OH, consistent with the results for TATP (Figure 5-6). All other rCYP isoforms showed about 20% reduction of TATP-OH, similar to the chemical degradation observed in buffer only. Since this was the only enzyme found to metabolize TATP-OH and it was very similar to the DLM, it may be fair to say that only CYP2B11 metabolizes TATP-OH and that TATP dominates a competition for this enzyme. While reversible competitive inhibition seems likely, determining the specific mechanism may not be easily performed since the initial substrate is also the metabolic inhibitor of its only metabolite.

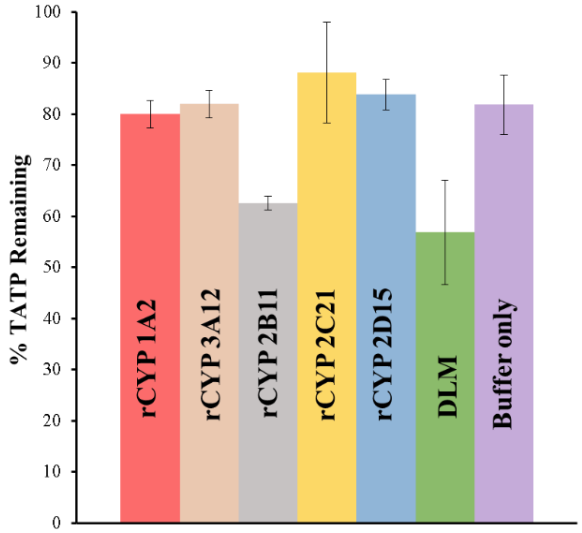

Figure 5-11. *TATP-OH incubated for 5 minutes in rCYP isoforms, DLM and buffer only at 5 µM substrate concentration.*

Conclusions:

TATP metabolism was characterized in canine liver microsomes. Only one hydroxylated metabolite was detected. Although the clearance was high, the low capacity of metabolism suggests that large exposure to TATP vapor could lead to significant systemic exposure. This is could be further evidenced by the lack of lung microsomal activity, since inhalation is the most likely route of exposure. With the assumption that absorption would not be much of a barrier, TATP may be sequestered in cells (and toxic) if its clearance does not progress by other means (cytosolic or Phase II metabolism). While TATP may be metabolized by more than one enzyme in

the microsomes, only CYP2B11 (in conjunction with cytochrome b5) was identified. Its only detected metabolite, TATP-OH, is metabolized by the same enzyme (CYP2B11 only) and TATP appears to dominate a reversible competitive inhibition of the TATP-OH metabolism. By comparing the TATP and TATP-OH levels following a 10 μM TATP incubation, their concentrations combine to account for all TATP initially added until approximately 15 minutes when the sum of these concentrations both begin to disappear. The data suggests that another metabolite is formed that is either not detected or non-specifically binds with some protein or other material related to the system. Whatever the fate of this second, unknown metabolite, it does not appear to affect the metabolism of TATP or TATP-OH, but its lack of detection is suggestive of high reactivity.

References:

1. Nuffield Council on BioEthics: Animal use in toxicity studies. (2005)
2. Parasuraman, S.: Toxicological screening. J. Pharmacol. Pharmacother. 2, 74–79 (2011). doi:10.4103/0976-500X.81895
3. Pearson, R.M.: In-vitro techniques: Can they replace animal testing? Hum. Reprod. 1, 559–560 (1986). doi:10.1093/oxfordjournals.humrep.a136473
4. Hughes, J.P., Rees, S.S., Kalindjian, S.B., Philpott, K.L.: Principles of early drug discovery. Br. J. Pharmacol. 162, 1239–1249 (2011). doi:10.1111/j.1476-5381.2010.01127.x
5. Emami, J.: In vitro - In vivo Correlation: From Theory to Applications. J.

Pharm. Pharm. Sci. 9, 31–51 (2006)

6. Amidon, G.L., Lennernäs, H., Shah, V.P., Crison, J.R.: A Theoretical Basis for a Biopharmaceutic Drug Classification: The Correlation of in Vitro Drug Product Dissolution and in Vivo Bioavailability, (1995)
7. Vineis, P., Ahsan, H., Parker, M.: Genetic screening and occupational and environmental exposures. Occup. Environ. Med. 62, 657–662 (2005). doi:10.1136/oem.2004.019190
8. Zhang, X., Lin, S., Funk, W.E., Hou, L.: Environmental and occupational exposure to chemicals and telomere length in human studies. Occup. Environ. Med. 70, 743–749 (2013). doi:10.1136/oemed-2012-101350
9. Channon, H.J., Mills, G.T., Williams, R.T.: The Metabolism of 2:4:6-trinitrotoluene (a-T.N.T.). Biochem. J. 38, 70–85 (1944)
10. Buedingg, E., Jolliffe, N.: METABOLISM OF TRINITROTOLUENE (TNT) IN VITRO. J. Pharmacol. Exp. Ther. 30–312 (1946)
11. Don Van Natta, J., Sciolino, E., Grey, S.: Details Emerge in British Terror Case. New York Times.
12. Bradley J. Fikes: REGION: Escondido “bomb house” controlled burn a model for nation, expert says. San Diego Union-Tribune. http://www, (2012)
13. Morris, S.: Terror suspect student “had suicide vest and explosives.” The Gaurdian.
14. Oxley, J.C., Smith, J.L., Moran, J., Nelson, K., Utley, W.E.: Training dogs to detect Triacetone Triperoxide. In: Proceedings of SPIE - The International Society for Optical Engineering (2004)

15. Boveris, A., Cadenas, E.: Mitochondrial production of hydrogen peroxide regulation by nitric oxide and the role of ubisemiquinone. IUBMB Life. 50, 245–250 (2000). doi:10.1080/15216540051080912

16. Hayyan, M., Hashim, M.A., Alnashef, I.M.: Superoxide Ion: Generation and Chemical Implications. Chem. Rev. 116, 3029–3085 (2016). doi:10.1021/acs.chemrev.5b00407

17. Karuzina, I.I., Archakov, A.I.: Hydrogen peroxide-mediated inactivation of microsomal cytochrome P450 during monooxygenase reactions. Free Radic. Biol. Med. 17, 557–567 (1994). doi:10.1016/0891-5849(94)90095-7

18. Kundu, T.K., Hille, R., Velayutham, M., Zweier, J.L.: Characterization of superoxide production from aldehyde oxidase: An important source of oxidants in biological tissues. Arch. Biochem. Biophys. 460, 113–121 (2007). doi:10.1016/j.abb.2006.12.032

19. Bayne, A.-C.V., Mockett, R.J., Orr, W.C., Sohal, R.S.: Enhanced catabolism of mitochondrial superoxide/hydrogen peroxide and aging in transgenic *Drosophila*. Biochem. J. 391, 277–284 (2005). doi:10.1042/BJ20041872

20. Jones, D.P., Eklöw, L., Thor, H., Orrenius, S.: Metabolism of hydrogen peroxide in isolated hepatocytes: Relative contributions of catalase and glutathione peroxidase in decomposition of endogenously generated H2O2. Arch. Biochem. Biophys. 210, 505–516 (1981). doi:10.1016/0003-9861(81)90215-0

21. Martins, D., English, A.M.: Catalase activity is stimulated by H2O2 in rich culture medium and is required for H2O2 resistance and adaptation in yeast.

Redox Biol. 2, 308–313 (2014). doi:10.1016/j.redox.2013.12.019

22. Vaz, A.D.N., Coon, M.J.: Hydrocarbon formation in the reductive cleavage of hydroperoxides by cytochrome P-450. 84, 1172–1176 (1987)

23. Chefson, A., Zhao, J., Auclair, K.: Replacement of natural cofactors by selected hydrogen peroxide donors or organic peroxides results in improved activity for CYP3A4 and CYP2D6. ChemBioChem. 7, 916–919 (2006). doi:10.1002/cbic.200600006

24. Degousee, N., Triantaphylides, C., Starek, S., Iacozio, G., Martini, D., Bladier, C., Voisine, R., Montillet, J.-L.: Measurement of Thermally Produced Volatile Alkanes: An Assay for the Plant Hydroperoxy Fatty Acid Evaluation. Anal. Biochem. 224, 524–531 (1995)

25. Litov, R.E., Matthews, L.C., Tappel, A.L.: Vitamine E Protection against in Vivo Peroxidation Initiated n Rats by Methyl Ethyl Ketone Peroxide as Monitored by Pentane. Toxicol. Appl. Pharmacol. 55, 96–106 (1981)

26. Hix, S., Kadiiska, M.B., Mason, R.P., Augusto, O.: In vivo metabolism of tert-Butyl hydroperoxide to methyl radicals. EPR spin-trapping and DNA methylation studies. Chem. Res. Toxicol. 13, 1056–1064 (2000). doi:10.1021/tx000130l

27. Hix, S., Augusto, O.: DNA methylation by tert -butyl A role for the transition metal ion in the production of DNA base adducts. 118, 141–149 (1999)

28. Młochowski, J., Brząszcz, M., Giurg, M., Palus, J., Wójtowicz, H.: Selenium-Promoted Oxidation of Organic Compounds: Reactions and Mechanisms. European J. Org. Chem. 2003, 4329–4339 (2003). doi:10.1002/ejoc.200300230

29. Tapiero, H., Townsend, D.M., Tew, K.D.: The antioxidant role of selenium and seleno-compounds. Biomed. Pharmacother. 57, 134–144 (2003). doi:10.1016/S0753-3322(03)00035-0

30. Tinggi, U.: Selenium: Its role as antioxidant in human health. Environ. Health Prev. Med. 13, 102–108 (2008). doi:10.1007/s12199-007-0019-4

31. Bozdemir, M.N., Yildiz, M., Seyhanli, E.S., Gurbuz, S., Kilicaslan, I., Karlidag, T.: Narrowing of airway caused by ingestion of methyl ethyl ketone peroxide. Hum. Exp. Toxicol. 30, 2002–2006 (2011). doi:10.1177/0960327111407230

32. Muraleedharan, K.M., Avery, M.A.: Progress in the development of peroxide-based anti-parasitic agents. Drug Discov. Today. 14, 793–803 (2009). doi:10.1016/j.drudis.2009.05.008

33. Jefford, C.W.: New developments in synthetic peroxidic drugs as artemisinin mimics. Drug Discov. Today. 12, 487–495 (2007). doi:10.1016/j.drudis.2007.04.009

34. Opsenica, D.M., Šolaja, B.A.: Antimalarial peroxides. J. Serbian Chem. Soc. 74, 1155–1193 (2009). doi:10.2298/JSC0911155

35. Antoine, T., Fisher, N., Amewu, R., O'Neill, P.M., Ward, S.A., Biagini, G.A.: Rapid kill of malaria parasites by artemisinin and semi-synthetic endoperoxides involves ROS-dependent depolarization of the membrane potential. J. Antimicrob. Chemother. 69, 1005–1016 (2014). doi:10.1093/jac/dkt486

36. Haynes, R.K., Cheu, K.W., Chan, H.W., Wong, H.N., Li, K.Y., Tang, M.M.K., Chen, M.J., Guo, Z.F., Guo, Z.H., Sinniah, K., Witte, A.B., Coghi, P., Monti, D.: Interactions between Artemisinins and other Antimalarial Drugs in Relation

to the Cofactor Model-A Unifying Proposal for Drug Action. ChemMedChem. 7, 2204–2226 (2012). doi:10.1002/cmdc.201200383

37. Ramasarma, T.: Generation of H2O2 in biomembranes. Biochim. Biophys. Acta - Rev. Biomembr. 694, 69–93 (1982). doi:https://doi.org/10.1016/0304-4157(82)90014-4

38. Oxley, J.C., Smith, J.L., Huang, J., Luo, W.: Destruction of peroxide explosives. J. Forensic Sci. 54, 1029–1033 (2009). doi:10.1111/j.1556-4029.2009.01130.x

39. Oxley, J.C., Smith, J.L., Luo, W., Brady, J.: Determining the vapor pressures of diacetone diperoxide (DADP) and hexamethylene triperoxide diamine (HMTD). Propellants, Explos. Pyrotech. 34, 539–543 (2009). doi:10.1002/prep.200800073

40. Oxley, J.C., Smith, J.L., Porter, M., McLennan, L., Colizza, K., Zeiri, Y., Kosloff, R., Dubnikova, F.: Synthesis and Degradation of Hexamethylene Triperoxide Diamine (HMTD). Propellants, Explos. Pyrotech. 41, 334–350 (2016). doi:10.1002/prep.201500151

41. Oxley, J.C., Smith, J.L., Shinde, K., Moran, J.: Determination of the Vapor Density of Triacetone Triperoxide (TATP) Using a Gas Chromatography Headspace Technique. Propellants, Explos. Pyrotech. 30, 127–130 (2005). doi:10.1002/prep.200400094

42. Colizza, K., Yevdokimov, A., McLennan, L., Smith, J.L., Oxley, J.C.: Reactions of Organic Peroxides with Alcohols in Atmospheric Pressure Chemical Ionization—the Pitfalls of Quantifying Triacetone Triperoxide

(TATP). J. Am. Soc. Mass Spectrom. In Press, (2017). doi:10.1007/s13361-017-1836-3

43. Minh, V.D., Dolan, G.F., Brach, B.B., Moser, K.M.: Functional residual capacity and body position in the dog. J. Appl. Physiol. 44, 291–296 (1978). doi:10.1152/jappl.1978.44.2.291

44. Barrett, K., Brooks, H., Boitano, S., Barman, S.: Ganong's Review of Medical Physiology. (2010)

45. Colizza, K., Mahoney, K.E., Yevdokimov, A. V., Smith, J.L., Oxley, J.C.: Acetonitrile Ion Suppression in Atmospheric Pressure Ionization Mass Spectrometry. J. Am. Soc. Mass Spectrom. (2016). doi:10.1007/s13361-016-1466-1

46. Colizza, K., Porter, M., Smith, J.L., Oxley, J.C.: Gas-phase reactions of alcohols with hexamethylene triperoxide diamine (HMTD) under atmospheric pressure chemical ionization conditions. Rapid Commun. Mass Spectrom. 29, 74–80 (2014). doi:10.1002/rcm.7084

47. Colizza, K., Yevdokimov, A., McLennan, L., Smith, J.L., Oxley, J.C.: Using Gas Phase Reactions of Hexamethylene Triperoxide Diamine (HMTD) to Improve Detection in Mass Spectrometry. J. Am. Soc. Mass Spectrom. (2018). doi:10.1007/s13361-017-1879-5

48. Oxley, J.C., Smith, J.L., Bowden, P.R., Rettinger, R.C.: Factors influencing triacetone triperoxide (TATP) and diacetone diperoxide (DADP) formation: Part 1. Propellants, Explos. Pyrotech. 38, 244–254 (2013). doi:10.1002/prep.201200116

49. Smith, M.E., Wall, C., Fitzgerald, M.: Characterisation of the major synthetic products of the reactions between butanone and hydrogen peroxide. Propellants, Explos. Pyrotech. 37, 282–287 (2012). doi:10.1002/prep.201100091

50. Court, M.H.: Canine cytochrome P450 (CYP) pharmacogenetics. NIH Public Access. 43, 1027–1038 (2014). doi:10.1016/j.cvsm.2013.05.001

51. Linder, C.D., Renaud, N.A., Hutzler, J.M.: Is 1-Aminobenzotriazole an appropriate in vitro tool as a nonspecific cytochrome P450 inactivator? Drug Metab. Dispos. 37, 10–13 (2009). doi:10.1124/dmd.108.024075

52. Bondoc, F.Y., Bao, Z., Hu, W.Y., Gonzalez, F.J., Wang, Y., Yang, C.S., Hong, J.Y.: Acetone catabolism by cytochrome P450 2E1: Studies with CYP2E1-null mice. Biochem. Pharmacol. 58, 461–463 (1999). doi:10.1016/S0006-2952(99)00111-2

53. Koop, D.R., Casazza, J.P.: Identification of ethanol-inducible P-450 isozyme 3a as the acetone and acetol monooxygenase of rabbit microsomes. J. Biol. Chem. 260, 13607–13612 (1985)

Appendix 1

Supplemental Information:

Supporting Information Table S1-1: Relative %signal (to 0 % ACN signal) for all compounds tested and standard deviation (±).

			%ACN								
Compound	Ion	Source	50	40	30	20	10	5	2	0	Comments
TATP	$[M+NH_4]^+$	APCI	14	15	19	22	29	37	59	100	
		±	2.3	1.3	2.0	1.3	1.3	1.1	2.3	0.63	
TATP	$[M+NH_4]^+$	ESI	8.0	9.0	11	14	25	42	63	100	Fisher ACN lot #147663
		±	0.54	0.48	0.23	0.22	1.3	1.3	4.7	3.3	
TATP	$[M+NH_4]^+$	ESI	8.5	8.7	11	16	27	43	65	100	Fisher ACN lot #124682
		±	0.62	0.81	0.63	0.62	0.74	0.80	2.6	0.92	
TATP	$[M+NH_4]^+$	HESI	6.6	6.9	12	17	33	51	80	100	333 ºC
		±	0.34	2.1	1.8	1.5	4.3	5.0	1.1	19	
HMTD	$[M+H]^+$	APCI	23	25	26	25	31	38	53	100	
		±	2.4	1.7	0.23	0.62	1.4	2.9	1.7	3.5	
HMTD	$[M+H]^+$	ESI	20	21	24	24	34	46	62	100	Fisher ACN lot #147663
		±	2.2	3.4	1.4	2.3	3.3	1.7	6.1	4.1	
HMTD	$[M+H]^+$	ESI	21	20	21	27	36	49	65	100	Fisher ACN lot #124682
		±	2.6	1.0	1.8	2.1	2.3	5.0	0.54	3.5	
Hexamine	$[M+H]^+$	ESI	91	103	105	109	108	105	106	100	
		±	4.7	9.8	3.8	3.6	6.9	4.8	7.2	6.7	
TBAH	M^+	ESI	112	116	110	111	109	115	116	100	
		±	7.3	5.5	5.0	8.0	1.6	3.8	5.4	2.6	
Michler's Ketone	$[M+H]^+$	ESI	105	94	95	109	112	115	122	100	
		±	2.8	8.2	3.3	4.4	3.0	3.2	4.7	7.5	

			%ACN								
Compound	Ion	Source	50	40	30	20	10	5	2	0	Comments
MEKP DHP1	$[M+NH_4]^+$	ESI	0.0	0.0	0.0	0.0	7.9	18	33	100	
		±					0.61	3.3	4.5	1.5	
MEKP DHP1	$[M+Na]^+$	ESI	0.0	1.5	1.7	4.5	7.8	20	34	100	
		±		0.02	0.73	1.3	0.59	3.4	2.3	8.5	
MEKP DHP2	$[M+NH_4]^+$	ESI	3.8	5.8	7.1	8.7	15	29	47	100	
		±	1.3	0.13	0.19	0.35	1.4	0.60	1.1	4.5	
MEKP DHP2	$[M+NH_4]^+$	HESI	7.1	8.9	11	12	30	30	51	100	200 ºC
		±	1.0	1.3	1.1	0.49	2.9	2.5	2.6	6.0	
MEKP C2	$[M+NH_4]^+$	ESI	14	18	20	23	28	41	58	100	
		±	1.2	0.82	0.48	0.21	1.2	1.1	0.94	4.6	
MEKP C2	$[M+NH_4]^+$	HESI	0.0	0.0	11	21	44	42	80	100	200 ºC
		±			1.8	3.5	9.2	3.9	1.3	13	
MEKP C3	$[M+NH_4]^+$	ESI	58	70	77	81	87	96	99	100	
		±	1.1	1.5	0.29	2.7	3.4	0.24	2.2	5.2	
MEKP C3	$[M+NH_4]^+$	HESI	18	26	33	49	61	67	82	100	200 ºC
		±	5.0	6.8	1.7	9.9	3.7	3.5	1.8	11	
MEKP DHP3	$[M+NH_4]^+$	ESI	68	75	87	90	99	107	112	100	
		±	7.0	3.9	1.5	1.7	1.6	2.6	1.0	3.0	
MEKP DHP3	$[M+NH_4]^+$	HESI	25	36	43	62	90	86	99	100	200 ºC
		±	4.6	5.1	2.2	8.4	9.6	6.6	5.0	5.4	
MEKP DHP4	$[M+NH_4]^+$	ESI	90	95	98	92	97	98	100	100	
		±	2.8	2.6	2.7	4.0	4.8	2.3	1.8	5.5	
MEKP DHP4	$[M+NH_4]^+$	HESI	91	100	95	105	102	90	96	100	200 ºC
		±	8.3	12	1.6	11	5.0	10	1.0	18	

			%ACN								
Compound	Ion	Source	50	40	30	20	10	5	2	0	Comments
MEKP C1	$[M+NH_4]^+$	ESI	34	29	28	38	36	48	62	100	
		±	4.2	2.0	2.3	1.5	3.4	5.4	6.2	0.86	
DADP	$[M+NH_4]^+$	ESI	2.2	2.2	4.0	9.0	12	21	36	100	
		±	0.39	0.25	0.84	0.53	2.3	3.3	8.1	6.1	
MEK/AP C2	$[M+NH_4]^+$	ESI	4.7	4.8	6.4	11	14	21	41	100	
		±	0.07	0.54	1.08	0.56	0.69	2.4	6.7	5.3	
AP DHP2	$[M+NH_4]^+$	ESI	1.7	1.8	2.7	4.8	8.5	17	36	100	
		±	0.04	0.59	0.90	0.38	1.5	3.7	5.8	3.0	
MEK/AP DHP2	$[M+NH_4]^+$	ESI	1.8	2.0	3.2	5.9	9.4	19	36	100	
		±	0.14	0.58	0.78	0.46	1.5	4.1	9.4	5.4	
MEK	$[M+H]^+$	ESI	4.3	5.3	6.8	10	18	31	51	100	
		±	0.39	0.45	0.74	0.20	0.68	0.40	4.2	1.9	
MEK	$[M+NH_4]^+$	ESI	5.0	6.2	8.6	12	21	32	53	100	
		±	0.69	0.51	0.53	0.73	1.0	0.85	1.2	2.1	
MEK	$[M+H]^+$	APCI	4.6	6.1	7.4	7.9	13	19	36	100	
		±	0.31	0.75	0.67	0.61	0.64	1.0	2.0	6.9	
MEK	$[M+NH_4]^+$	APCI	6.0	7.3	9.4	13	22	33	55	100	
		±	0.40	0.70	0.11	0.64	0.54	1.2	0.76	1.5	
Acetone	$[M+H]^+$	ESI	8.9	11	9.3	10	12	31	52	100	
		±	1.4	1.3	1.2	2.0	1.1	1.1	3.9	0.64	

			%ACN								
Compound	Ion	Source	50	40	30	20	10	5	2	0	Comments
Menadione	$[M+H]^+$	ESI	11	9.5	9.2	10	13	22	39	100	
		±	0.14	0.36	0.58	0.78	1.8	0.64	8.6	2.9	
Menadione	$[M+NH_4]^+$	ESI	6.2	4.8	5.0	5.7	8.8	17.7	40	100	
		±	2.4	1.5	0.23	1.5	2.5	2.2	5.4	3.3	
Menadione	$[M+H]^+$	APCI	11	14	17	20	31	42	58	100	
		±	0.34	1.3	0.34	0.61	0.96	1.7	1.7	2.6	
Menadione	$[M+NH_4]^+$	APCI	27	28	23	29	37	52	62	100	
		±	4.8	1.6	4.0	1.1	1.8	2.4	3.1	2.8	
Cyclopentanone	$[M+H]^+$	ESI	0.0	0.0	0.0	5.6	13	35	55	100	
		±				1.8	0.50	1.8	2.8	5.4	
Cyclopentanone	$[M+NH_4]^+$	ESI	5.7	8.0	10	14	28	45	64	100	
		±	0.57	0.16	0.17	0.73	0.30	0.75	0.55	1.7	
Cyclohexanone	$[M+H]^+$	ESI	5.0	7.8	13	12	13	25	53	100	80% aqueous
		±	0.21	0.27	0.39	0.35	0.24	0.40	1.8	3.0	
Cyclohexanone	$[M+NH_4]^+$	ESI	11	15	21	21	22	33	54	100	80% aqueous
		±	0.10	0.33	0.25	0.54	0.30	0.18	0.50	0.51	
Cyclohexanone	$[M+H]^+$	ESI	8.9	6.6	6.4	9.5	19	39	68	100	50% aqueous (standard analysis)
		±	0.73	0.54	0.58	0.91	1.4	1.5	0.77	2.6	
Cyclohexanone	$[M+NH_4]^+$	ESI	5.9	7.9	11	16	29	44	68	100	50% aqueous (standard analysis)
		±	0.22	0.37	0.25	0.30	0.31	0.53	0.35	2.6	

			%ACN								
Compound	Ion	Source	50	40	30	20	10	5	2	0	Comments
Cyclohexanone	$[M+H]^+$	ESI	2.5	2.5	4.7	10	24	43	65	100	20% aqueous
		±	0.14	0.17	0.12	0.33	1.5	3.2	1.1	2.3	
Cyclohexanone	$[M+NH_4]^+$	ESI	4.1	5.3	7.7	13	24	39	57	100	20% aqueous
		±	0.08	0.13	0.04	0.42	0.54	0.65	0.80	0.96	
Cyclohexanone	$[M+H]^+$	ESI	5.5	7.7	6.5	8.9	19	37	49	100	5% aqueous
		±	0.82	0.47	0.69	0.42	1.7	1.4	4.9	7.1	
Cyclohexanone	$[M+NH_4]^+$	ESI	4.7	5.9	7.1	11	20	35	49	100	5% aqueous
		±	0.04	0.19	0.37	0.28	0.84	0.68	2.5	3.2	
Cyclohexanone	$[M+H]^+$	ESI	4.6	6.3	9.6	14	24	41	63	100	Fluka ACN lot #SHBG1053V
		±	0.56	0.55	0.91	1.1	1.2	2.3	0.56	9.6	
Cyclohexanone	$[M+NH_4]^+$	ESI	7.9	9.8	15	19	29	43	61	100	Fluka ACN lot #SHBG1053V
		±	1.4	1.1	0.57	0.50	0.48	0.77	1.5	6.1	
Cyclohexanone	$[M+NH_4]^+$	ESI	8.6	11	14	18	27	44	54	100	0% aqueous with ACN
		±	0.10	0.46	0.19	0.88	1.4	1.2	7.8	6.0	
Cyclohexanone	$[M+H]^+$	ESI	6.3	7.5	9.7	14	22	43	53	100	0% aqueous with ACN
		±	0.41	0.27	0.19	0.10	0.63	1.2	8.5	9.2	
Cyclohexanone	$[M+NH_4]^+$	ESI	2.3	2.8	4.0	5.8	8.4	15	25	100	0% aqueous with tert-butyl nitrile
		±	0.15	0.33	0.18	0.22	0.32	0.04	0.56	4.1	
Cyclohexanone	$[M+H]^+$	ESI	0.0	0.0	0.0	0.0	3.0	6.1	14	100	0% aqueous with tert-butyl nitrile
		±					0.43	0.54	0.63	6.5	

			%ACN								
Compound	Ion	Source	50	40	30	20	10	5	2	0	Comments
Cyclohexanone	$[M+NH_4]^+$	ESI	2.4	2.8	4.8	7.7	15	29	57	100	With Cyanamide (not ACN)
		±	0.53	0.50	0.40	0.65	0.18	1.1	2.4	2.0	
Cyclohexanone	$[M+H]^+$	ESI	0.0	0.0	0.0	0.0	4.4	18	44	100	With Cyanamide (not ACN)
		±					1.5	1.6	3.3	2.5	
Cyclohexanone	$[M+NH_4]^+$	ESI	52	51	60	72	85	93	105	100	With BromoACN
		±	0.31	0.55	1.8	3.4	4.8	5.9	4.7	2.4	
Cyclohexanone	$[M+H]^+$	ESI	48	47	56	69	84	93	108	100	With BromoACN
		±	0.82	0.70	0.91	2.7	5.9	7.2	4.3	3.1	
Cyclohexanone	$[M+H]^+$	ESI	2.1	2.2	3.4	8.6	17	31	63	100	50% aqueous w/1% formic acid
		±	0.11	0.32	0.12	0.18	0.54	1.4	0.68	5.6	
Cyclohexanone	$[M+NH_4]^+$	ESI	4.5	5.6	6.5	11	18	33	62	100	50% aqueous w/1% formic acid
		±	0.22	0.15	0.11	0.02	0.28	0.30	1.1	0.58	
Cyclohexanone	$[M+H]^+$	ESI	4.1	3.8	5.9	11	26	48	71	100	50% aqueous no NH4OAc
		±	0.38	0.16	0.15	0.17	0.32	2.0	4.4	2.2	
Cyclohexanone	$[M+NH_4]^+$	ESI	5.0	7.1	10	16	28	45	66	100	50% aqueous no NH4OAc
		±	0.95	0.12	0.15	0.15	0.33	0.24	1.3	0.06	
Cyclohexanone	$[M+H]^+$	APCI	15	24	21	29	37	55	71	100	No NH4OAc, no MP NH4OAc, 50% ac
		±	6.8	1.05	3.43	0.99	0.77	0.22	0.51	2.9	

			%ACN								
Compound	Ion	Source	50	40	30	20	10	5	2	0	Comments
1, 2, 4-Triazole	$[M+H]^+$	APCI	14	15	18	25	42	61	82	100	
		±	0.67	0.68	0.73	1.7	3.2	1.3	2.7	3.9	
1, 2, 4-Triazole	$[M+H]^+$	ESI	20	16	20	28	54	64	82	100	
		±	2.2	1.3	1.3	6.7	2.7	8.0	7.2	2.0	
1, 2, 4-Triazole	$[M+H]^+$	HESI	6.2	10	16	23	35	48	78	100	250 ºC
		±	0.43	0.60	1.7	1.7	2.0	4.3	4.9	7.8	
Diphenyl isophthalate	$[M+NH_4]^+$	ESI	2.4	3.6	6.0	7.2	13	24	54	100	Exactive
		±	0.14	0.36	0.51	0.16	0.09	0.48	2.0	2.1	
Diphenyl isophthalate	$[M+H]^+$	ESI	0.7	0.9	1.4	3.1	9.2	19	51	100	Exactive
		±	0.05	0.09	0.09	0.78	0.63	0.94	1.9	1.3	
Diphenyl isophthalate	$[M+NH_4]^+$	HESI	2.0	4.8	7.2	9.3	14	24	57	100	250 ºC
		±	1.0	0.22	1.7	1.2	1.3	1.1	0.98	3.7	
Diphenyl isophthalate	$[M+H]^+$	HESI	1.6	3.9	5.9	8.1	14	24	56	100	250 ºC
		±	0.59	0.92	1.2	0.69	0.98	0.65	7.0	11	
Diphenyl isophthalate	$[M+NH_4]^+$	HESI	5.1	5.5	6.0	11	18	34	58	100	No NH4OAc, no MP NH4OAc, 50% aqueous
		±	0.53	1.4	1.8	1.8	0.86	2.3	1.4	4.2	
Diphenyl isophthalate	$[M+H]^+$	HESI	6.5	6.3	7.1	13	18	34	58	100	No NH4OAc, no MP NH4OAc, 50% aqueous
		±	0.74	0.81	0.98	2.6	2.4	1.3	2.4	3.0	
Diphenyl isophthalate	$[M+NH_4]^+$	HESI	5.4	5.1	5.2	6.4	20	33	63	100	No NH4OAc, no MP NH4OAc, 50% MeOH
		±	1.4	0.35	0.07	1.0	0.97	3.1	4.1	2.6	
Diphenyl isophthalate	$[M+H]^+$	HESI	7.3	4.4	5.8	7.0	22	36	66	100	No NH4OAc, no MP NH4OAc, 50% MeOH
		±	2.9	0.52	0.25	1.1	0.21	3.2	3.0	2.2	

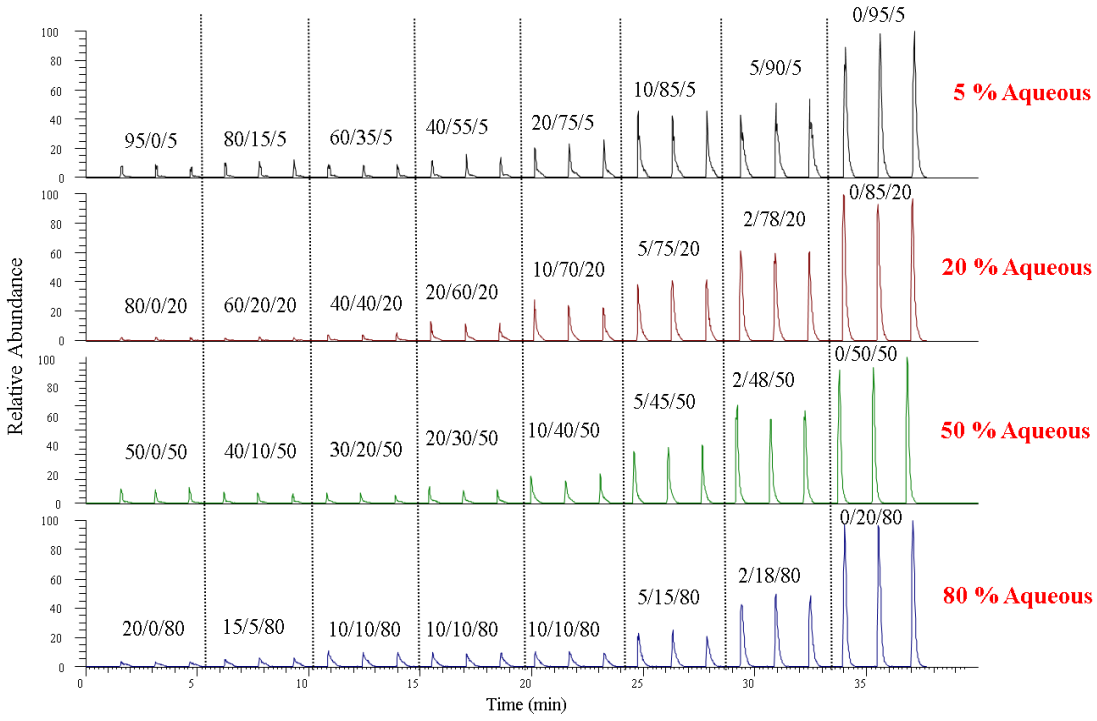

Supporting Information Figure S1-1: *FIA XIC of cyclohexanone $[M+H]^+$ response in ESI with decreasing ACN while varying aqueous content. Concentrations are given as ACN/MeOH/10 mM NH_4OAc located above 3 injections made for each sample.* (Note that for 80% aqueous at 10/10/80, three replicates were prepared and each injected 3 times.)

Supporting Information Table 1-2: NIST Gas Phase Basicity (GPB) and Proton Affinity (PA) in kJ/mol.

Compound	GPB	PA
H_2O	660	691
MeOH	724.5	754.3
ACN	748	779.2 (787.4)
Acetic acid	752.8	783.7
Cyanamide	774.4	805.6
Pivalonitrile	780.2	810.9
Acetone	782.1	812
Cyclopentanone	794	823.7 (828)
MEK	795.5	827.3
Cyclohexanone	811.2	841
Ammonia	819	853.6
1,2,4-triazole	855.9	886

Appendix 2

Supplemental Information:

Reactions of Organic Peroxides with Alcohols in Atmospheric Pressure Chemical Ionization—the Pitfalls of Quantifying Triacetone Triperoxide

Kevin Colizza, Alexander Yevdokimov, Lindsay McLennan, James L. Smith and Jimmie C. Oxley

Supporting Information:

Table S2-1. Stability of TATP, HMTD and TMDDD reported as % accuracy to nominal concentration.

		TATP			HMTD*			TMDDD*		
	Level	Day 7	Day 40	Day 60	Day 7	Day 40	Day 60	Day 7	Day 40	Day 60**
Room Temp	10000	**108**	**108**	**104**	**97**	**86**	**87**	**100**	**100**	**112**
(~22°C)	2500	**103**	**104**	**101**	**99**	**85**	**81**	**94**	**107**	**110**
	1000	**101**	**100**	**98**	**99**	**83**	**84**	**97**	**131**	**115**
Refrigerator	10000	**112**	**105**	**104**	**97**	**100**	**94**	**101**	**102**	**114**
(4°C)	2500	**109**	**103**	**102**	**95**	**99**	**93**	**95**	**108**	**110**
	1000	**103**	**100**	**97**	**101**	**98**	**93**	**95**	**114**	**114**
Freezer	10000	**108**	**105**	**101**	**97**	**100**	**94**	**105**	**91**	**108**
(-20°C)	2500	**103**	**100**	**98**	**99**	**100**	**93**	**100**	**106**	**106**
	1000	**100**	**93**	**95**	**101**	**100**	**94**	**102**	**107**	**106**
Autosampler	10000	**7**			**203**			**194**		
(8°C)	5000	**11**			**201**			**177**		

*HMTD standard contains 1.00% TMDDD and TMDDD standard contains 1.57% HMTD

**Increase at day 60 may be due to a new batch of TMDDD standard.

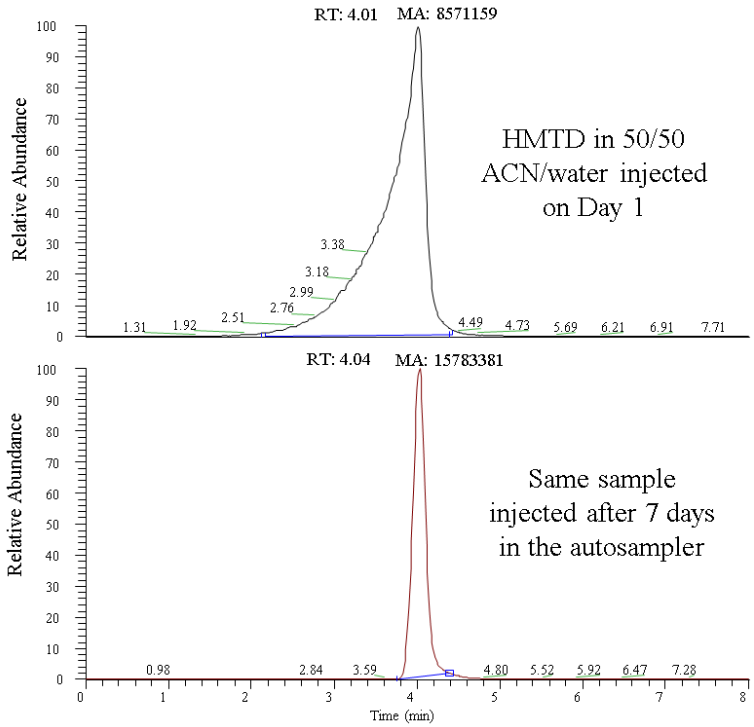

Figure S2-1. The same HMTD standard curve sample (10000 ng/mL) injected on day 1 and day 7 for autosampler stability.

Table S2-2. Mean concentration (N=3) of TATP in vapor by direct sampling and analysis by LC/MS.

Vessel	Mean (ng TATP/mL vapor)	SD (+/- ng/mL vap)
A 1L	354	34
B 1L	388	54
A 500mL	384	1.6
B 500mL	379	64
Mean	376	
Standard Error	8	

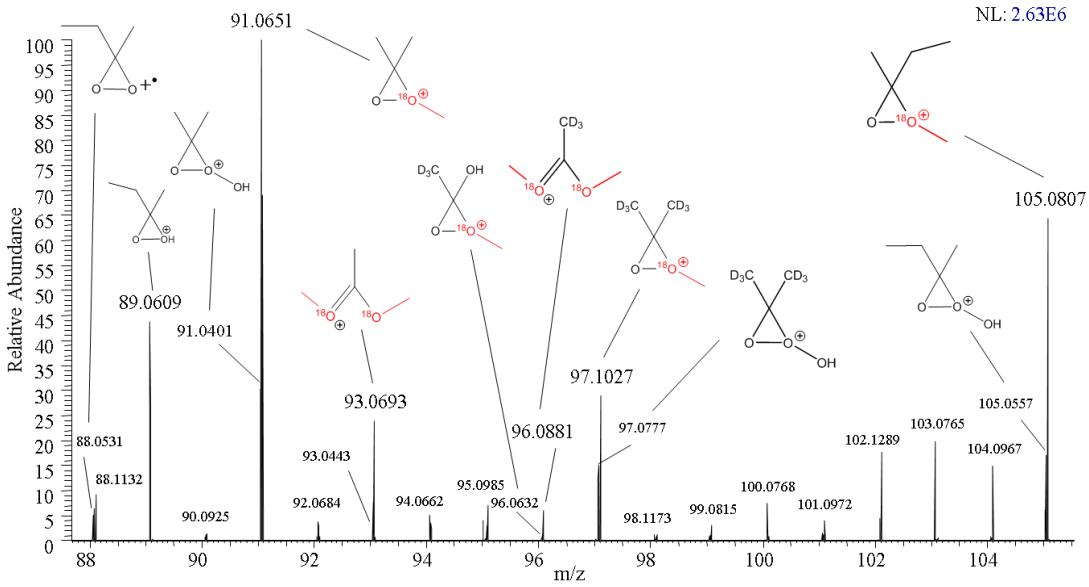

Figure S2-2. Infusion of TATP, d_{18}-TATP & MEKP onto APCI source in $Me^{18}OH$ and 10 mM NH_4OAc solution.

Appendix 3

This appendix is intentionally left blank to keep consist numbering between chapters and appendices.

Appendix 4

Supporting Information:

Using Gas Phase Reactions of Hexamethylene Triperoxide Diamine (HMTD) to Improve Detection in Mass Spectrometry

Supplemental information

Table S4-1. Stability of TATP, HMTD and TMDDD reported as % accuracy to nominal concentration.

		TATP			**HMTD***			**TMDDD***		
	Level	Day 7	Day 40	Day 60	Day 7	Day 40	Day 60	Day 7	Day 40	Day 60**
Room Temp	10000	**108**	**108**	**104**	**97**	**86**	**87**	**100**	**100**	**112**
(~22°C)	2500	**103**	**104**	**101**	**99**	**85**	**81**	**94**	**107**	**110**
	1000	**101**	**100**	**98**	**99**	**83**	**84**	**97**	**131**	**115**
Refrigerator	10000	**112**	**105**	**104**	**97**	**100**	**94**	**101**	**102**	**114**
(4°C)	2500	**109**	**103**	**102**	**95**	**99**	**93**	**95**	**108**	**110**
	1000	**103**	**100**	**97**	**101**	**98**	**93**	**95**	**114**	**114**
Freezer	10000	**108**	**105**	**101**	**97**	**100**	**94**	**105**	**91**	**108**
(-20°C)	2500	**103**	**100**	**98**	**99**	**100**	**93**	**100**	**106**	**106**
	1000	**100**	**93**	**95**	**101**	**100**	**94**	**102**	**107**	**106**
Autosampler	10000	**7**			**203**			**194**		
(8°C)	5000	**11**			**201**			**177**		

*HMTD standard contains 1.00% TMDDD and TMDDD standard contains 1.57% HMTD

**Increase at day 60 may be due to a new batch of TMDDD standard.

Table S4-2. % Area for Each Related Species at a given Vaporizor Temp on PFP Column with 30 AU N2 flow

APCI Probe Temperature	TMDDD		HMTD			
	m/z = 207.0611	m/z = 224.0877	m/z = 207.0611	m/z = 224.0877	m/z = 207.0975	m/z = 209.0768
210 °C	6.01	94.0	0.00	2.31	67.5	30.2
250 °C	6.29	93.7	0.80	11.5	63.0	24.8
300 °C	4.84	95.2	2.40	32.3	45.9	19.3

Table S4-3. % Total Area for Each Related Species over all Vaporizor Temps on PFP Column with 30 AU N2 flow

APCI Probe Temperature	TMDDD		HMTD			
	m/z = 207.0611	m/z = 224.0877	m/z = 207.0611	m/z = 224.0877	m/z = 207.0975	m/z = 209.0768
210 °C	1.71	26.7	0.00	0.66	19.2	8.57
250 °C	2.18	32.5	0.30	4.30	23.6	9.27
300 °C	1.79	35.1	0.82	11.0	15.7	6.60

Table S4-4. % Total Area for Each Related Species over all Gas Flows Run with a PFP Column and 250°C Vaporizor Temperature

Nitrogen Gas Flow (AU)		TMDDD % Area		TMDDD %Area	TMDDD
Sheath	Auxillary	m/z 207.0612	m/z 224.0877	Over All Gas Flows	Averge %RSD
25	5	14.1	85.9	32.9	34.3
5	25	22.8	77.2	3.01	5.39
15	15	13.5	86.5	15.7	2.61
20	20	18.5	81.5	14.3	1.08
25	25	22.6	77.4	13.1	2.43
30	30	25.9	74.1	11.1	4.25
35	35	29.6	70.4	9.82	2.96

Nitrogen Gas Flow (AU)		HMTD % Area				HMTD %Area	HMTD
Sheath	Auxillary	m/z 207.0612	m/z 224.0877	m/z 207.0975	m/z 209.0768	Over All Gas Flows	Averge %RSD
25	5	1.49	3.89	79.2	15.4	26.0	8.79
5	25	1.88	3.63	76.6	17.9	9.06	2.98
15	15	2.03	5.63	77.9	14.5	19.3	2.28
20	20	2.43	5.19	73.7	18.6	15.0	2.39
25	25	2.39	4.32	71.4	21.9	12.5	1.08
30	30	3.00	4.81	67.1	25.1	9.89	4.35
35	35	3.17	4.29	64.9	27.7	8.22	3.12

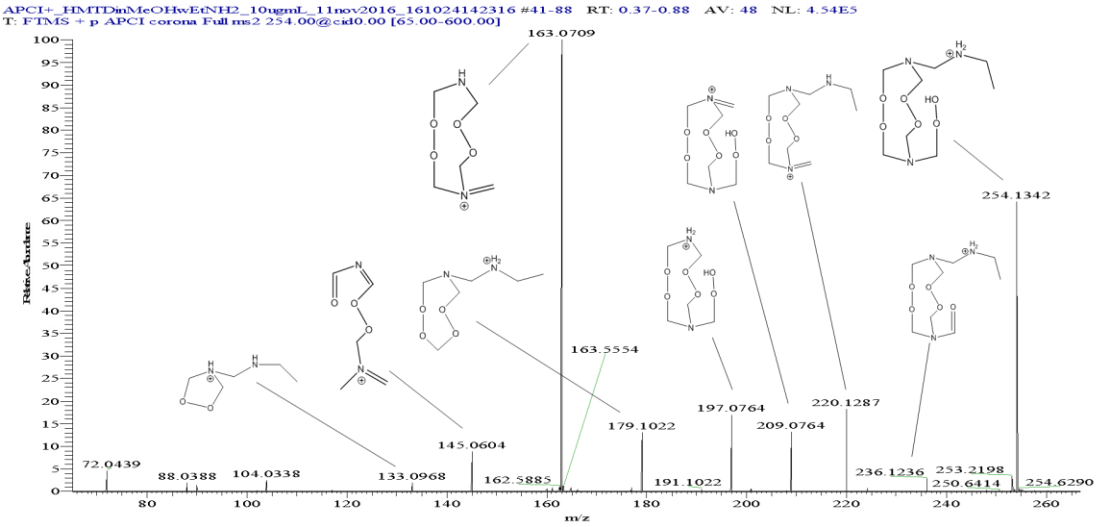

Figure S4-1. HMTD spectra of m/z 254.1347 when infused with ethylamine.

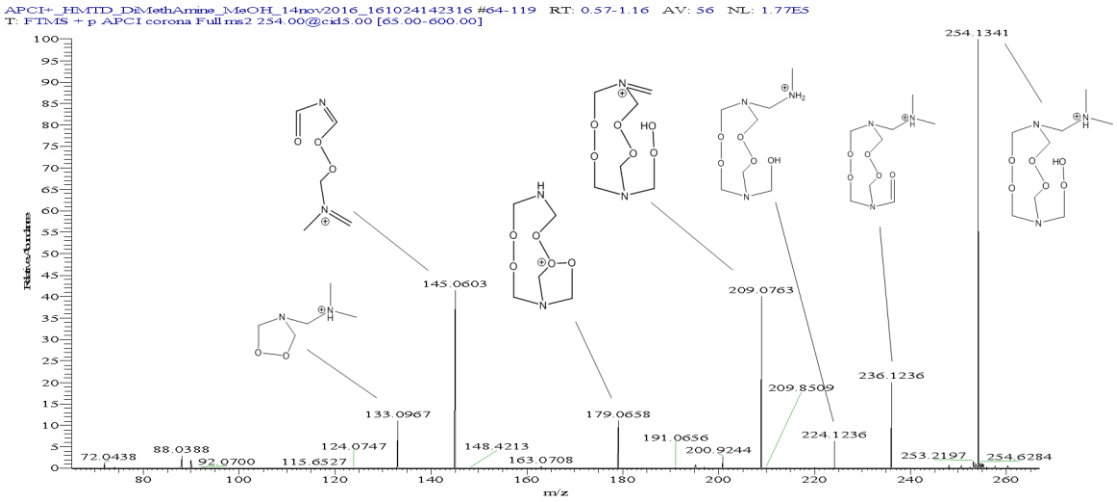

Figure S4-2. HMTD spectra of m/z 254.1347 when infused with dimethylamine.

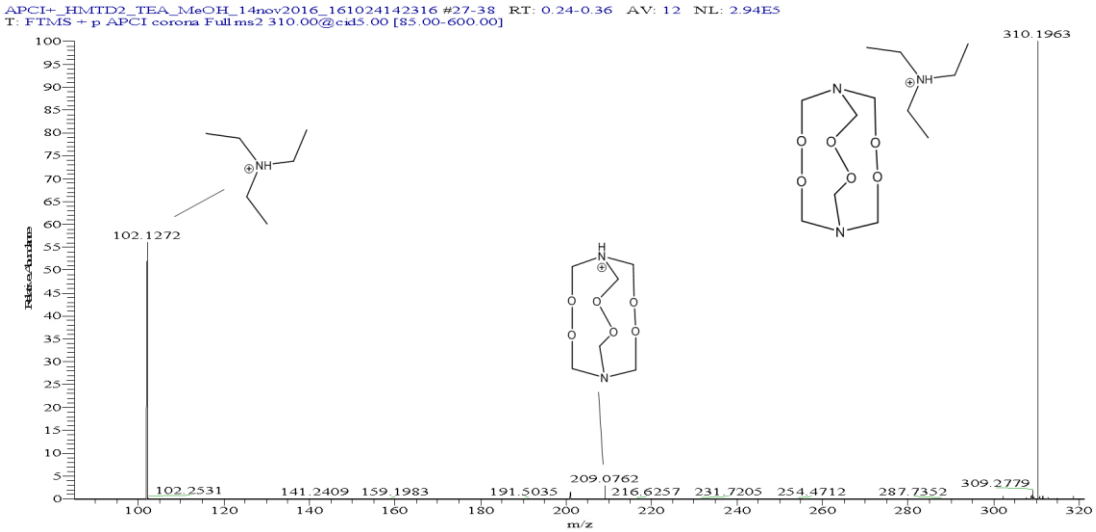

Figure S4-3. HMTD spectra of m/z 310.1973 when infused with triethylamine.

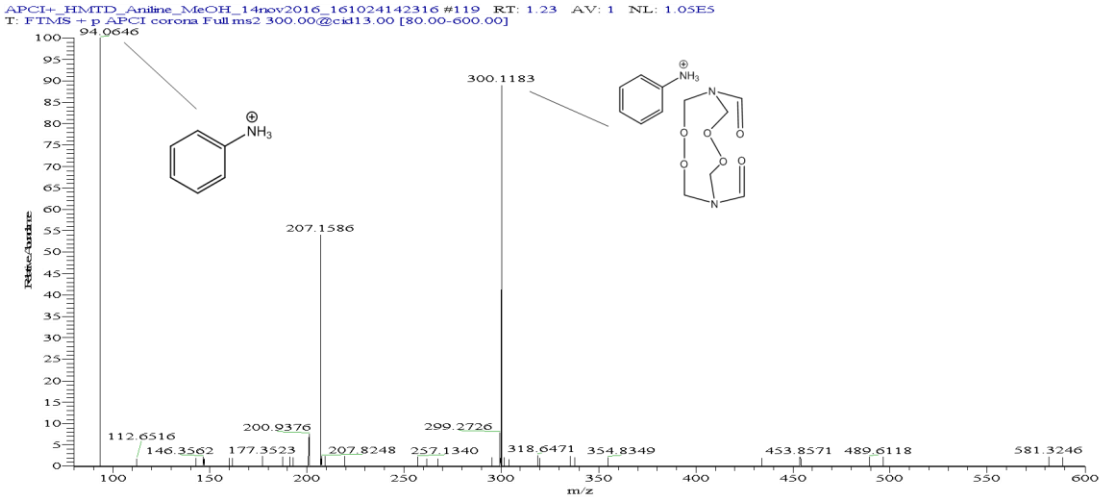

Figure S4-4. TMDDD spectra of m/z 300.1183 when infused with aniline. Note: 207.1586 is not the TMDDD $[M+H]^+$; this mass was not identified.

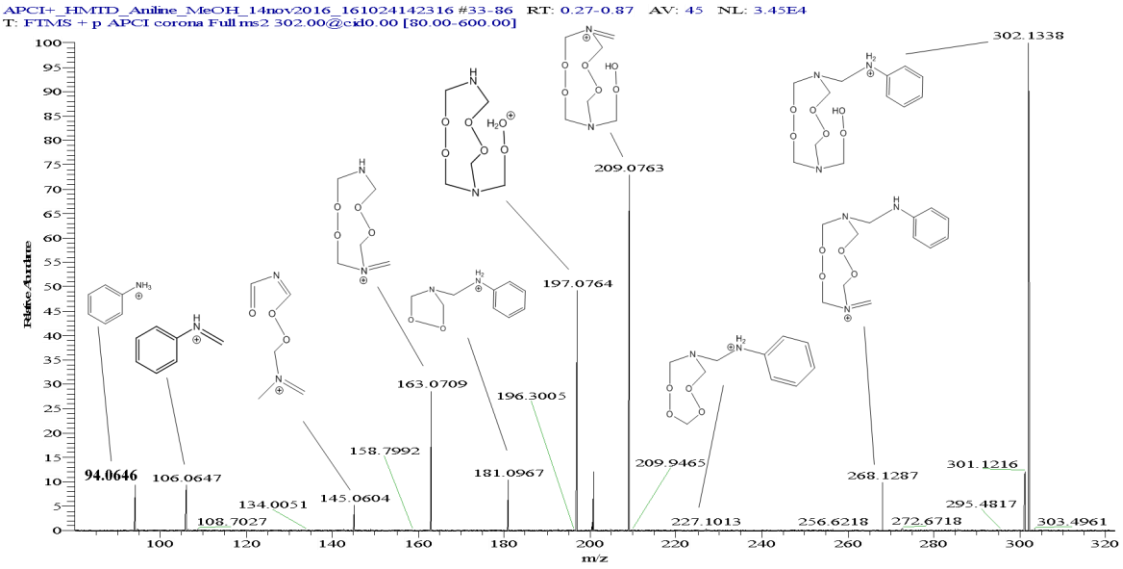

Figure S4-5. HMTD spectra of m/z 302.1347 when infused with aniline.

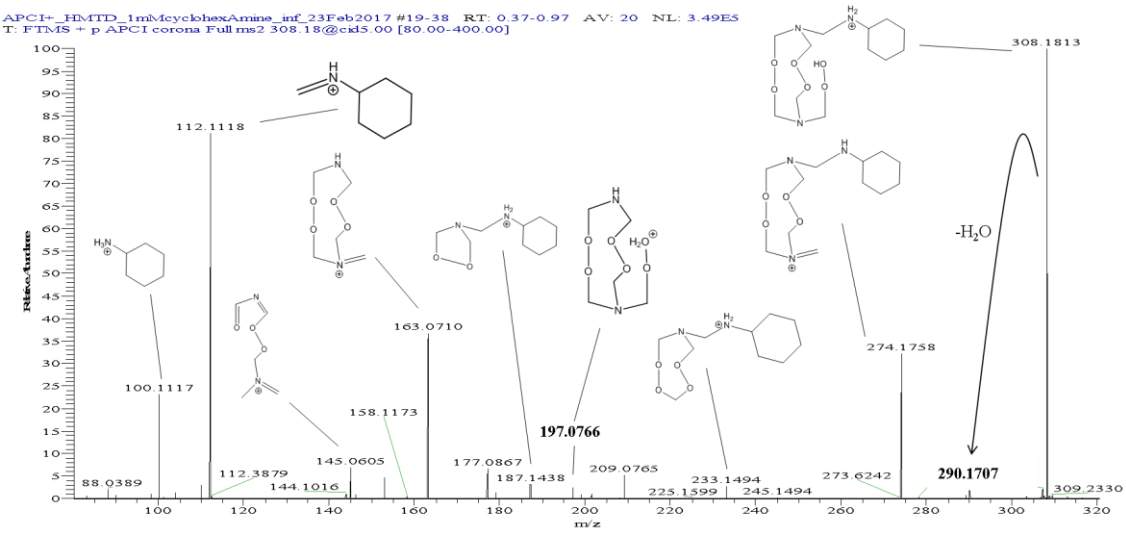

Figure S4-6. HMTD spectra of m/z 302.1347 when infused with aniline.

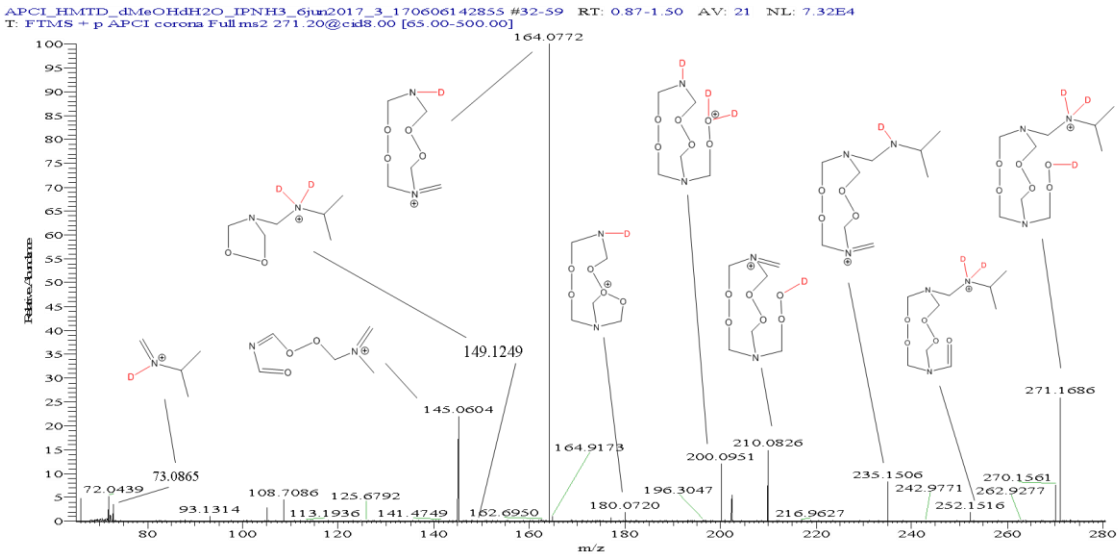

Figure S4-7. HMTD spectra of m/z 271.1691 when infused isopropyl amine and deuterated solvent.

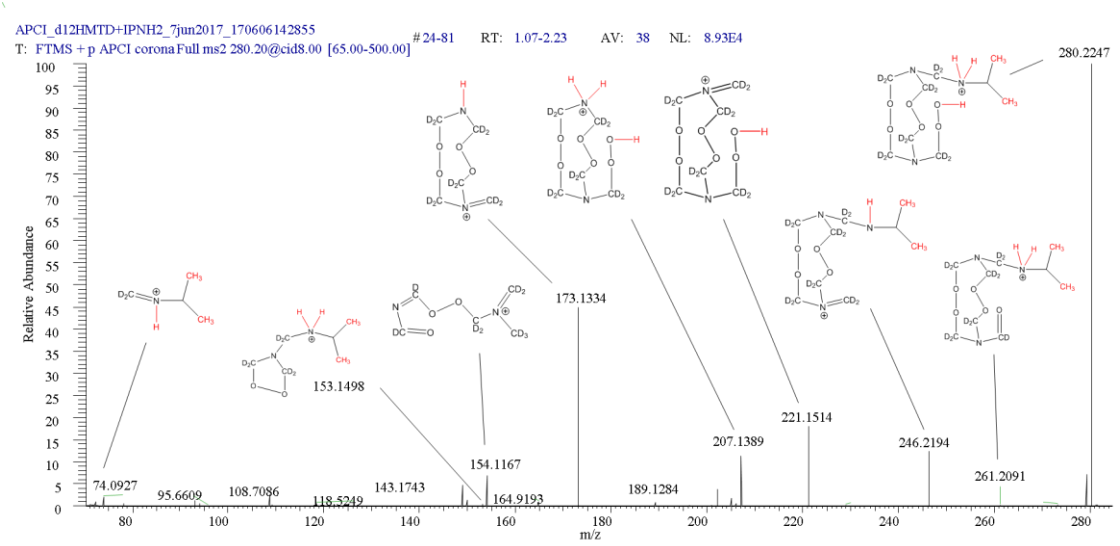

Figure S4-8. d_{12}-HMTD spectra of m/z 280.2256 when infused isopropyl amine.

Appendix 5

Supporting Information:

In Vitro Metabolism and Potential Toxicity of Triacetone Triperoxide (TATP) in Canines

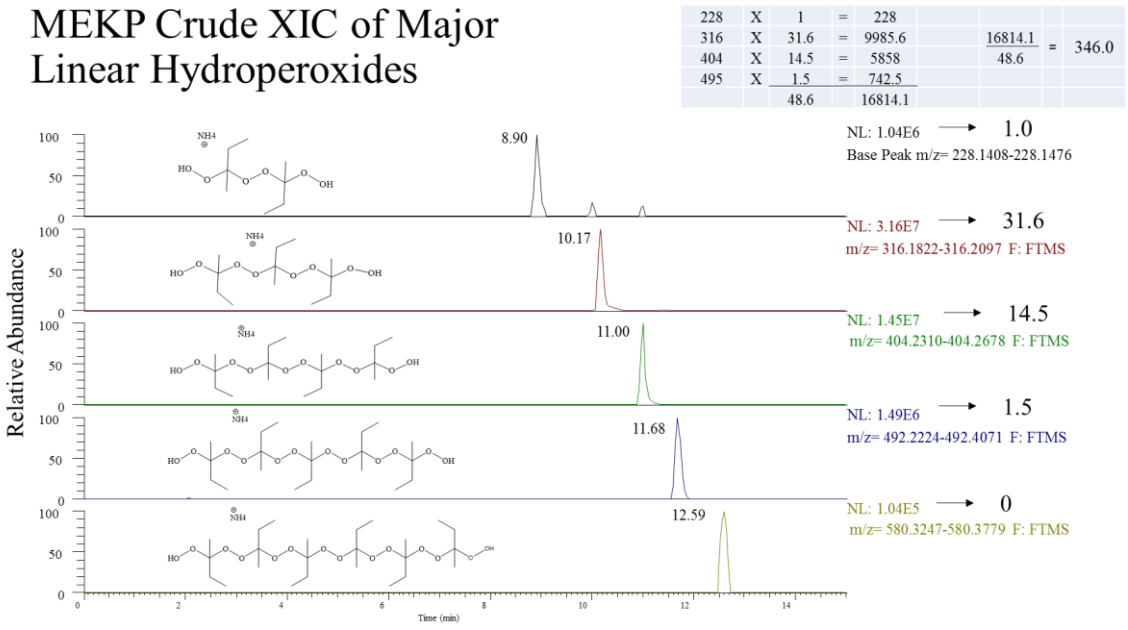

Calibration Curve and QC Samples for TATP Analysis

Curve data

	Calculated Concentration (ng/mL)					
Exp Amt	**Curve 1**	**Curve 2**	**Mean**	**% Acc**	**SD**	**%CV**
25	28	24	26	104	2.5	9.5
50	54	45	49	98	6.4	13.0
100	97	98	98	98	0.5	0.5
150	133	146	139	93	8.8	6.3
250	225	237	231	92	8.3	3.6
500	469	484	477	95	10.7	2.2
1000	1003	951	977	98	36.9	3.8
5000	5206	5073	5139	103	93.8	1.8
10000	10781	10636	10708	107	102	1.0
20000	23785	21030	22408	112	1948	8.7

QC data

	Calculated Concentration (ng/mL)					
Exp Amt	**QC1**	**QC2**	**Mean**	**% Acc**	**SD**	**%CV**
15000	16679	15934	16307	109	527	3.2
1500	1606	1559	1582	105	33.2	2.1
75	77	78	77	103	0.8	1.0

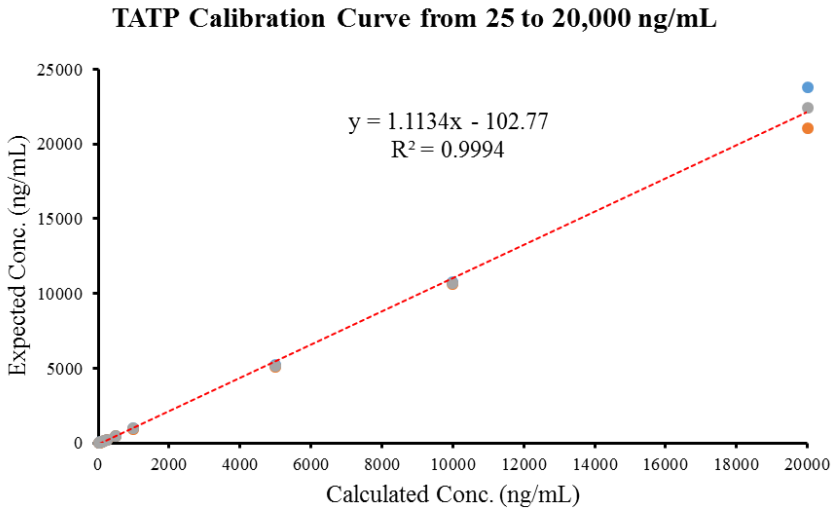

Positive control, Verapamil, incubated in DLM in an open and closed container. No NADPH was run in an open container.

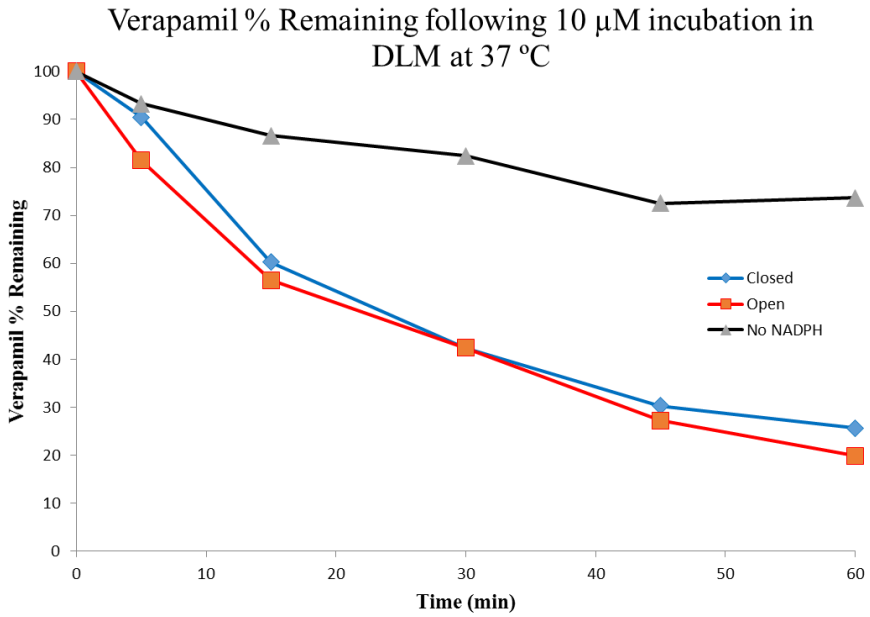

	Neg Control	Open	Closed	
k	0.0052	0.0264	0.0236	1/min
T1/2	133.27	26.25	29.36	min
V	1000.00	1000.00	1000.00	µL/mg
Clint	5.2	26.4	23.6	µL/min/mg

k = -slope of time vs. ln[S]

$T_{1/2} = 0.693/k$

V = Vol/mg protein

$Cl_{int} = V \bullet k$

Data Used to Determine Km and Vmax for TATP in DLM.

1 µM	Slope (µM/min)	Rate (µM/min/mg)	Mean Rate	SD
Tr1	0.2232	0.4464	0.4136	0.039
Tr2	0.2117	0.4234		
Tr3	0.1855	0.371		

2.5 µM	Slope (µM/min)	Rate (µM/min/mg)	Mean Rate	SD
1	0.3011	0.6022	0.581	0.019
2	0.2826	0.5652		
3	0.2885	0.577		

5 µM	Slope (µM/min)	Rate (µM/min/mg)	Mean Rate	SD
1	0.3227	0.6454	0.758	0.114
2	0.3768	0.7536		
3	0.4371	0.8742		

10 µM	Slope (µM/min)	Rate (µM/min/mg)	Mean Rate	SD
1	0.3575	0.715	0.887	0.151
2	0.4765	0.953		
3	0.4969	0.9938		

20 µM	Slope (µM/min)	Rate (µM/min/mg)	Mean Rate	SD
1	0.5233	1.0466	1.035	0.024
2	0.5039	1.0078		
3	0.5251	1.0502		

30 µM	Slope (µM/min)	Rate (µM/min/mg)	Mean Rate	SD
1	0.5914	1.1828	1.076	0.151
2	0.4845	0.969		
3	~~0.2652~~	~~0.5304~~		

50 µM	Slope (µM/min)	Rate (µM/min/mg)	Mean Rate	SD
Tr1	0.5834	1.1668	1.095	0.064
Tr2	0.5375	1.075		
Tr3	0.5214	1.0428		

	Initial Rate	
[TATP] (µM)	V0 (µM/min/mg)	SD
1	0.414	0.039
2.5	0.581	0.019
5	0.758	0.114
10	0.887	0.151
20	1.035	0.024
30*	1.076	0.151
50	1.095	0.064

*Two trials µsed dµe to error with third trial

Lineweaver-Burke Plots for TATP Loss

[TATP] = 1, 2.5 and 5 µM

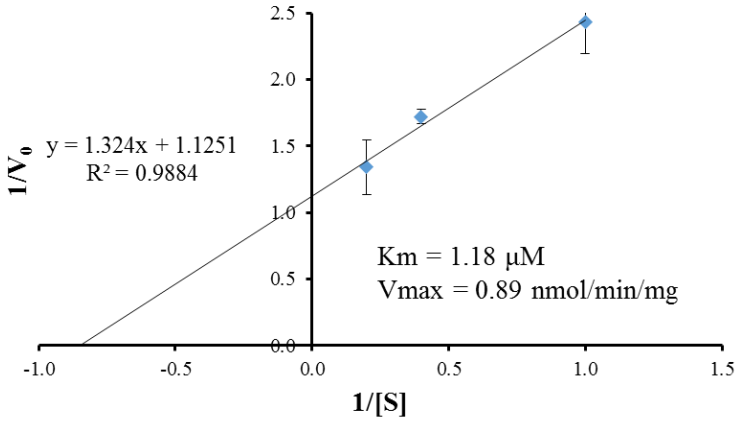

[TATP] = 10, 20, 30 and 50 µM

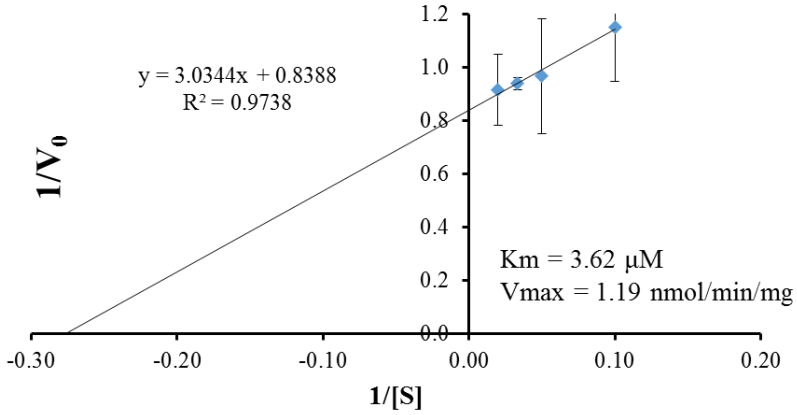

[TATP] = 1 to 50 µM

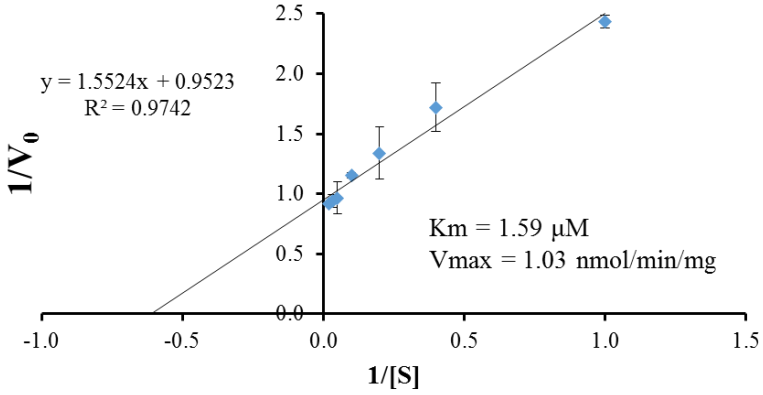

Hanes Plot for TATP Loss

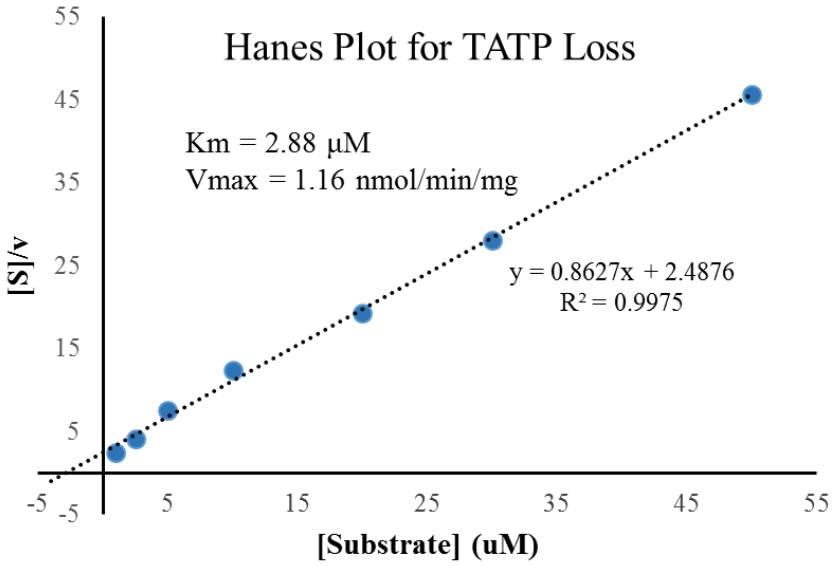
Hanes Plot for TATP Loss
Km = 2.88 µM
Vmax = 1.16 nmol/min/mg
y = 0.8627x + 2.4876
R² = 0.9975
[S]/v
[Substrate] (uM)
55
45
35
25
15
5
-5
-5
5
15
25
35
45
55